UNIVERSITÀ DI TRENTO | Department of Industrial Engineering

XXXIV cycle

Doctoral School in Materials, Mechatronics and System Engineering

The Role of Photovoltaic Generation and Electric Mobility in Future Distribution Systems

Mattia Secchi

October 2022

The Role of Photovoltaic Generation and Electric Mobility in Future Distribution Systems

Candidate: Mattia Secchi

Email: mattia.secchi@unitn.it - mattia.secchi@eurac.edu

Prof. Dario Petri, Advisor
Dept. of Industrial Engineering
University of Trento, Italy

Dr. Grazia Barchi, Co-Advisor
Institute for Renewable Energy
Eurac Research, Bolzano, Italy

University of Trento

Department of Industrial Engineering

October 2022

University of Trento - Department of Industrial Engineering

Doctoral Thesis

Mattia Secchi - October 2022
Published in Trento (Italy) - by University of Trento

Abstract

In order to meet the worldwide limits on greenhouse gases emissions, a shift from a fossil fuels to a renewable energy-based electric system is required. As this process goes on, both the power generation and consumption profiles are changing in daily pattern and magnitude, so the power grid needs to become more and more flexible in order to handle this variability. At the distribution level, photo-voltaic (PV) systems are, by far, the most widespread distributed energy resource, mostly due to the recent drop in the cost at the residential level. As more and more consumers become also producers (the so called "prosumers") and the volatile solar energy production increases, a higher number of storage systems is required to both avoid grid destabilisation and minimise the CO_2 emissions. At the same time, since the transportation sector is responsible for a sizeable part of the total CO_2 emissions, electric vehicles (EVs) are bound to replace traditional internal combustion engine vehicles. However, two main issues may arise when a large number of vehicles are connected to the existing power grid at the same time. The first issue is that the electricity required to charge them needs to be renewable, while the second is that, a rapid electrification of the existing vehicles fleet could destabilise the grid. In this context, this thesis aims at partially addressing these two issues by analysing different ways to reduce the impact of both PV systems and EVs on low (LV) and medium (MV) voltage grids. After the introduction and a chapter dealing with the most closely related research work, a novel optimisation algorithm, aimed at obtaining the optimal storage capacity for each prosumer belonging to a "renewable energy community" is presented. The algorithm minimises the dependence of the community on the main grid, which is one of the main purposes of this new model, while minimising the total installed storage capacity. The algorithm is tailored to the specific case study, because it keeps track of the willingness of the users to install a battery and keeps the voltage levels between regulatory limits in the optimisation process. In the second part instead, the effects of "uncontrolled" and "smart" EV-charging the electric vehicles with the aim of reducing the power fluctuations at the MV/LV transformer level are analysed. In particular, the interaction between PV production and EV charging is investigated, while considering the grid voltage fluctuations, the distribution line losses and the transformer loading levels at the same time. The broader impact of smart charging is also analysed by performing a simplified economic and battery wear analysis. Results help in understanding if storage devices can reduce the dependence of a renewable energy community on the main grid, and to what extent it is possible and economically viable to do so. Moreover, results quantify a realistic range of EV and PV system penetration in a LV grid that still allows for a combined minimisation of their impact on the power grid.

Contents

List of Figures

List of Tables

List of Abbreviations

AC	Alternating Current
BESS	Battery Energy Storage System
BEV	Battery Electric Vehicle
DC	Direct Current
DER	Distributed Energy Resource
DOD	Depth-of-discharge
DSO	Distribution System Operator
DSM	Demand Side Management
ESS	Energy Storage System
EV	Electric Vehicle
HC	Hosting Capacity
HP	Heat Pump
HV	High Voltage
LV	Low Voltage
MV	Medium Voltage
NLV	Net-load Variance
P2G	Peer-to-grid
P2P	Peer-to-peer
PHEV	Plug-in Hybrid Electric Vehicle
PS	Primary Substation
PSO	Particle Swarm Optimisation
PV	Photo-Voltaic
REC	Renewable Energy Community
RMS	Root-mean-square
SOC	State-of-charge
SS	Secondary Substation
V2G	Vehicle-to-grid

Chapter 1

Introduction

1.1 Research Context

The worldwide regulation on climate change, first introduced in the Kyoto protocol (1994), then confirmed in the Paris agreement (2016), identified a temperature increase threshold of 1.5°C compared to pre-industrial levels as the target value to mitigate the effects of global warming and prevent irreversible changes in our ecosystems. The Intergovernmental Panel for Climate Change (IPCC) on its 6th Report showed how different Shared Socio-Economic Pathways (SSPs) produce different levels of emitted CO2 per year, as shown in Figure 1.1 [1]. In turn, the SSPs correlate to different temperature rise gradients, hence the targets.

The Authors of the report described SSP2-4.5 (expected 2°C increase by 2050) as the "most likely" one, based on the current worldwide situation. In that scenario, "the world follows a path in which social, economic, and technological trends do not shift markedly from historical patterns. Global and national institutions work toward but make slow progress in achieving sustainable development goals. The overall intensity of resources and energy use declines." In order to shift to SSP1-1.9 or SSP1-2.6 (expected 1.6-1.7 °C increases by 2050), "the consumption needs to be strongly oriented towards low material usage and lower resource and energy intensity."

Aside from this important message, the IPCC also provided a current greenhouse gases emissions inventory based on data from 2019. The greenhouse gases emissions at present depend by around 22% on agriculture, forestry and land use, 33% on energy supply, 15% on transportation, and 24% on industry. A detailed breakdown is shown in figure 1.2.

In order to decrease the 33% of the emissions depending on energy supply, the generation paradigm needs to shift from a fossil fuels-based model, to a clean energy sources-driven one. This is the reason why, in the recent years, the electric system has undergone some major changes. Those changes mainly involve shifting from a *centralised* type of electricity generation, based on large scale coal/gas, nuclear and hydro power plants to a *decentralised* one, where the generation/consumption at the consumers' side is governed by the so-called Distributed Energy Resources (DERs). Recently, it was shown that DERs generate more competitive, clean and resilient systems [2]. Thus, the number of DERs connected to the grid is increasing every year. However, while from a theoretical standpoint the higher the share of DERs, the lower the greenhouse gases emissions are, there are complex *economic and technical limitations* that have slowed down the transition to a cleaner energy system. Those limitations stem from the way the electric grid was originally designed, i.e. as an Alternating Current (AC) system whose core elements, such as transformers, lines, circuit breakers, were designed assuming the power transmission and distribution to be *unidirectional*, from High-Voltage (HV) through Medium-Voltage (MV), down to Low-Voltage (LV). Instead , the ever-increasing share of DERs connected at the distribution side can create *reverse power flows* from LV to MV, generally due to large quantities of power simultaneously injected into the grid at moments of low consumption. This may occur when photo-voltaic (PV) systems produce large quantities of power during the central hours of the day. Moreover, the production of electricity by fossil fuels-based sources is generally fully *controllable* and able to meet any load demand, whereas DERs are mostly volatile due to their dependence on natural resources.

Those power injections can destabilise the *grid voltage*, create *congestion over the lines*, *overload the transformers* or endanger the electric equipment designed for a unidirectional power flow, such as circuit breakers [3]. Additionally, DERs are generally direct current (DC) sources, and require the transformation of the injected currents into AC via non-linear power electronics that increase the harmonic content of the current and voltage waveforms. Finally, DERs generally do not provide any inertial response to restore the grid frequency in the case of sudden connections or disconnections of

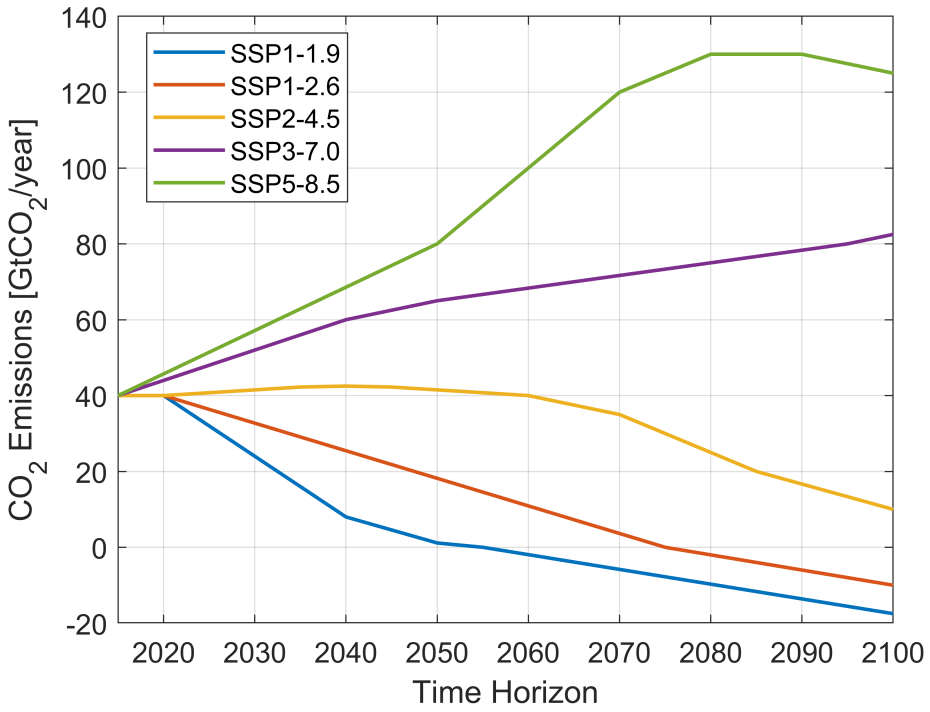

FIGURE 1.1: SSPs and related CO2 emissions from the IPCC 6-th Report [1].

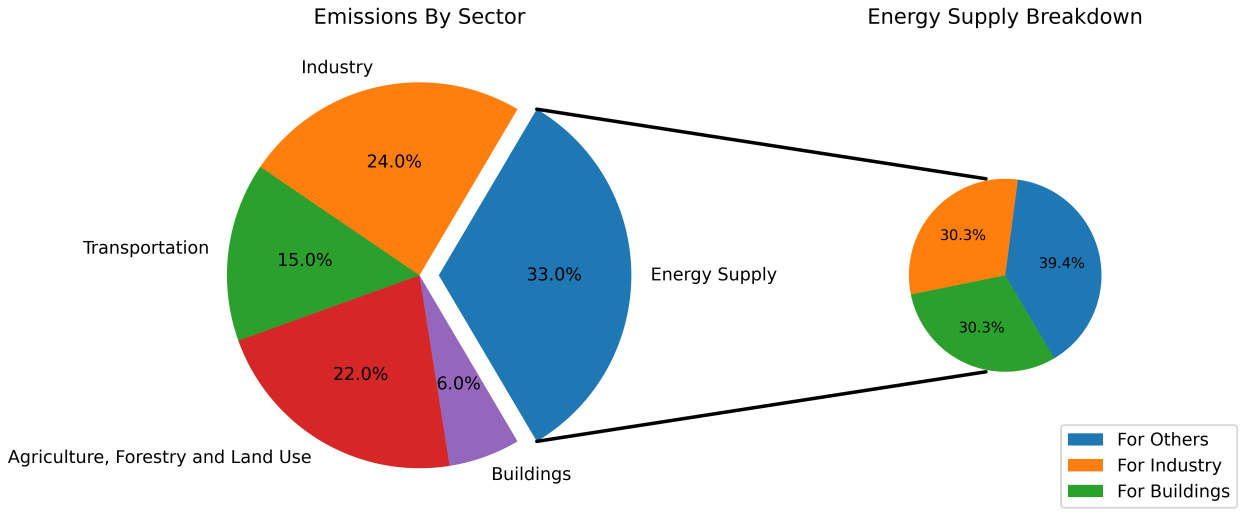

FIGURE 1.2: Greenhouse Gases Emissions Breakdown from the IPCC 6-th Report [1].

large loads or generators. Understanding these issues is essential to accommodate larger shares of DERs in the power grid without expensive reinforcements.

1.2 Objectives

Over the last years PV systems have become very competitive due to the decrease in their levelised cost of electricity [4], i.e. the cost to produce electricity that considers the entire lifetime of the panel. Differences persist all over the world regarding the economic value [5–7], but from the grid side, the main issue is always the simultaneous injection of electricity during the central hours of the day, when the consumption is often at its lowest. In order to mitigate this impact, battery energy storage systems (BESSs) need to be properly placed, sized and controlled, so that the payback time of the combined PV+BESS system is minimised. As such, the *first* objective of this work is to understand how BESSs can be properly controlled and sized to increase the hosting capacity of the grid and provide an economic benefit to the users. For this reason, a novel BESS sizing algorithm with the goal of maximising collective self-sufficiency in a renewable energy community (REC), while minimising the total BESSs installed capacity, will be presented. RECs are legal entities, composed by citizens, municipalities or small-enterprises that pool their production, consumption and storage resources to improve the "collective" self-sufficiency. This is done by enforcing the electricity exchanges between the REC members themselves. To this end, different BESS control strategies can be used. In this dissertation, two policies will be analysed.

Recently, the cost of electric vehicles (EVs), more specifically plug-in ones (PEVs) has also decreased [8] and studies report that PEVs could break-even with an equivalent internal combustion engine vehicle in six years [9]. Hence, a more sustainable way of transportation could be available to everyone in a very short time. Those EVs however, need to be charged through the electric grid, and the peak consumption values of EV charging stations generally happen when people are home. That may overload the electric network, especially if domestic appliances simultaneously consume electricity. Thus, the *second* objective of this work is exploring the possibilities of smart PEVs charging and its interactions with the PV production on a LV grid. Thus, the capabilities of a smart charging algorithm for PEVs to smooth the active power curve through the LV/MV transformer will be investigated in a variety of realistic scenarios, including PV production. The desired objective is achieved by either allocating the EVs charging sessions at low-demand times of the day or during high-PV production periods, in order to maximise the use of renewable energy and avoid impacting the grid. In the simulations, the actual EV use and willingness of the uses are also considered.

In conclusion, the thesis is structured as follows: Chapter 2 provides an overview of the scientific literature regarding the aforementioned topics, when either BESS or smart EV charging stations with smart charging capabilities and residential PV systems are simultaneously considered. In Chapter 3 and 4 instead, two alternative solutions to both problems are validated through real-world simulations and supported by a broader analysis of their grid-related, environmental and economic impacts. Chapter 5 expands the results of Chapter 4 by presenting the analysis of the EV uptake impact on a large MV/LV distribution network. Chapter 6 draws the main conclusions of the work and provides an overview of ongoing and future activities.

Chapter 2

Background

In this Section, the different parameters affected by the introduction of PV systems and EV stations on the electric network are presented, along with a number of examples taken from the literature. Then, different techniques to reduce those impacts are presented, mostly concerning stationary BESS and smart EV charging or vehicle-to-grid (V2G) algorithms.

2.1 DERs Grid Impact

Following the scheme introduced by Caballero-Pena et al. [3], DERs can impact the electric distribution systems by altering its most important electric parameters, e.g. the root-mean-square (RMS) amplitude of bus voltages and line currents, the grid frequency and total harmonic distortion (THD), the power losses over the lines and the power quality in general (voltage unbalance, flicker, frequency and harmonics).

Numerous studies about the impact of PV systems and EV charging stations on the electric network can be found in the literature. In the following Section, each specific parameter will be individually analysed and some examples will be provided.

2.1.1 Voltage Magnitude Changes

In order to demonstrate how a power injection/absorption influences the voltage levels, we can assume, without loss of generality, to analyse the simple system composed by one fixed power generator, one load, one line and a MV/LV transformer, such as in Figure 2.1.

The equation (2.1) relating the power injection-absorption to the voltage levels is presented by Ghiani et al. [10]:

$$\Delta V = V_1 - V_2 = \frac{R \cdot (P_l - P_g) + X \cdot (Q_l - Q_g)}{V} \cdot L \tag{2.1}$$

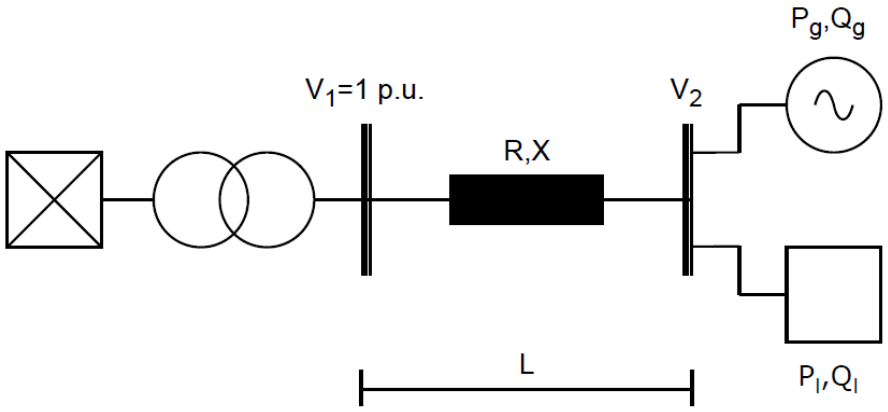

FIGURE 2.1: Example system to show how voltage is influenced by power injections and absorptions.

where index 1 refers to the slack bus, whose voltage level is set to the nominal one ($V_1 = V$), P_g and Q_g are the active/reactive power injections at node 2 (both positive), P_l and Q_l are the absorptions at the same node, R and X are the line resistance and reactance per unit length and L is the line length. Even if Equation (2.1) holds for any voltage level, a LV feeder is going to be considered for this example. This choice stems from two reasons: firstly, LV networks are much more subject to voltage fluctuations than MV and HV ones are. This happens both because of the intrinsic characteristics of the LV lines and because a much higher power injection/absorption is required to destabilise a MV grid. Secondly, the work presented in chapters 3 and 4 is going to be based on the IEEE LV Test Feeder.

In order to show that a power injection from a DER always produces a voltage rise, let us assume that the load is negligible ($P_l = 0$ and $Q_l = 0$), which means that $P_l - P_g < 0$ and $Q_l - Q_g < 0$, so that there is a surplus of power injected at node 2. If we assume that the DERs are PV systems, this situation is likely to happen during the central hours of the day. In that scenario, we obtain equation (2.2) and by setting $\Delta V < 0$, it is possible to solve for R/X while remembering that $P_g = S_g \cdot \cos(\alpha_g)$, $Q_g = S_g \cdot \sin(\alpha_g)$ and $PF_g = \cos(\alpha_g)$. In these equations S_g is the apparent power injection, α_g is the phase angle between the voltage and current signals produced by the PV inverter and PF_g is the associated power factor.

$$\frac{R}{X} > -\frac{Q_g}{P_g} = -\frac{\sin(\arccos(PF_g))}{PF_g} \qquad \Delta V < 0 \tag{2.2}$$

On the contrary, when $P_g = 0$, $Q_g = 0$ and $\Delta V > 0$, which represents the voltage decrease condition at the end of the line, equation (2.3) is obtained

$$\frac{R}{X} > -\frac{Q_l}{P_l} = -\frac{\sin(\arccos(PF_l))}{PF_l} \qquad \Delta V > 0 \tag{2.3}$$

where PF_l is the load power factor.

It is clearly visible that all the positive PF_g values satisfy the inequality in (2.2), since $\frac{R}{X}$ is usually positive in LV networks. Thus an overvoltage always occurs when injecting both active and reactive power into the grid. Dual conclusions can be drawn from (2.3) for the case of a purely passive consumer connected at bus 2. This means that a voltage decrease always happens when both the active and reactive absorbed powers are positive.

In order to quantify the magnitude of the voltage fluctuations, and show that they are influenced by the R/X line ratio and line length L, let us take as an example the R/X ratios for the primary and secondary lines of the IEEE 906 Bus LV Test Feeder. That ratio ranges from 1.30 to 6.20 for primary lines and from 9.43 to 40.10 for secondary ones. The magnitude of the fluctuation of the voltage at bus 2 (V_2) is directly proportional to the modules of P and Q (either consumed or generated), the R/X ratio and the line length L. Moreover, under specific circumstances, e.g. high PF_l and PF_g and high R/X ratios, it is possible to obtain an approximation of the voltage at bus 2, $\hat{V_2}$, as shown in equation (2.4).

$$\hat{V_2} = V_1 - \frac{R \cdot (P_l - P_g)}{V_1} \cdot L \tag{2.4}$$

Note that in general, the relative approximation error, expressed in % as $\Delta E = (1 - \overline{V_2}/V_2) \cdot 100$ is small enough. Under the aforementioned circumstances, it is possible to generalise that for LV lines with a high R/X ratio and both PF_g and PF_l close to unity, the impedance and reactive power effects are mild and can be neglected.

Tables 2.1 and 2.2 justify the conclusions drawn by assuming two line lengths L (0.2 km and 1 km) and different R/X ratios (1.3 and 40). Note how the "modules" of the active and reactive power $|P|$ and $|Q|$ are used in the tables, because the power can be either absorbed (in that case $|P| = P_l$, $|Q| = Q_l$) or injected ($|P| = P_g$, $|Q| = Q_g$). The tables also show the voltage fluctuations at bus 2 (V_2), the associated current variations ΔI normalised by the line ampacity and the value of the aforementioned approximation error ΔE.

It is thus confirmed that the voltage and current fluctuations are higher in magnitude for highly resistive and long lines, such as the ones connecting the LV users to the secondary grid substations. As such, the standard for LV systems EN50160:2010 [11] specifies that the 10-minutes RMS value of the voltage levels should not be over 1.1 p.u. or under

L=0.2 km		Overvoltage			Undervoltage			Overcurrent
|P| [kW]	**|Q|** [kVAr]	$\mathbf{V_2}$ [V]	**V2** [p.u.]	**ΔE** [%]	$\mathbf{V_2}$ [V]	**V2**[**p.u.**]	**ΔE** [%]	**ΔI** [%]
0.00	0.00	240.00	1.00	0.00	240.00	1.00	0.00	0.00
2.00	0.41	240.86	1.00	0.05	239.14	1.00	-0.05	3.97
4.00	0.81	241.71	1.01	0.10	238.29	0.99	-0.10	7.94
6.00	1.22	242.57	1.01	0.14	237.43	0.99	-0.15	11.90
8.00	1.62	243.43	1.01	0.19	236.57	0.99	-0.19	15.87
10.00	2.03	244.28	1.02	0.24	235.72	0.98	-0.24	19.84
L=1 km		Overvoltage			Undervoltage			Overcurrent
|P| [kW]	**|Q|** [kVAr]	$\mathbf{V_2}$ [V]	**V2** [p.u.]	**ΔE** [%]	$\mathbf{V_2}$ [V]	**V2**[**p.u.**]	**ΔE** [%]	**ΔI** [%]
0.0	0.00	240.00	1.00	0.00	240.00	1.00	0.00	0.00
2.0	0.41	240.86	1.00	0.05	239.14	1.00	-0.05	3.97
4.0	0.81	241.71	1.01	0.10	238.29	0.99	-0.10	7.94
6.0	1.22	242.57	1.01	0.14	237.43	0.99	-0.15	11.90
8.0	1.62	243.43	1.01	0.19	236.57	0.99	-0.19	15.87
10.00	2.03	244.28	1.02	0.24	235.72	0.98	-0.24	19.84

TABLE 2.1: Voltage and current fluctuations for a *primary line* of length 0.2 km or 1 km due to power injections or absorptions $|P|$ and $|Q|$: R/X=1.31, Ampacity=210 A.

L=0.2 km		Overvoltage			Undervoltage			Overcurrent
|P| [kW]	**|Q|** [kVAr]	$\mathbf{V_2}$ [V]	**V2** [p.u.]	**ΔE** [%]	$\mathbf{V_2}$ [V]	**V2**[**p.u.**]	**ΔE** [%]	**|ΔI|** [%]
0.00	0.00	240.00	1.00	0.00	240.00	1.00	0.00	0.00
2.00	0.41	246.65	1.03	0.01	233.30	0.97	-0.03	14.88
4.00	0.81	253.30	1.06	0.03	226.61	0.94	-0.07	29.76
6.00	1.22	259.95	1.08	0.04	219.91	0.92	-0.11	44.64
8.00	1.62	266.60	1.11	0.05	213.21	0.89	-0.15	59.52
10.00	2.03	273.25	1.14	0.06	206.52	0.86	-0.19	74.40
L=1 km		Overvoltage			Undervoltage			Overcurrent
|P| [kW]	**|Q|** [kVAr]	$\mathbf{V_2}$ [V]	**V2** [p.u.]	**ΔE** [%]	$\mathbf{V_2}$ [V]	**V2**[**p.u.**]	**ΔE** [%]	**|ΔI|** [%]
0.00	0.00	240.00	1.00	0.00	240.00	1.00	0.00	0.00
2.00	0.41	273.25	1.14	0.06	206.52	0.86	-0.19	14.88
4.00	0.81	306.50	1.28	0.11	173.03	0.72	-0.46	29.76
6.00	1.22	339.75	1.42	0.15	139.55	0.58	-0.86	44.64
8.00	1.62	373.00	1.55	0.18	106.07	0.44	-1.51	59.52
10.00	2.03	406.25	1.69	0.21	72.59	0.30	-2.75	74.40

TABLE 2.2: Voltage and current fluctuations for a *secondary line* of length 0.2 km or 1 km due to power injections or absorptions $|P|$ and $|Q|$: R/X=40, Ampacity=56 A.

0.85 p.u. at any time during the year, and that it should be limited between 0.9 p.u. and 1.1 p.u. for 95% of the time. Thus, particular care should be devoted to ensure that those limits are not exceeded.

2.1.2 Overloading and Losses

If the system in Figure 2.1 is taken as a reference once more, another consequence of a greater power mismatch at bus 2 is the increase in the power and current flowing through the lines. In order to see that, assuming that R/X is sufficiently high (so that the reactance effects are negligible) and that both $PF_g \longrightarrow 1$ and $PF_l \longrightarrow 1$, it is possible to use Ohm's Law to calculate the current increase ΔI associated to the voltage fluctuation ΔV, through Equation (2.5)

$$|\Delta I| = \frac{\Delta V}{R} = \frac{|P| \cdot L}{V_1} \tag{2.5}$$

where $|P|$ is the magnitude of the injected or absorbed power and $|\Delta I|$ is the magnitude of the additional current produced by $|P|$. Overcurrent values, reported in tables 2.2 and 2.1 as a percentage of the lines ampacities (indicated in the captions to the tables), may range from a few % points to about 20% in the case of primary lines, and up to 74% for secondary ones. Reminding Joule's law, linking the power dissipated through a conductor to the current flowing through it, an increase in the current flowing through the conductor produces a quadratic increase in the system losses, thus it is important to avoid lines overloading. The Italian regulation [12] for electric systems with a nominal voltage

lower than 1 kV [12] prescribes that currents should not be higher than 140% of the ampacity of the line. Electric equipment manufacturers may however indicate even stricter limitations to avoid damage to the cables.

2.1.3 Power Quality

Under the generic term of "power quality", it is possible to find different issues affecting electric systems, which can also be caused by DERs.

2.1.3.1 Frequency Stability

A first important one is the *frequency stability*, which depends on the power mismatch between generation and consumption. Dixon [13] proposes equation (2.6) to determine the rate of change of the rotational speed of a synchronous system $\frac{d\omega}{dt}$ in the case of a sudden power mismatch:

$$P_{resp}^{GEN} + P_{non-resp}^{GEN} - P^{LOAD} = 2 \cdot H_{eq} \cdot \omega \cdot \frac{d\omega}{dt} \tag{2.6}$$

where

- P_{resp}^{GEN} represents the aggregated power of "responsive" generators, which automatically change their rotational speed to interact with the power mismatch;
- $P_{non-resp}^{GEN}$ represents the "non-responsive" generators aggregated power, which do not change their speed automatically to restore the frequency;
- P^{LOAD} is the total electric load connected to the grid;
- H_{eq} is an empirically-derived constant calculated as the total system kinetic energy over the nominal apparent power system rating, as in Chapter 3 of [13].

Since the rotational speed ω in stationary conditions must be constant, Equation (2.6) also shows how both an increase/decrease of P^{LOAD} or $P_{non-resp}^{GEN}$ may significantly affect the system frequency, especially in the case of unplanned connection/disconnection events. DERs, such as PV systems and EV stations, are indeed generators and loads which inject/absorb AC power through DC/AC power electronics converters, which do not produce any inertial response in case of frequency fluctuations. Thus, their connection/disconnection or a variation in their power absorption/consumption profiles could pose a threat to system stability. The regulation for synchronous LV networks connected to the MV/HV grid [11] prescribes that deviation of the 10 s average of the fundamental frequency does not exceed $\pm$ 1% for more than 0.5% of the year, and that it never exceeds +4%/-6%.

2.1.3.2 Voltage Unbalance

An uneven distribution of loads and DERs on the single phases of a network could lead to voltage and currents unbalance in the three-phase systems, possibly causing different malfunctions. The most common indicator for voltage unbalance, is the Voltage Unbalance Factor VUF (equation (2.7))

$$VUF[\%] = \frac{V^{NEG}}{V^{POS}} \cdot 100 \tag{2.7}$$

where V^{NEG} and V^{POS} are the 10 minutes RMS values for the negative and positive sequence components of the three-phase AC voltage waveform. The regulation [11] prescribes that 90% of the V^{NEG} values should be within $\pm$2% of V^{POS}, or similarly that $98\% < VUF < 102\%$ for 90% of the time.

2.1.3.3 Harmonics

Since most of the modern DERs are connected to the grid via power converters that represent highly non-linear loads, the harmonic content of the voltage and current waveforms is steadily growing. The most common indicator for the *harmonic content* is the "total harmonic distortion" (THD) coefficient, which is calculated, for example for voltage levels, as in (2.8)

$$THD_V[\%] = \sqrt{\sum_{n=1}^{N} \left(\frac{V_n}{V_1}\right)^2} \cdot 100 \tag{2.8}$$

where V_n is the RMS value of the n-th harmonic voltage, N is the number of harmonics, and V_1 is the RMS harmonic voltage value of fundamental frequency. In power electronic converters, the RMS value of the 3rd, 5th and 7th harmonics can be very large. Thus, they should be limited and properly filtered via passive or active filters, i.e. series or parallel circuits designed to prevent harmonic currents from entering the system. Power transformers are mostly affected by harmonics. Thus, particular care should be placed in mitigating this issues. The regulation around harmonics [11] prescribes that 95% of the 10 min RMS voltage values for the single harmonics $\frac{V_n}{V_1}$ should be lower than specific thresholds based on the harmonic order n, and that THD_V should be less than 8% if n=1,...,40.

2.1.3.4 Flicker

Flicker happens instead due to low voltage magnitude fluctuations with a very short time period, causing variations in lighting intensity of lamps. The main causes of flickering are industrial loads with a fluctuating consumption such as welding machines, mills, arc furnaces and compressors. Several studies tried to determine the effects of flickering on human health, but it was found that it is highly subjective, and a flickering level which causes a headache in one person is harmless to another. Nonetheless, flickering is quantified by "disturbance" curves that depend on both the voltage fluctuation magnitude and the number of flickers per minute. As such, it is possible to distinguish between the short term flicker severity $P_{st,i}$, measured over 10 minutes by flickermeters and the long term one P_{lt}, obtained as in (2.9)

$$P_{lt} = \sqrt[3]{\sum_{i=1}^{12} \frac{P_{st,i}^3}{12}} \tag{2.9}$$

where $P_{st,i}$ is the short-term flicker intensity over the i-th 2-hours interval of the day and P_{lt} is the daily long-term flicker intensity. The existing regulation [11] prescribes that the weekly $P_{lt} < 1$ for 95% of time. A new directive by the EU [14] tackles instead the issue of flickering in the much more widespread LED lights. In that regulation, the limit of 1 is also set for the short term flickering index at full load. That value means that the probability for the user to perceive flickering is 50%.

There is a vast literature regarding the impact of DERs on the electric grid, covering all the aspects that were outlined up to here. In the following, a number of them will be presented and described.

2.1.4 Literature Review on PV Impact

As of now, the concept of "hosting capacity" (HC) and "penetration" of DER are going to be extensively used in the following literature review. HC is used in the literature to define the maximum allowable installed capacity of DERs that does not produce any violation of the specific thresholds prescribed by some regulation. It must be noted, that the HC for voltage violations could be different from the one for the current loading levels, or voltage unbalance. The concept of DER "penetration" instead, is generally defined for PV systems, as in Equation (2.10), i.e.

$$PV_{pen} = \frac{\sum_{m=1}^{M} P_m^{PV}}{\sum_{n=1}^{N} S_n^{LOAD}} \tag{2.10}$$

where P_m^{PV} is the nominal installed capacity of the m-th PV generator on the grid and S_n^{LOAD} is the nominal apparent power of the n-th load on the grid. The definition for EVs is similar, but is less frequently found in the literature. It has to be noted that, even if the penetration is a very easy-to-understand and useful indicator, there are several shortcomings in the specific case of DERs, since most of the times neither PV systems nor EVs absorb their nominal power. Thus, the penetration is not very indicative of the actual production/consumption balance in a system.

A number of examples of how the impacts of PV systems and EV stations on the electric network are analysed and mitigated in the literature is provided in Table 2.3.

Parameter	PV Systems	EV Charging Stations
Voltage Magnitude	[15–46]	[46–59]
Lines Loading	[25, 26, 29, 31, 33–35, 37, 44–46, 58–60]	[46, 48, 49, 51, 54, 57, 61–63]
Transformer Loading	[32, 33, 45, 46, 53, 60]	[46, 50–52, 54, 61]
Losses	[29, 36, 40, 44, 64–67]	[48–50, 57, 68, 69]
Frequency	[70–72] (impact) - [73] (support)	[46, 48, 49, 51, 54, 57, 61–63] (support)
Voltage Unbalance	[22, 23, 36, 42, 44, 46, 60, 64, 65, 67, 74–76]	[46, 57, 63, 69, 77–79]
Harmonics	[30, 44, 58, 59, 80–83]	[77, 84–87]
Voltage Flicker	[25, 39, 88–90]	[87, 91–93]

TABLE 2.3: Review of the literature around PV and EV impact on the grid.

Since the analysis is quite different depending on whether MV or LV systems are considered, in the rest of this Section the related studies will be separately described.

2.1.4.1 PV Impact on MV Feeders

Several Authors analysed and tackled the issue of voltage stability due to the injection of PV power in MV test feeders provided by IEEE. For example, Joshi et al. [40] analysed the IEEE 13-bus feeder, finding that both the voltages and losses are not impacted by PV, and never trespass the MV limits ($\pm$0.1 p.u). The same network was analysed by Emmanuel et al. [65], who calculated the voltage magnitude variation, unbalance, transformer and lines overload and electric losses due to PV units. They found out that overvoltages are the main source of HC limitation. Balamurugan et al. instead [36], focused on the IEEE 34 node MV test feeder and observed that there are specific buses where introducing three-phase PV systems is particularly risky in terms of voltage unbalance. That happens even though both the voltage profile and losses benefit from the introduction of PV systems. Other Authors analysed bigger MV networks, such as Begovic et al. [41], that studied the IEEE 123-bus test feeder and realised that even stochastic PV placement may provide peak load shaving and CO2 emissions reduction. Liu et al. also studied the same network [29] and tested a particle swarm optimisation-based (PSO) network reconfiguration methodology. They found that both the losses and overvoltage issues are eliminated by changing the grid topology, and that the required grid reconfiguration is reduced by smart capacitors and transformer control. Moreover, Ceylan et al. [24] applied tap changing and reactive power control to mitigate the impact of PV systems on the 123-bus grid. They found out that distributed PV generation has a much lower impact on the grid than PV power concentrated on one node only. Finally, Daud et al. [17] analysed several IEEE MV test feeders and observed that both losses and overvoltage issues are minimised when the PV penetration is between 60 and 80%. Over that value, the PV production is unmatched by the load, reverse power flow happens and the aforementioned issues appear.

When real MV grids are instead considered, as Ampofo et al. [35] did, voltage rise is found to be maximum when the PV systems are far from the transformer and the available load consumption is low. Heilscher et al. instead [33] realised that, even if the PV systems are evenly distributed along a MV grid in Germany, their impact on the transformer and lines loading keeps being relevant and severely limits the grid HC. Dhlamini et al. [18] modelled the transmission/distribution networks in the South African region of North Cape and observed that, due to the high solar irradiance in the area, voltage stability is greatly affected by the installation of PV systems. Luthander et al. [32] analysed two feeders in Sweden with increasing levels of PV uptake, up to 100% of the load consumption. Batteries and power curtailment are used to increase the HC while reducing overvoltage, overcurrent and transformer overloading events. Other Authors, like Pormousavi et al. [72] analysed voltage and frequency stability on a typical American MV grid and realised that up to 30% PV penetration can be reached without creating issues. However, the provision of ancillary services is required to keep the frequency under the allowed limits. Feilat et al. [70] instead, analysed the entire national grid from Jordan, and found that the maximum PV HC considering current and voltage limitations is 10% of the total load demand. If frequency is considered instead, the installation of PV and wind power plants can cover 40% of the total demand without any issues. A smaller network composed by 14 buses was analysed by Reno et al. [28], who investigated the extent to which smart inverters with volt-var control could improve the PV HC, showing that up to 100% PV penetration is allowed. A very simple MV network was analysed by Shayani et al. [31], who showed that both overvoltage and overcurrents are a bottleneck to PV HC. The former can moreover be solved by setting the transformer taps to a lower p.u. value, so that the PV generation can grow up to twice the load capacity.

Finally, Navarro et al. [21] analysed a 25-bus system at the interface between the LV and MV grid, and found out that the LV side limits the PV HC, while the MV side is not influenced.

As far as voltage unbalance is concerned, Ding et al. [42] tested capacitor switching on the IEEE 123-bus grid, by maximising the PV HC with a mixed-integer linear programming approach and monitoring the voltage levels, the unbalances and current loading. They found out that, even though a positive impact is detected, the system has to be supported by storage system. On the same topic, Wang et al. [75] analysed the IEEE 13 and 123-bus networks and solved the BESS siting problem with the objective to maximise the use of PV-produced energy. They compared the results with normal HC maximisation methods and highlighted the advantages of the proposed solution. Farmer et al. [51] instead, focused on the lines loading only while analysing a MV grid in Vermont, and observed that both the cables and transformers could be loaded up to 60% more, although in general the expected average increase is around 15%.

Darussalam et al. [71] investigated how PV influences the system frequency in a MV Indonesian grid, and realised that 20% PV penetration is the HC. Other Authors focused on the harmonic injection due to PV. Barutcu et al. [80] for example, analysed how the voltage and current RMS values in three 7, 13 and 25-bus MV systems react to high PV injections in terms of total and single harmonic distortions. They found that when the irradiance is low, the current harmonics limit the HC value, whereas when the irradiance is high, voltage harmonics are more severely affected.

2.1.4.2 PV on LV Feeders

Many Authors showed that LV grids typically suffer more than MV ones from the introduction of PV systems due to larger R/X values and long lines. Aziz et al. [16] for example, showed that if the PV power is concentrated on one LV bus, a PV penetration of 2.5% is enough to destabilise the grid, whereas if the PVs are spread over the grid, the HC value may increase up to 110% PV penetration. Dubey et al. [23] found out that both voltage magnitude and unbalance are affected by the increasing penetration of PV systems, especially when most of the PV capacity is installed far from the transformer. Additionally, increasing the base-load consumption (e.g. power through the transformer when no PV is installed) improves the PV hosting capacity. Haghi et al. [26] instead, compared various techniques to increase the PV hosting capacity of a Californian grid, finding that Volt-VAR is the best technique to avoid PV curtailment due to overvoltage issues. Mohammadi et al. [25] analysed how the LV network protections are affected by PV systems and proposed "smart" ones that reduce the overvoltage, overcurrent and flicker events. Smith et al. [38] instead, observed that the feeder they analysed already suffers from both overvoltage and voltage unbalance issues at the furthermost buses from the transformer for a 20% PV penetration. Tang et al. [22] showed once more that smart inverters with volt-VAR capabilities help in reducing the voltage magnitude variations and unbalances, improving the PV HC from a 140-200 % to a 250-270 % PV penetration. Tevar-Bartolomé et al. [19] analysed the cost of upgrading a very vast MV/LV network of 80000 customers. Up to 30% PV penetration, no grid upgrading is required, while above that value, the upgrade costs increase quadratically with the installed PV capacity. Moreover, 30% PV penetration is the optimal value that minimises the losses and does not involve any economic expenditure for additional operation and maintenance. Stetz et al. [45] analysed a LV network in Germany where smart inverter capabilities, on-load tap changers and grid reinforcements are used to mitigate the voltage, line currents and transformer loading issues. They realised that reactive power support from smart PV inverters is the most profitable and efficient strategy. Torquato et al. [60] instead, performed a Montecarlo analysis and found that overvoltages and voltage unbalances are the most restrictive limitations to PV HC, which can be accurately estimated also by selecting a limited amount of feeders. Hu et al. [64] implemented inverter reactive power consumption and on-load tap changing to improve the PV HC from 40 to 70% in a Danish feeder. Interestingly, both the techniques improve the voltage profile, but could create voltage unbalance and slightly increase the losses. Finally, Rahman et al. [74] investigated voltage magnitude fluctuations and unbalance on an Australian network and showed that demand-side management (DSM) and on-load tap changing can be optimally controlled by using a modified PSO algorithms to minimise the upgrading costs.

Finally, some Authors studied a very common example of European LV Grid, which is going to be considered in this thesis too: the IEEE 906 Bus LV Test Feeder. Indeed, Gonzalez-Moran et al. [20] used this grid model together with irradiance data from the north of Spain, finding that coordination between the PV systems is required to avoid overvoltages and that the installed PV capacity needs to be tailored to the load profile of each user. Kitworawut et al. [44] instead, studied how voltage magnitude, unbalance, lines and transformer overloads, as well as voltage harmonics

are impacted by PV production. They found out that voltage rise and lines loading are the limiting factors for HC, which is around 150% PV penetration. Voltage unbalance, harmonics and transformer loading are not outside of the regulatory limits, but they increase as the PV penetration does. The electric losses instead, start to increase when the PV penetration exceeds 50%.

Some other Authors focused their efforts on voltage unbalance issues on LV grids instead, such as Schwanz et al. [67], who analysed two Swedish and one German LV network, finding that PV redistribution and size reduction is key to reduce the unbalance. The introduction of 6 kW PV for each phase produces around 1% unbalance. Moreover, Su et al. [76] analysed how reactive power support from small-scale PV inverters can help reducing the voltage unbalance in Perth, Australia, and observed that it has a very positive impact.

2.1.4.3 PV and Power Quality

A number of Authors analysed the problem of harmonics injection from PV generators. Deng et al. [83] realised that a simple LV grid can be impacted by a high PV penetration due to multi-resonance peaks at the point of common coupling of each PV system. Those peaks can be mitigated by passive damping resistors. Hu et al. [82] instead, studied how the resonance of LCL filters for PV systems could affect the additional harmonic content in a North American power system. They found that the harmonic content reduction far outweighs the introduction produced by the filters. Sakar et al. in both [58] and [59], analysed how introducing PV system impacts the voltage levels, current loading and single/total voltage and current harmonic distortion levels. They also introduced two new optimised filters that maximise the PV HC and outperform traditional THD minimising ones. Finally, flickering issues were analysed by some Authors. For example, Ari et al. [88] showed that a LV grid in Nevada does not experience violations of the voltage flicker limits due to PV power fluctuations, provided that the adopted time-step is small enough to capture the irradiance fluctuations. Arshad et al.[90] instead, analysed a number of Finnish LV grids and observed that while urban areas do not suffer from flicker, even when the PV penetration is high, the rural ones do. They also propose an active/reactive inverter-based power profile compensation to reduce those issues. Finally, Ferdowsi [89] et al. analysed a LV grid from Lousiana and realised that flickering issues start arising when 10% of the customers install 7 kW PV systems, and become severe when a share of 30% is reached.

2.1.5 Literature Review on EV Impact

A vast literature exists regarding the impact of charging plug-in hybrid electric vehicles (PHEVs) and battery electric vehicles (BEVs) on LV and MV grids. What follows is a review of some significant papers concerning the results of EV HC on the grids.

2.1.5.1 EVs on MV Feeders

Dulau et al. [48] investigated the IEEE 13-bus MV system, finding that the lines loading, losses and voltage drops are heavily impacted by the EV penetration, especially in fast EV charging scenarios. Lopes et al. instead [62], found that both voltage levels and line congestions on a grid in Portugal are greatly impacted by large scale plug-in electric vehicle (PHEV) integration and that time-of-use tariffs produce a mild effect on the grid HC value. Johansson et al. [54] extended their analysis to a large-scale EV integration plan for a Swedish LV-MV network and showed that 50% EV penetration is HC for undervoltages, overcurrents and transformer overloads. If the charging power increases, the maximum allowed penetration decreases to 25%, with the transformers being the most vulnerable elements in the system. Masoum et al. [50] instead, analysed a LV/MV distribution feeder with a large number of PHEV charging stations. They found out that, when 80% PHEV penetration is reached, the transformers are impacted by both slow and fast charging, whereas at 20% those impacts are almost negligible. Voltages are impacted too, with deviations up to -0.14 p.u. at 20% and 0.43 p.u at 80 % PEV penetrations respectively. Losses generally increase alongside the PHEV penetration, and generally occur when the number of charging events is higher. Finally, Schlee et al. [53] investigated the impact of large scale PHEV penetration on a LV/MV distribution feeder from Idaho, and observed that the maximum undervoltage magnitude is around -0.14 p.u and that transformer loading increases by up to 8%. Both issues can be efficiently handled by smart scheduling the charging sessions based on time-of-use tariffs.

2.1.5.2 EVs on LV Feeders

Some Authors analysed the impact of EVs on LV feeders instead. Dubey et al. [55], for example, investigated the impact of EV charging on the voltage levels of a very large LV grid, and realised that the voltage drop is directly proportional to the distance from the transformer. They also found that increasing the size of closely connected EV chargers greatly impacts the voltage drops, and that wires with a higher ampacity (primary feeders) are less affected than the others. Kelly et al. [52] showed that transformers are the most impacted element in the system, as peak EV charging happens almost always at the same time of the day in both the urban and rural analysed LV feeders. Leemput et al. [56] analysed a Flemish LV feeder instead, finding that smart charging strategies, such as voltage droop control, reduce the minimum voltage levels but do not improve the overall grid performance enough to respect existing regulation. The combination of peak shaving and voltage droop control instead, provides the best results as it avoids grid reinforcement at all. Islam et al. [63] analysed coordinated EV charging, finding out that the voltage unbalances are solved, while the current unbalance issues are greatly improved. The voltage levels issues instead, are only marginally solved. Al Essa et al. [57] analysed a generic UK LV network and found out that voltage unbalance and magnitude fluctuations are the most restrictive limitations to HC, whereas lines and transformers are significantly impacted, but without overcoming the threshold levels. Additionally, losses are increased by EV deployment. Finally, Putrus et al. [77] analysed a typical UK LV grid and observed that voltage magnitude and current unbalance are impacted above 20% EV penetration, whereas harmonics are significantly impacted only at much higher penetration levels.

The issue of transformer overloading was analysed by Taylor et al. [61], who presented preliminary results from a study by EPRI in the US. They realised that the transformer close to the customers are the most influenced by PHEVs, since they do not benefit from the aggregation of EV profiles, which typically smooths out the power curve. Temporal and spatial diversity of the PHEVs, in general, reduces the overloads frequency by 2-8%. About the topic of current and voltage unbalance instead, Islam et al. [69] investigated a MV/LV grid from Queensland, Australia, proposing a controller to reduce the EV impact on the system by performing coordinated charging. They found that the application of the controller to the most impacted set of nodes is the most efficient to increase the HC value. Klayklueng et al. [79] showed that if the EV stations are concentrated on one phase only, the voltage unbalance may increase up to thrice. Losses are generally increased by EV connection too, as Pieltain-Fernandez et al. show [68]. Indeed, losses at off-peak consumption moments of the day can increase by 14%-40% due to simultaneous charging from all EV stations.

2.1.5.3 EVs and Power Quality

As far as the system frequency is concerned, Dechanupaprittha et al. [94] analysed micro-grid frequency control when EVs are connected, and realised that charging scheduling optimisation is required to keep the frequency close to the nominal level. Banol-Arias instead [95], analysed the possibility of rewarding EV owners for their participation in frequency regulation, and found that the EVs provide an operational reserve for grid stabilisation. Finally, model predictive control [96, 97] and adaptive optimal control [98] were used to reduce the EVs load impact on grid frequency and provide primary frequency regulation with very positive results. Since the expectations of the EV owners need to be included, as explained in [99, 100], simulations were performed and proved that the optimisation models do not influence the quality of service for the users. With regards to harmonic content, instead, Gomez et al. [84] studied how the transformer lifetime is impacted by the current THD in a system with EV chargers, and showed that the THD should be limited to 25-30% to achieve a reasonable transformer life expectancy. Flickering from EV chargers is analysed in [93] on the MV 4-bus IEEE test system. The Authors found out that fast charging EV stations from 150 to 350 kW violate the voltage flicker limitations, even though the results depend on the adopted time-step. Basta et al. [91] analysed the MV IEEE 34 bus system in terms of harmonic distortion and voltage flicker, finding out that the order of the harmonics heavily depends on the type of charger and manufacturer. Regarding flicker instead, the long-term effects are more important than the short term ones, which are within an acceptable range. Finally, Blavette et al. [92] analysed voltage flicker at the connection of EV charging stations, and observed that it is important to avoid saturating the grid with an EV capacity close to the pre-connection base-load. Also, even though the simultaneous introduction of PV systems could reduce the congestion levels due to EVs, the higher allowable EV penetration could in-turn increase voltage flicker issues.

2.1.6 Review on Combined PV and EV Impact

Recently, various Authors started analysing the combined impact of PV and EV on electric systems. Raouf et al. for example [46] analysed to which extent BESS deployment can mitigate both the impact of EV charging stations and PV systems on a LV network from Ireland. Results show that voltage unbalance is much more impacted than voltage magnitude. Finally, the voltage magnitude, together with cables loading and transformer power, are impacted much faster by an increase in EV rather than PV capacity. Carollo et al. [37] analysed an extensive real LV feeder with both EV and PV, and realised that the PV overvoltage issues are just mildly mitigated in very high EV uptake scenarios. Gabdullin et al. [15] analysed a real LV test feeder from Malta and found that if the PV penetration is under 30%, none of the analysed feeders show any overvoltage issue. Moreover, uncontrolled EVs charging does not produce any PV HC increase. Finally, Fachrizal et al. [47] analysed the combined PV-EV HC on the IEEE 906 Bus LV Test Feeder, finding that smart EV charging and PV curtailment are the most effective ways of minimising the net-load peaks, respectively leading to a 20% and a 40% increase in the number of users equipped with a PV system or an EV station.

In the following sections, techniques to improve the combined PV/EV HC making use of Energy Storage Systems (ESSs) and smart vehicle-to-grid (V2G) charging algorithms are going to be showcased.

2.2 PV Systems Impact Mitigation

There are many types of stationary ESSs that can be used to mitigate the impact of DERs in general, and more specifically of PV systems and EV stations. The most important parameters that have to be checked when choosing which solution to use are the energy and power density, lifetime, response time, round-trip efficiency and cost. A small review of the most relevant ones is going to be henceforth presented.

2.2.1 Types of ESSs

The stationary ESSs are roughly divided in two categories, as reported by various Authors [101, 102]: the *mechanical* and *electro-chemical* ones.

Among *mechanical* storage devices, it is possible to find machines that use heat, water or air with compressors, turbines and similar devices to store the electricity. For example, compressed air systems store the electricity by compressing air and then releases it by expansion. Pumped hydro instead, stores it by pumping water to a higher altitude, then releases it by running a turbine while the water flows back to a lower stage. Liquid air storage uses electricity to cool air until it liquefies, and then brings the liquid back to a gas, which is then used to run a turbine and produce electricity. Thermal and pumped thermal energy storage instead use a heat pump (HP) to store energy inside a medium like gravel or water, then gets it back with any heat engine used to run a turbine to produce electricity. Flywheels store the electricity as kinetic energy and release it by working as a traditional generator *Electro-chemical* storage devices instead store electricity in the chemical reactions between the acids in the batteries themselves, and examples of that are Li-Ion and Redox Flow Batteries. Super capacitors are also included in this category, and store energy through the electric field created between two metal plates which are separated by a dielectric medium. All of the mechanical methodologies generally have longer lifetimes (25–50 years), lower energy ($< 80\ \mathrm{kW\,m^{-3}}$) and power ($< 2\ \mathrm{kW\,m^{-3}}$) densities, and lower round-trip efficiencies ($< 80\%$) than Li-Ion batteries. Thermal energy storage devices are the exception to that rule, having much higher power and energy density, but rather low minimum efficiencies (45-75%). Flywheels instead, have a very short response time and high power density (1000-2000 $\mathrm{kW\,m^{-3}}$), but are still extremely expensive compared to Li-Ion batteries. Among the electro-chemical ESSs instead, Redox Flow Batteries have much longer lifetimes than Li-Ion ones, but fall short in terms of energy/power densities and round-trip efficiencies. Supercapacitors instead have the highest power density of all ESSs, but a much lower energy density than Li-Ion batteries (same level as Redox-Flow ones). Moreover, they generally are still very expensive.

Since both power and energy densities are required for PV energy storage and due to their recent cost drop, Li-Ion batteries are the most widespread and mature storage technology. Thus Li-Ion batteries, henceforth dubbed as BESS, are the only type of ESS which is going to be considered.

2.2.2 BESS sizing

As introduced in Chapter 1, in order to support DER generation on a LV grid, the BESSs need to be properly sized and controlled. The analysis of the literature highlights three different, but equally important, aspects for BESS sizing: the *input modelling*, the *BESS control* and the *sizing algorithm*.

2.2.2.1 Input Profiles Modelling

Since BESSs sizing results are only as good as the modelling of the input profiles is, the choice regarding how the input data to the sizing algorithms are modelled is vital. Two categories can be defined:

- *Deterministic Modelling*: the input profiles are obtained through one extensive measurement campaign or field trials, and no statistic modelling is performed.
- *Probabilistic Modelling*: stochastic distributions are used to describe the input load and production profiles or abstract representative profiles from several measurement campaigns.

In *deterministic* modelling, the input data is not statistically processed to be as representative as possible of the daily or seasonal behaviour of a system. Thus, it requires no pre-processing, and more faithfully represent the reality of the specific electric system the measurement campaign considered.

In *probabilistic* methods instead, the input data should statistically represent the consumption and production profiles on the analysed grids, thus the sizing results are more easily generalised for similar networks and depend way less on the specific analysed case study. However, the results of the sizing algorithm for one specific case study may not be as accurate as in the case where the modelling was deterministic, due to the inevitable degree of randomness in the input profiles.

Both of these ways to model the input data are used to create load/production profiles, which are then fed into sizing algorithms to obtain the battery capacity.

2.2.2.2 Sizing Algorithm Classification

Another important aspect is the sizing algorithm, which, as reported in [103, 104], can be classified in two categories:

- *Analytic:* a set of different power system configurations are evaluated against an ESS capacity change, while all the other input profiles generally stay the same. The best solution is showed by sorting a performance indicator or objective function.
- *Search-Based:* an optimal solution is found with mathematical or heuristic optimisation methodologies, by minimising or maximising a specific objective function.

The first type, *analytic* methods, are generally not very time-efficient if the BESS capacity increase for each scenario is small, since a lot of possibilities need to be analysed. These algorithms are, essentially performing a "sensitivity analysis" on a set of parameters which change due to the BESS size increase. The results of the sizing procedure are evaluated at every iteration and the "best" solution is chosen as the optimal one.

Whenever the computational burden of analysing such a wide array of network configurations is too high, however, *search-based methods* are preferred. In those algorithms an optimisation algorithm is used to minimise some objective function, either by making use of mathematical optimisation algorithms or heuristic ones:

- *Mathematical:* the search is guided by means of a *mathematical optimisation algorithm* that minimises/maximises a particular objective function. Those algorithms rely on mature mathematical optimisation algorithms such as linear or quadratic programming that converge to optimal solutions. The range of objective functions that can be represented is however limited to the ones that can be mathematically represented as a function of the decision variables.
- *Heuristic:* the search is guided by *heuristic algorithms* that mimic naturally existing behaviours to find an optimal path to the objective. An example could be copying how insects fly in a swarm or bees move inside a colony.

Methodology	Pros	Cons	Examples
Analytic	• Easier to understand • Very flexible in all simulation environments • Provides clear and stable outputs	• Very dependent on the choice of scenarios • Generally computationally intensive • May miss global optimum if scenarios are not carefully chosen	[105–108] [109–113]
Search-Based - Mathematical	• Based on stable mathematical methods • Fast and robust if problem is linear • Usually able to reach global optimum	• Explicit mathematic representation is required (no hybrid KPIs) • Computational burden increases with problem complexity • May require complex linearization techniques to be solved	[114–117]
Search-Based - Heuristic	• No complex mathematical representation • Widely applicable to all sorts of sizing problems	• Less stable/reliable than mathematical optimisation for linear problems • May miss global optimum	[105, 118–121]
Hybrid	• No high computational resources requirement • Combines strong points of different methods	• Complexity increases and easiness of results interpretation decreases	[122–124]

TABLE 2.4: Pros and cons of different BESS sizing methodologies, along with some examples related to PV.

These methods allow for a very wide range of objective functions to be minimised/maximised and act as "sorting" algorithms that find the optimal search direction. Those algorithms generally reduce the computational time requirements of the mathematical ones and allow for the minimisation/maximisation of multiple objective functions at the same time, but are not guaranteed to always reach the global optimum.

Finally, hybrid methods combine the best features of the other methodologies, for example algorithms operating on different stages that perform a mathematical optimisation of one parameter, then use it as the input to a sensitivity analysis or a heuristic search-based method.

It has to be noted that the "search-based" sizing algorithms could also not require a BESS control, because they are also capable of scheduling the BESS to achieve an optimisation objective. The analytic ones instead, usually simulate a number of scenarios and then evaluate the objective function. Thus, they almost always need a BESS control to optimise the instantaneous charge/discharge and achieve a global, usually sub-optimal, value of the objective function.

Tables 2.4 details the main pros and cons of each sizing method and gives some specific examples of how they were used in the literature for PV-related BESS sizing. In the following, those examples are going to be shortly described.

Among the *Analytic* methods, Nazaripouya et al. [106] minimised the total BESS capacity and solved the siting problem for a number of BESS placed on the IEEE MV 14-bus test feeder. They regulate the active and reactive power flows by applying inverter controls to reduce the overvoltage issues. Ru et al. [107] instead, analysed how BESSs influence a single user yearly saving thanks to the PV-related self-sufficiency. Their approach tries to find a critical BESS capacity threshold over which the savings due to the installation of storage systems are null, and the results show that between 9.4 and 16 kWh per user is the most appropriate BESS size range. Yang et al. [108] minimised the system costs by deploying BESS systems on a MV test feeder with high PV penetration. They found out that the BESS costs are still too high to ensure the payback time is reached before the BESS end-of-life. The same results are obtained by Zheng et al. [105], who analysed the IEEE 14-bus test feeder instead. Yue et al. [125] performed BESS sizing on a test 68-bus feeder where 35% of the traditional generation is replaced by PV systems. By deploying a Monte-Carlo approach, they observed that, in order to address the frequency issues arising from replacing generators with PV systems, a BESS capacity from 53 MWh to 16 GWh is required. Cervone et al. [123], paired a Markov Chains stochastic approach for input data creation to a deterministic optimisation to size the BESS for a PV-powered grid. They realised that in this particular case study, lead-acid BESS achieve a payback period of 8 years while the costs of Li-ion ones are too high to be considered yet. In Long et al. [126], the Authors propose a centralised BESS control algorithm to maximise the district-level self sufficiency of a community of 100 grid users spread over a vast LV network. The Authors show that a reduction in the electricity costs up to 30% is achievable, along with an increase in the self-consumption values by 10-30% and self-sufficiency by 20%. Moreover, the more users participate in district electricity trading, the more the BESS size tends to reduce. As a consequence, a self-consumption value of 80% requires each user to install a 3 kWh BESS instead of a 10 kWh one. Another example is found in Rodrigues et al. [127], where a centralised energy sharing BESS control algorithm was applied to a university campus system to understand which is the most economically profitable BESS ownership scenario. When a centralised BESS control is applied, the model where the users purchase the BESSs has the lowest payback period, provided the initial investment is not too high for them. The scenario where a company purchases the BESSs instead, is only profitable to attract the users, since it has a longer payback period for the company but requires no initial user investment. In both these examples, the BESSs are centrally controlled by a company, thus the charging/discharging can be "coordinated" and provide the highest benefits. As such, the classification splitting the BESS controls in "decentralised" and "centralised" is very important, so in Section 2.2.2.3, the main differences between these two categories are going to be presented.

Some of the *search-based* methods rely on *heuristic* algorithms to minimise or maximise some particular objective function. Shang et al. [121] for example, used a PSO algorithm to simultaneously minimise dispatch costs and lower the cost of electricity in a LV grid in Singapore. The Authors showed that, as the renewable energy penetration covers more and more of the total electricity demand, the cost of electricity decreases from 0.26 to 0.18 $/kWh. Ai et al. [118] instead, make use of a Binary Firefly Algorithm to solve the BESS siting/sizing problem in the IEEE 69-bus MV test feeder, in order to minimise the overvoltage events due to the installation of a large 3.66 MW PV generator at one bus. They also report that the overvoltage events are neutralised by the BESSs. Babacan et al. [120] used a genetic algorithm to solve the BESSs sizing/siting problem on the IEEE 8500-Node test feeder. They observed that the installed BESS capacity increase with the PV penetration is sub-linear and the higher the installation costs, the lower the installed capacity, as the nodes least affected by PV will not be supported anymore. Finally, if only one centralised BESS is installed, the scale-economy allows for a higher total installed BESS capacity. Saboori et al. [119] analysed how the profits of an electric distribution company managing a MV system can be maximised by optimally sizing and managing BESSs with a PSO algorithm. It is shown how a 60% annual profit increase can be obtained when PV and BESSs are properly sized and coordinated, whereas when there is no storage capacity, a 45% increase only is reached. If there is no PV instead, the increase stops at 37%. Zheng et al [105] tested how a fuzzy-programming based PSO can be used to minimise the Distribution System Operator (DSO) system costs on the IEEE 15-bus test feeder. They realised that, in this specific case study, Li-ion batteries are better than lead-acid ones, and that the best solution is to place the BESSs at the PV systems' location, a solution requiring the installation of a BESS nominal power equal to 30% of the PV capacity only.

Some other search-based methods rely on *mathematical* optimisation techniques. Fortenbacher et al. [116] proposes an optimal power flow approach to size the BESSs in a test grid from CIGRE with a high PV penetration. The installed PV systems in fact, produce up to 100% of the load consumption, and decentralised BESS control results as the most profitable solution since it prevents PV curtailment.ù Johnson et al. [115] instead, studied a real UK LV test feeder, and optimised the BESS size by means of Mixed-Integer Linear Programming to control active and reactive BESS exchanges. In this case study, the authors found that BESSs are not economically as viable as traditional grid reinforcement techniques. Nick et al. [114], investigated how BESSs can perform grid support in terms of voltage, currents and losses in the IEEE 34-bus MV system. By adopting a mixed-integer cone programming approach, they showed BESSs efficiently eliminate line congestion and load curtailment, mitigate overvoltages and minimise the electricity cost. Nick et al. [117] analysed a larger MV system too with a total connected PV capacity of 5 MW and solved the sizing/siting problem by using an alternating direction method of multipliers algorithm. They found out that compared to the work in [114], the simulation is much faster. Finally, Dragicevic et al. [124] paired a robust optimisation model for PV uncertainty to a search-based method based on mixed-integer linear programming to minimise the systems cost, considering battery degradation as well. They observed that traditional lead-acid batteries are not economically as viable as Li-ion ones due to their higher replacement frequency.

2.2.2.3 Centralised vs. Decentralised BESS Controls

ESSs in general, but more specifically BESSs try to mitigate the lack of contemporaneity between the PV production and the load consumption. As such, a control algorithm is usually required to regulate the power exchanged with the battery. A typical situation is shown in Figure 2.2, where the PV production (P_{PV}) is mostly available from 08:00 to 17:00, whereas the consumption (P_{LOAD}) is concentrated in the 06:00-08:00 and 18:00-21:00 intervals.

This active power mismatch is visible in the profile of the power exchanged with the grid $P_{NET} = P_{LOAD} - P_{PV}$, which is negative during overproduction hours and positive for underproduction. This issues can be smoothed by charging or discharging the battery (P_{BESS}), in order to smooth the P_{NET} curve to $P_{NET} + P_{BESS}$, Simultaneously, the battery state-of-charge (SOC_{BESS}) profile will reflect the injected/absorbed power. Summing up, the batteries are charged when there is a surplus of PV generation E_{PV} and discharged when the PV production is not enough to cover the load demand E_{LOAD}, in order to minimise the amount of energy exchanged with the grid E_{NET}. Even if both Decentralised and Centralised charging algorithms follow the same generic BESS principle, they generally select grid-level or single-user level objective functions to optimise.

For example, centralised controls require a "coordinator", an entity that receives information about the state of the storage devices and instructs them on how to efficiently use their capacity to achieve a global optimal value of some

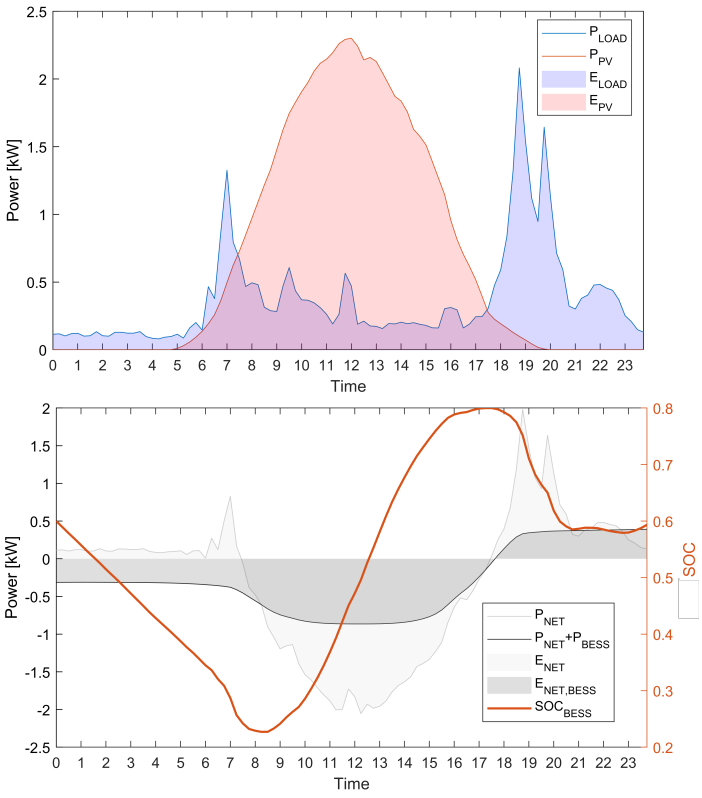

FIGURE 2.2: Working principle of a stationary storage system to increase the exploitation of the PV-produced energy.

objective function. As such, in Figure 2.3 the effects of *centralised* battery charging strategies on the aggregated net power of an LV/MV transformer, are compared to the effects of *decentralised* charging.

Since this Figure considers a "grid-level" objective function, i.e. the batteries are used to minimise the dependence of the *entire* network on the main grid, it can be easily seen that the centralised algorithm outperforms the decentralised one. In fact, the latter makes a less efficient use of the available installed capacity by only optimising user-level self sufficiency. The results are confirmed by the net-power P_{NET} curve in figure 2.3b, which is only smoothed when the batteries are centrally coordinated ($P_{NET} + P_{BESS}$).

If instead, the disaggregated net-power is plotted, which means considering the net load P_{NET} of any of the single users instead of the MV/LV transformer, the situation showed in Figure 2.3 changes to the one displayed in Figure 2.4.

It is clearly visible that now, the P_{NET} curve is smoothed only in Figure 2.4a since the centralised coordination shown in Figure 2.4b charges and discharges the battery following a control policy that considers the entire network. However, this is clearly not beneficial to optimise the single-user self sufficiency.

Summing the whole BESS sizing process up, Figure 2.5 shows how these elements relate to each other.

2.3 EV Stations Impact Mitigation

Among the different solutions to reduce the impacts of EV charging on the grid, the most promising one is the V2G control policy, which can either be applied as unidirectional (also called G2V) or bidirectional (also dubbed V2G). The latter is harder to implement, as it requires modern power converters to charge and discharge the EV battery based on the supply-demand requirements (check Figure 2.6).

The possibility of not only "smart charging" the EV, but also "smart discharging" based on the grid requirements, allows the bi-directional V2G to provide an additional range of grid services, as shown in Table 2.5.

The V2G algorithms can be classified based on the methodology they adopt, and in the following a review of the literature is presented.

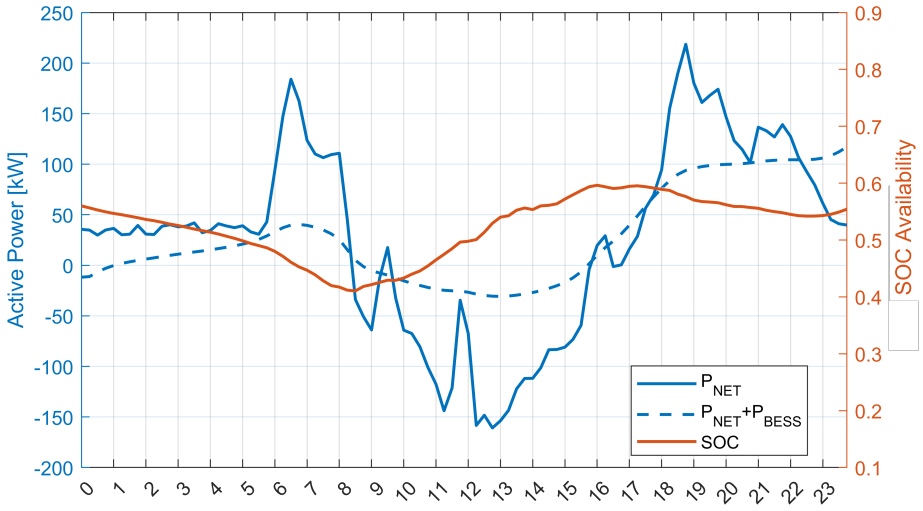

(A) Decentralised

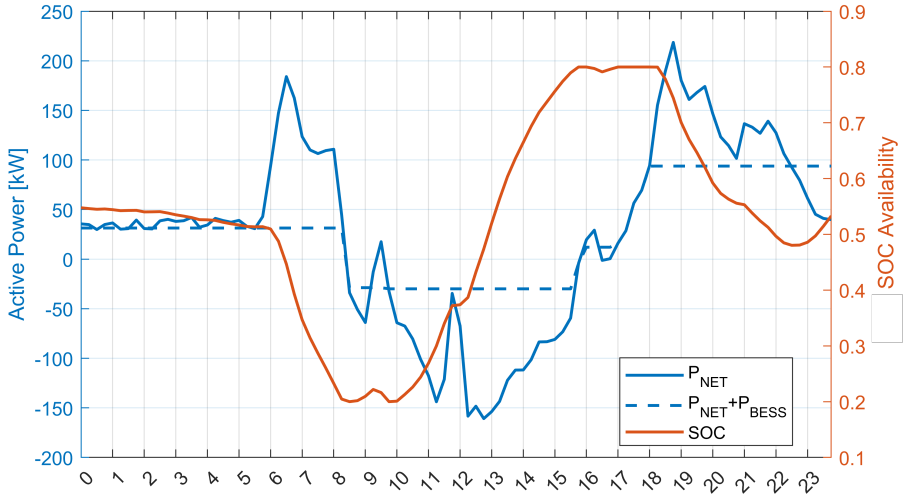

(B) Centralised

FIGURE 2.3: Net power flow P_{NET} across a LV/MV transformer with and without BESS controls for the same total installed storage capacity on the grid.

	Unidirectional	**Bidirectional**
Name	G2V	G2V+V2G
Complexity	Lower	Higher
Social Barrier	Lower	Higher
Battery Degradation	Lower	Higher
Required	• Communication Infrastructure	• Communication Infrastructure • Bidirectional Inverter
Services	• Frequency regulation • Spinning Reserve • Voltage Regulation • Load Shifting	• Frequency regulation • Spinning Reserve • Voltage Regulation • Demand Response • Peak Shaving • RES Integration • Harmonic Filtering

TABLE 2.5: Comparison between uni and bi-directional EV charging.

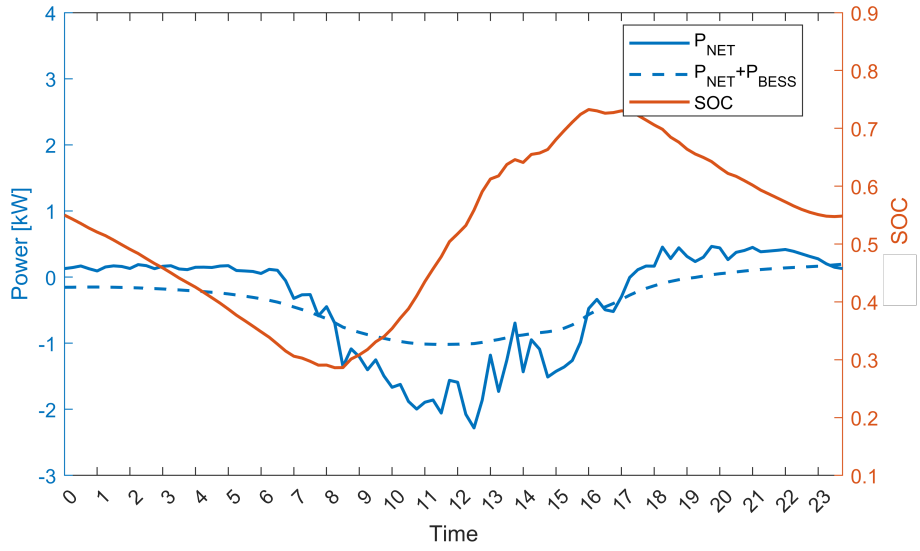

(A) Decentralised

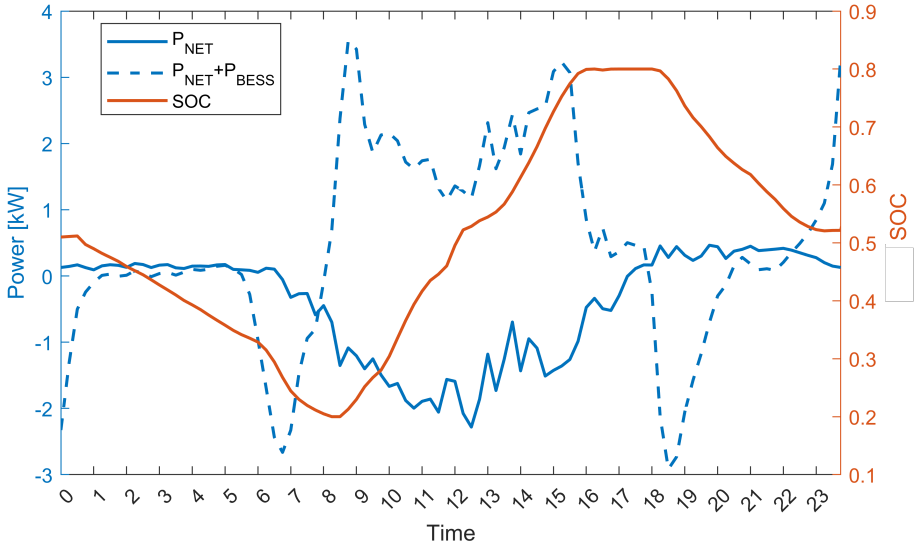

(B) Centralised

FIGURE 2.4: Net power flow P_{NET} of a single user with and without centralised or decentralised BESS controls for the same total installed storage capacity on the grid.

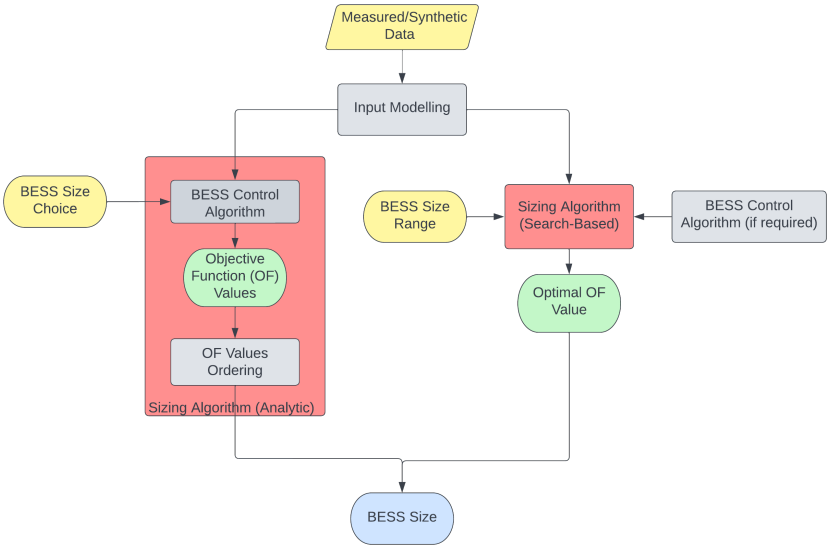

FIGURE 2.5: Analytic vs. Search-Based BESS sizing as most commonly find in the literature.

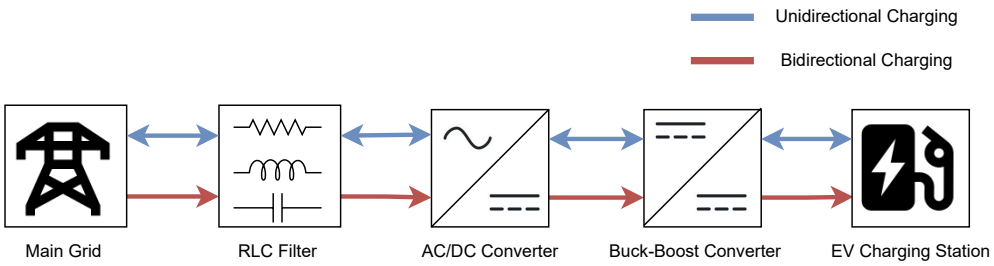

FIGURE 2.6: EV connection schemes for uni and bi-directional V2G.

2.3.1 Review on V2G Methodologies

V2G charging algorithms can be roughly classified in three categories: *analytic*, *heuristic* and *model predictive controls*.

- *Analytic* methods are guaranteed to converge to a global optimum of some selected objective function. They are based on mature optimisation techniques, but are generally tied to the representation of the optimisation problem in mathematical terms.
- *Heuristic* methods reduce the number of solutions to analyse and generally do not require complex mathematical formulations. They allow for an arbitrary number of objective functions but could get stuck in locally optimal minima/maxima.
- *Model predictive* techniques rely on controls based on the production vs. consumption mismatch forecasting. Generally paired to traditional analytical techniques, they do not assume a perfect forecast of the network conditions in the future.

Some examples are presented in Table 2.6, and will hereafter be shortly described.

Among the *analytic methods*, linear programming ones are generally deployed to minimise objective functions that are a linear combination of the decision variables. For example, some Authors minimise the EV charging costs [128–130] or maximise the normalised PV utilisation [131]. Another type of optimisation algorithm that is usually deployed to speed up the simulations is mixed-integer linear programming, which constrain some decision variables to be integers and applied linear programming. Papers that use that methodology usually minimise the charging costs [132] or the overall system costs [133, 134]. Other aspects may involve maximising PV utilisation, as in [135], and minimising frequency deviation, as performed by Kaur et al. [136]. Whenever the objective algorithm is not a linear combination of the decision variables, non-linear programming methods have to be used. An example of that is the reduction of the net-load profile variance at the secondary substation transformer, as performed by Ioakimidis et al [137], or the minimisation of battery ageing, as in [138, 139]. A particular type of non-linear optimisation is quadratic programming, which can be, for instance, aimed at minimising the net-load variance of a power profile, as in [140–143]. Sometimes, quadratic programming is used because it allows for the inclusion of a linear term too, as performed by Palmiotto et al. [144] who also include the minimisation of system costs in the problem. Again, whenever speed is essential, mixed-integer quadratic programming algorithms are used, for example to maximise PV utilisation [145]. Sometimes, optimisation problems can be represented as sub-problems which are easier to analyse and solve. Since a relation between the solutions of the sub-problems and the main problem persists, it is possible to break the big problem down, as Dynamic Programming approaches do. Some examples of that are shown in [146–148].

Among the variety of *heuristic* approaches, oftentimes mimicking natural behaviours to sort and select the solutions of an optimisation problem, one of the most common is Particle Swarm Optimisation. For example, some authors [149–156] use it for V2G optimisation in a number of situations, ranging from the classic maximisation of the use of PV-produced energy to the minimisation of system costs and net-load variance at the same time. Artificial Bee, Ant Colony optimisations and Genetic Algorithms are also used to minimise charging costs [157], minimise users' waiting time at the charging station [158, 159] and minimise the net-load profile variance [160]. An additional benefit of heuristic optimisation algorithms is that the number of optimised objective functions is arbitrary, even if some limitations persist due to computational requirements.

Model predictive controls provide a more realistic view of the algorithms performance than deterministic or heuristic methods, especially if they need to be implemented on real devices. Among the typical optimisation objectives based on model-predictive control, it is possible to find the minimisation of both the total system costs [161, 162] and the charging costs [163–165], the maximisation of the benefit for the users' aggregator [166], the minimisation of the peak net-load demand [167, 168] and the maximisation of the PV utilisation [169].

Finally, it has to be noted that all of these algorithms can be found either in a "centralised" or "decentralised" form, which is an additional layer of classification in the V2G algorithms. Table 2.6 details this particular aspect for each of the reviewed papers. The main methodological differences will be detailed in the following Section.

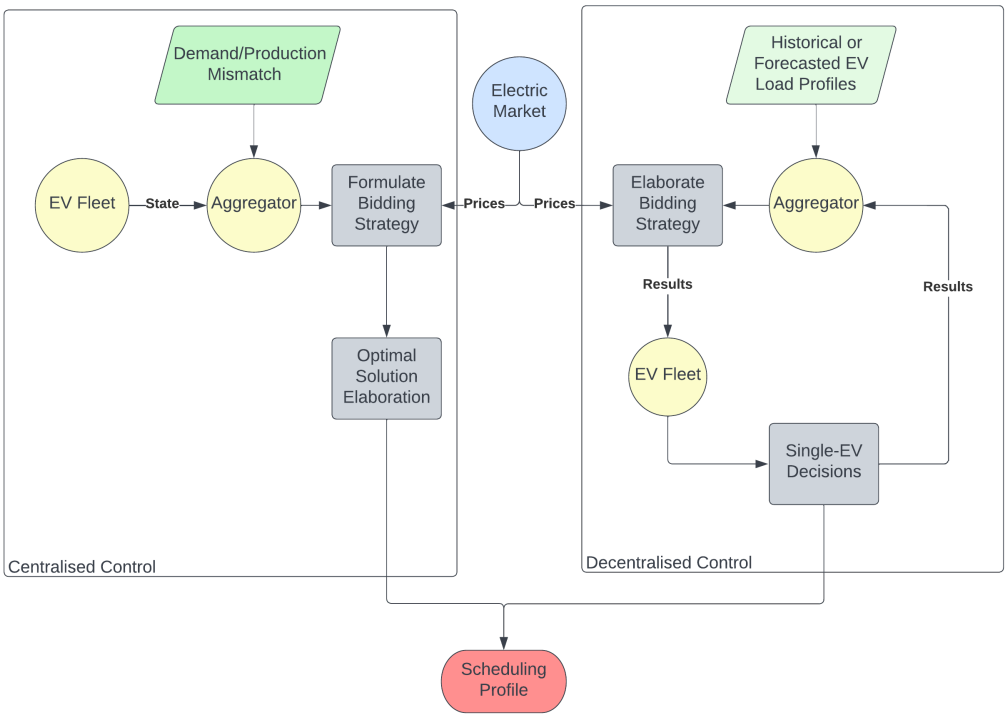

FIGURE 2.7: Centralised and Decentralised charging, a comparison.

2.3.2 Decentralised and Centralised V2G

EV charging techniques are classified in the literature as coordinated or uncoordinated. While in the latter the EVs connect to the stations and absorb the nominal power until the max SOC is reached, coordinated or "smart" charging shifts the charging sessions to avoid overloading the grid. The latter type is further split into centralised and decentralised EV charging. This classification is displayed in Figure 2.7, while some examples are provided in Table 2.6.

In *centralised* charging, the aggregator first gathers information regarding the EVs SOC, connection state and charging requirements. Then, based on the grid production-consumption mismatch and other grid parameters, elaborates a bidding strategy that is submitted to the market. If the bidding is successful, the optimal charging solution is obtained and the control signals sent to the EVs. In *decentralised* charging instead, the aggregator elaborates a bidding strategy based on historical or forecasted EV demand profiles, then sends the bidding results to the single EVs, which can decide whether to charge or not in that time slot. The results are then sent to the aggregator, which can then decide whether to modify the bidding or not. When the final solution is reached, the scheduling profile is obtained. While centralised charging charging only requires a one-way communication between the EVs and the aggregator, has an overall low computational burden for the single EVs and allows for grid stabilisation, the EVs need to entirely demand the charging process to the aggregator, which also experiences a higher computational burden. Decentralised charging instead, shifts the computational burden from the aggregator to the single users, and generally requires more than one iteration to find the optimal solution that satisfies both the single EVs and the market. The communication infrastructure needs to be bidirectional, and thus becomes more expensive, but the single EV can decide whether to charge or not based on their own payback plan.

As mentioned before, a centralised V2G control can include grid-level objectives in the smart scheduling process and more efficiently exploit all the EVs connected to the grid. An example can be seen in Figure 2.8, where two scenarios (low and high EV penetration) are compared. In those figures, the objective is smoothing the net active power curve through a MV/LV transformer.

Two different aspects should be underlined by looking at figures 2.8a and 2.8b. Firstly, the centralised algorithm is able to smooth the P_{NET} curve efficiently in both cases, though major differences can be spotted between the high and low EV penetration scenarios. Secondly, the high number of EVs in the high penetration scenario reduces the use of each

Classification	Method	Objective(s)	Type	Examples
Analytic	Non-Linear Programming	NLVR	Decentralised	[137]
		Minimize Battery Ageing Cost	Decentralised	[138]
		Maximize Profit and Battery Life	Decentralised	[139]
	Linear Programming	Maximising PV Utilisation	Centralised	[131]
		Minimize User Costs	Decentralised	[128–130]
	Mixed-Integer Linear Programming	Minimising System Costs	Centralised	[133, 134]
		Minimising Charging Costs	Decentralised	[132]
		Maximising PV Utilisation and Profit	Centralised	[135]
		Minimise Frequency Deviation	Decentralised	[136]
	Quadratic Programming	NLVR	Decentralised	[47, 140–143]
		NLVR+Minimize System Costs	Centralised	[144]
		NLVR	Centralised	[140, 141]
	Dynamic Programming	Minimise EV Management Costs	Decentralised	[146–148]
	Mixed-Integer Quadratic Programming	Maximise PV Utilisation	Centralised	[145]
Heuristic	Hierarchical Control Architecture	Minimise Charging Costs	Centralised	[170]
	Particle Swarm Optimisation	Maximise PV Utilisation	Centralised	[171]
		Peak Shaving	Centralised	[149–152]
		Minimise Charging Costs	Centralised	[153–155]
		Minimise System Costs + NLVR	Centralised	[156]
	Artificial Bee Colony	Minimise Charging Costs	Centralised	[157]
	Ant Colony Optimisation	Minimise Users' Waiting Time	Centralised	[158, 159]
	Genetic Agorithm	NLVR	Centralised	[160]
Model Predictive Control		Minimise Total Costs	Centralised	[161, 162]
		Minimise Charging Costs	Decentralised	[163–165]
		Maximise Aggregator's Benefits	Centralised	[166]
		Minimise Peak Demand	Centralised	[167, 168]
		Maximise PV Utilisation	Decentralised	[169]

TABLE 2.6: Overview of bidirectional V2G optimisation techniques and objectives.

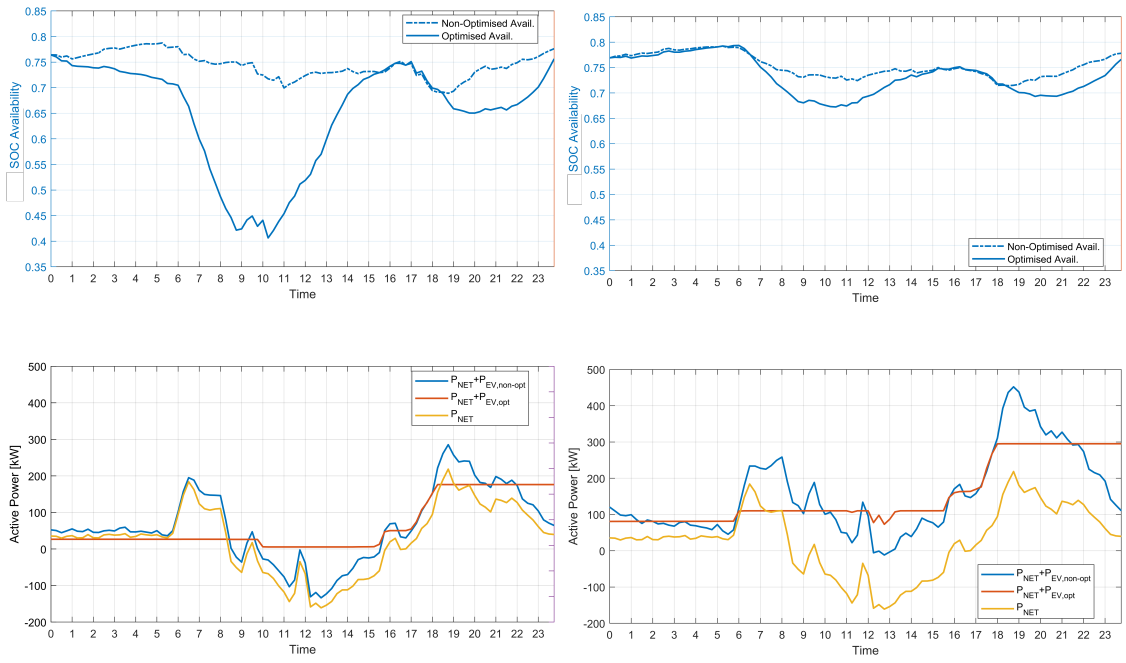

(A) Low EV Penetration

(B) High EV Penetration

FIGURE 2.8: Net power flow P_{NET} across a LV/MV transformer with and without centralised V2G charging for high and low EV penetration scenarios.

vehicle, since the "cumulative" SOC curve of the EV fleet never decreases under 65%. The latter consideration supports the idea that the more EV stations are involved in the coordinated charging, the less the system needs to rely on the individual users.

If the disaggregated net power flows in Figure 2.9 at each user are considered instead and then both centralised and decentralised V2G charging are compared, it is possible to confirm that the single user P_{NET} is smoother in the "decentralised" V2G scenario only.

This happens because users may be forced to discharge their EVs when their installed PV system is overproducing, in order to supply another user which is instead underproducing. The inability to optimise charging based on, for

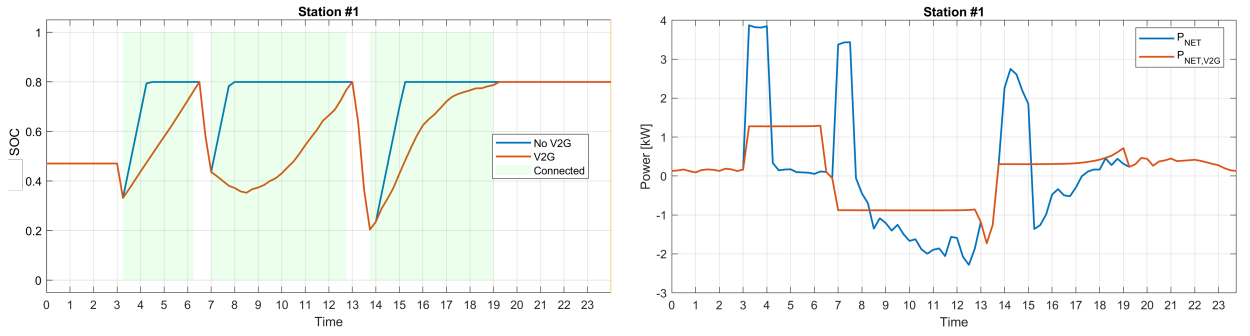

(A) Decentralised

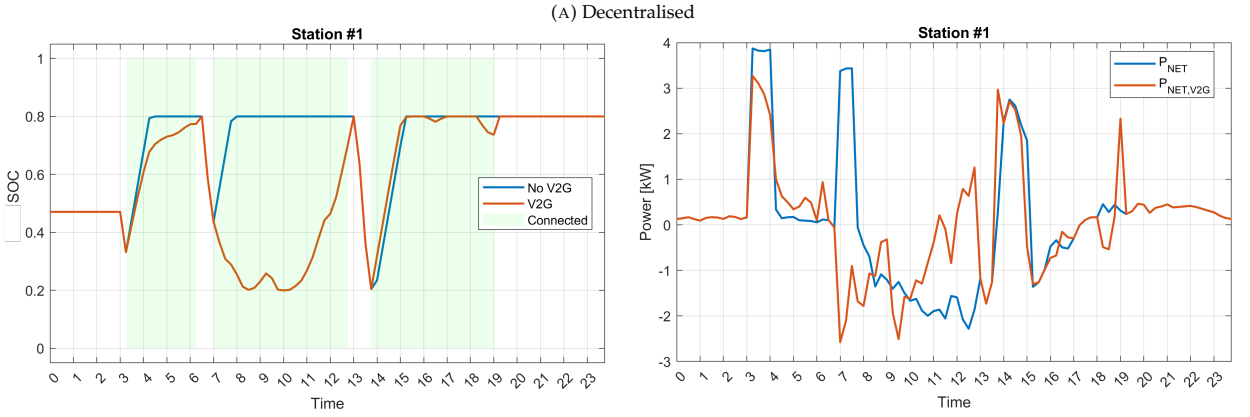

(B) Centralised

FIGURE 2.9: Net power flow P_{NET} for a single grid connected user with and without centralised or decentralised V2G charging.

example, time-of-use tariffs, is generally positive for the system but detrimental to the single users.

Summing up, the choice between a decentralised or centralised V2G policy influences both the grid support capabilities and the users' revenue, thus becoming as important as the optimisation method itself.

2.4 Conclusions

The problem of mitigating the multi-faceted impact of the increasing penetration of both PV systems and EV stations on the electric network can be addressed in a variety of ways.

The literature review in Section 2.1.4 made it clear that, at the LV side, RMS voltage and current variations are the most important issues to consider. Thus, in the papers presented in chapters 3 and 4, the results of power flow simulations will be used to analyse possible voltage levels fluctuations. Additionally, in Chapter 4, the transformer and lines loading level are going to be considered.

As presented in Section 2.2, heuristic techniques are often deployed for BESS sizing, due to their ability to handle any optimisation objective and speed up the convergence process. For this reason, in Chapter 3 the results of an innovative BESS sizing algorithm based on the Non-Sorted Genetic Algorithm II (NSGA-II) will be described and applied to the context of Renewable Energy Communities (RECs). In particular, two different controls are compared, and their effect on the battery sizing results is presented, together with a wider analysis of their impact on the network. The first one is a centralised peer-to-peer control, that specifically favours exchanges between the users, while the second is a decentralised peer-to-grid one, which is considered as the business-as-usual control strategy for BESSs.

Moreover, as presented in Section 2.3, smart charging is a very promising technique to both reduce the EV impact on the grid and maximise the use of PV-produced energy. In Chapter 4, the results of a centralised EV smart charging algorithm, aimed at reducing the production/consumption mismatch at the transformer level, are going to be presented.

Chapter 3

Optimal BESS Sizing for PV Impact Mitigation on the Distribution Grid

In this Chapter [1], a novel algorithm to optimise the size of the BESSs within a REC is presented. According to the European Renewable Energy Directive 2018/2001 [172] a REC is a legal entity, aggregating prosumers and consumers who share their energy generation resources and storage capabilities to decrease the prices of electricity and increase the district-level self-sufficiency. Even if, in the future, REC members could participate to the electricity market, the first step should be pooling their own storage resources to increase the district-level self consumption and lower the electricity prices. Thus, sizing the storage systems needs to keep track of new requirements that were usually not included in the classic methodologies presented in 2.2.2.2.

3.1 Review and Motivation

Many Authors simultaneously solve the issue of optimal sizing and siting, but in this case study, the BESS are deployed at the users' premises, thus the problem is a pure sizing one. Since none of the papers presented in Section 2.2.2.2 analysed RECs as a case study, their Authors never considered that some grid nodes could be "unavailable" for storage placement. On the contrary, in this work, it is assumed that a percentage of users does not want or cannot purchase a BESS, thus requiring to be excluded from the optimisation problem. To the best of the Authors' knowledge, only Rodrigues et al. [127] optimally sized the batteries based on a prosumer-driven peer-to-peer sharing control which makes that case study comparable to a REC. The Authors, however, only considered six buildings, and did not include a grid impact analysis, which is usually a DSO's responsibility. Moreover, even though several Authors considered the grid impact in their BESS sizing algorithms (as explained in Section 2.4), none of them considered energy sharing in a REC as a case scenario at the same time.

In the following, a multi-objective optimisation strategy is presented. The objectives are to minimise the energy absorbed by the REC from the grid (as recommended by the EU in the REC definition) and minimise the total installed BESS capacity (to avoid the related installation costs). Such objectives are concurrent and thus, the best trade-off solutions are obtained by a custom NSGA-II. Based on the classification presented in Section 2.2.2.2, the algorithm hereafter described is classified as *search-based* and *heuristic*, because the Pareto front search is performed through a genetic algorithm.

Two different control strategies are considered: a traditional decentralised peer-to-grid (P2G) one (each user manages its own battery) and a REC-oriented centralised peer-to-peer (P2P) one (the batteries are controlled based on the requirements of the entire REC).

3.2 Problem Formulation

If $\mathbf{x} = [x_1, \ldots, x_N]^T$, i.e. the BESS capacities for each prosumer, the problem can be formulated as follows:

[1] Part of this chapter was published in M.Secchi, G. Barchi, D.Macii, D.Moser and D. Petri, "Multi-objective battery sizing optimisation for renewable energy communities with distribution-level constraints: A prosumer-driven perspective", Applied Energy, Vol.29, September 2021, https://doi.org/10.1016/j.apenergy.2021.117171

$$\min_{\mathbf{x}} \quad (C_T(\mathbf{x}), G_A(t_0, T, \mathbf{x})) \tag{3.1}$$

subject to:

$$C_{\min} \leq x_n \leq C_{\max} \qquad n = 1, \ldots, N \tag{1a}$$

$$\Pr\left\{V_L \leq V_b^p(t_0, T, \mathbf{x}) \leq V_U\right\} \geq q_\alpha \qquad \begin{matrix} b = 1, \ldots, B \\ p = 1, 2, 3 \end{matrix} \tag{1b}$$

$$U\mathbf{x} = \mathbf{0} \tag{1c}$$

where C_T represents the total capacity of all BESSs deployed in the REC:

$$C_T(\mathbf{x}) = \sum_{n=1}^{N} x_n \tag{3.2}$$

and G_A is the grid absorption coefficient

$$G_A(t_0, T, \mathbf{x}) = \frac{E_G(t_0, T, \mathbf{x})}{E_L(t_0, T, \mathbf{x}) + \sum_{n=1}^{N} E_{D_n}(t_0, T)} \cdot 100 \tag{3.3}$$

representing the share of energy the REC users need to purchase from the grid $E_G(t_0, T, \mathbf{x})$ in the analysed time interval $[t_0, t_0 + T]$, to cover their requirements. In equation 3.3, the G_A value is expressed as a percentage of the total energy demand $E_L(t_0, T, \mathbf{x}) + \sum_{n=1}^{N} E_{D_n}(t_0, T)$, which is the sum of the load demand and the electricity losses (due to both line and battery charging). All the parameters are evaluated for a generic n-th REC member out of the total N ones. The simplest scenario is the one where all of the users are passive, a.k.a. they do not produce their electricity via PV. In that case, $G_A(t_0, T, \mathbf{x})$ is 100%, whereas its value decreases as the installed PV and BESS capacity grows.

Three constraints are considered in the optimisation problem:

- Constraint (1a) ensures the installed BESS capacity does not exceed the smallest C_{min} or largest C_{max} domestic BESS sizes due to technology or regulatory requirements.
- Constraint (1b) makes sure the joint over and undervoltage probability for the RMS voltages $V_b^p(t_0, T, \mathbf{x})$ of the B three-phase buses the REC members are connected to, does not overcome $1 - q_\alpha$, with reference to the upper (V_L) and lower (V_U) limits set by the national and international regulation (EN50160 [11]). Generically, $B \geq N$ due to the presence of zero-injection buses, frequently found at the distribution level.
- The linear equality constraint (1c) assigns a BESS only to the users that are willing to install it. In fact, the non-zero diagonal elements of U identify the REC members to be excluded from optimal BESS sizing.

Since both the objective function (3.3) and the constraint (1b) are not only strongly nonlinear, but they can also hardly be formulated in an explicit analytical form, both the grid absorption coefficient and the probability of voltage violation have to be estimated through numerical simulations. Moreover, the results are influenced by the actual PV generation, the load power profiles and the energy sharing policy adopted by the REC members. Hence, the choice of a heuristic optimisation technique, guiding the search for the optimal combination of G_A and C_T.

3.2.1 Problem solution

The BESS optimisation problem (3.1) was solved by means of a custom implementation of the NSGA-II algorithm. The BESS capacity values of the N REC members (namely the decision variables of problem (3.1)) are regarded as the genes of an $N-$sized chromosome. The NSGA-II algorithm requires an initial $2M-$sized population of chromosomes, M of which change at every iteration as a result of the evolutionary process. Of course, the value of M as well as the genetic variety of the initial population must be large enough to ensure a thorough exploration of the solution space.

A simplified flowchart of the developed implementation is shown in Fig. 3.1. The genetic algorithm is applied to a multi-parametric REC model, whose behaviour depends on a variety of inputs, such as

a) the *load consumption profiles*, which depend on the profile temporal resolution, the type of load (e.g., residential or commercial), the buildings occupancy [173], the users' behaviour and habits, the grid geographical location and the season of the year;

b) the *grid model*, which includes the network topology, the line parameter values, the transformer features and the nominal load values;

c) the *PV generation profiles*, which depend on both the maximum power of the PV generators deployed at REC members' locations and on the daily solar irradiance and temperature patterns in different seasons of the year.

d) the *BESSs capacity values* could potentially take any real value within $[C_{min}, C_{max}]$, but in practice are quantized. This is due to the fact that the capacity of a single cell cannot be arbitrarily small, but depends on the battery technology. Therefore, even if the optimal BESS sizing problem formally is continuous, in practice it becomes discrete (i.e., combinatorial), thus justifying the use of a genetic algorithm to solve (3.1). Note that if there are sites where BESSs cannot be installed due to constraint (1c), the corresponding genes are steadily set to 0 in all chromosomes and for all generations.

A quasi steady-state power flow analysis is repeatedly performed in OpenDSS [2] for each chromosomes of the population in the time interval $[t_0, t_0 + T]$, with a predefined time step. This iterative power flow analysis returns accurate time series of the power flows within the REC, the corresponding losses (used to compute (3.3)) and the bus voltage values. The probability of exceeding the ends of interval $[V_L, V_U]$ has to be checked to meet constraint (1b).

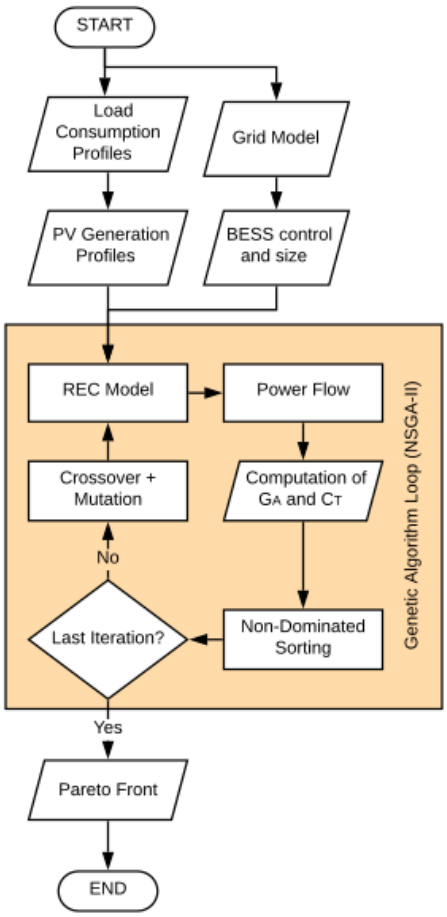

FIGURE 3.1: Simplified flowchart of the algorithm implemented to solve the BESS sizing optimisation problem.

It is important to emphasise again that such grid-level simulation results also depend on the energy sharing policy chosen by the REC members, as briefly introduced at the beginning of this chapter. In the present study, two alternative BESS control policies are implemented, i.e. the classic P2G approach and a custom P2P policy (firstly introduced in [126] and then improved in [174]). In the P2G approach each REC member manages its own BESS, regardless of the state of the others and the neighbours' needs. In this case, power flows between the REC peers are possible but not implemented through a specific BESS control. Conversely, the P2P policy specifically promotes the exchange of energy between prosumers depending on their actual supply and demand as well as the SOC of all the BESSs at a given time. Further details on P2G and P2P BESS control rules are summarised in the Section 3.3.2. The losses due to BESS charging and discharging are also taken into account in the simulations since they may significantly affect the outcome of this study, as it will be shown in Section 3.5. Once the results of the OpenDSS quasi steady-state power flow simulations are completed for all the chromosomes of the available population, the objective functions (3.2)-(3.3) are computed and the constraint conditions (1a)-(1c) are checked. The feasible solutions are kept and ranked on the basis of the so-called *non-dominated sorting criterion* [175]. With reference to cost functions (3.2) and (3.3), a solution $\mathbf{x}_i$ dominates a solution $\mathbf{x}_j$ if

$$\begin{cases} G_A(T, \mathbf{x}_i) < G_A(T, \mathbf{x}_j) \\ C_T(\mathbf{x}_i) \leq C_T(\mathbf{x}_j) \end{cases} \vee \begin{cases} G_A(T, \mathbf{x}_i) \leq G_A(T, \mathbf{x}_j) \\ C_T(\mathbf{x}_i) < C_T(\mathbf{x}_j) \end{cases} \tag{3.4}$$

[2] OpenDSS: Open Distribution System Simulator v9.0.0, R.Dugan, D.Montenegro, A.Ballanti, https://www.epri.com/pages/sa/opendss

By repeatedly applying condition (3.4), the $2M$ chromosomes of a given generation are partitioned into subsets (called "fronts") in such a way that the objective function values associated with all the members of the $f-$th front are *dominated* by the solutions of the $(f-1)-$th front only. The first front, which contains the solutions that are not dominated by any other, is the "Pareto front" of the considered population. In addition, the so-called *crowding distance* associated to each solution of a given front is computed, as explained in [175]. Given that just M of the existing solutions have to be selected to create a new generation, if the chromosomes of the non-dominated front are more than M, only those with the largest crowding distance are retained. Conversely, if the Pareto front elements are less than M, the missing ones are taken from the following ordered dominated fronts, always starting from the chromosomes with the largest crowding distance values. The algorithm returns a population of M chromosomes, whose genes are combined through binary tournament, crossover and mutation, as customary in genetic algorithms, to obtain M new solutions that are added to the parent ones. The results of this last step are fed back into the REC model and the algorithm runs until the chromosomes of the Pareto front no longer significantly change. The number of generations needed to reach convergence depends on the features of the considered case study.

3.2.2 Problem implementation

The algorithm shown in Figure 3.1 is implemented in Matlab and interfaced with the open-source software OpenDSS, which is used to run power flow simulations within the optimisation loop. The NSGA-II algorithm required a custom implementation in Matlab, since it needed to be interfaced with OpenDSS, which is used to run power flow simulations within the optimisation loop to calculate the objective function values from Equation (3.3).

Since the power flow simulations are very time consuming, the NSGA-II algorithm was chosen because the crossover, mutation and sorting sections of the algorithm can be parallelised into multiple parallel threads implemented by making use of the Matlab Parallel Computing Toolbox. This greatly speeds up the process and allows for the simulations to conclude within a reasonable time. On top of the parallelisation of the genetic algorithm, the OpenDSS parallel machine features were further exploited to speed-up the grid solving process. The simulations were split up into 30 threads, running on 15 cores and supported by two 3600 MHz DDR4 32 GB RAM banks. The objective function is computed by a single thread that saves the results in Matlab structures that are finally merged and sent to the non-dominated sorting section of the NSGA-II algorithm. The processor frequency, which is nominally 3.6 GHz in single core but here limited to 2.2 GHz due to multi-threading. This does not allow for a 1:1 relationship between the number of cores and the speedup, but the parallelised solution still runs 12 times faster than the baseline one, in accordance to what reported in [176].

3.3 Case Study

The grid model used to test the BESS optimisation strategy is the IEEE Low Voltage Test Feeder. That feeder was chosen because 1) it is a well-known and studied test case in the scientific literature, 2) the grid parameters are publicly available on the IEEE PES website [3], 3) it is representative of a LV European test feeder, whose extension and electric features are suitable to describe the connection between REC members. The structure of the grid is shown in Fig. 3.2.

The proposed study requires the REC members to be connected to the grid buses highlighted with red dots in Figure 3.2. Since for the IEEE LV Test Feeder the nominal load values are provided only, we replaced them with time-dependent profiles generated with Load Profile Generator (LPG) [4], a bottom-up generator mimicking the user consumption behaviours for different age groups and occupations. We aimed at representing the typical house composition of a REC in the city of Bolzano in the Italian Südtirol-Alto Adige autonomous province, and selected the number of households for multi and single-apartment buildings and the related occupancy profiles accordingly. Those parameters were obtained through a preliminary urban and demographic analysis based on the main database from ASTAT [177] and then used as an input to the load profiles generation process in LPG.

Moreover, since the future electric grid will feature both loads for standard appliances and heating devices, we decided to include one scenario in which HPs are included in the electric consumption. Thus, two different scenarios will be analysed:

[3] IEEE Test Feeders Database: https://site.ieee.org/pes-testfeeders/
[4] LPG: A Bottom-Up Customizable Load Generator, Noah Pflugradt, `https://www.loadprofilegenerator.de`

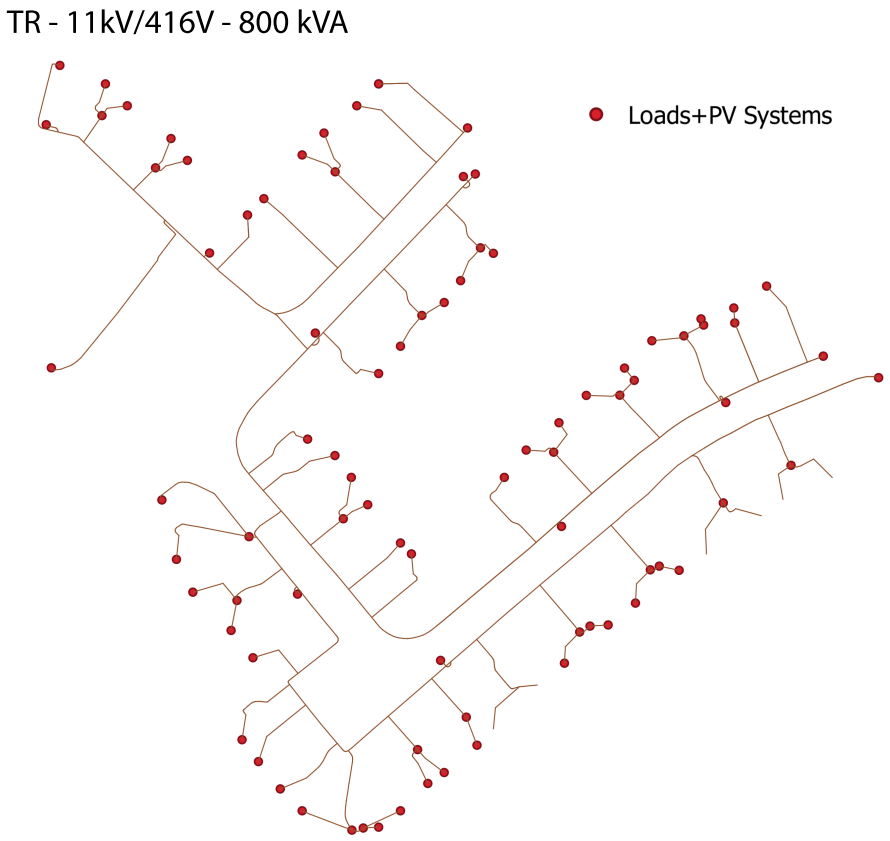

FIGURE 3.2: Structure of the IEEE 906-bus LV Test distribution system.

- *Present scenario*: the impact of heating and cooling on the total electrical energy consumption is assumed to be negligible;
- *Future scenario*: heating and cooling are provided by highly efficient electrical HPs, which increase the overall load.

In order to give the reader a more realistic view, the increase in total yearly energy demand for scenarios including HPs is around 40%, which is very close to the values presented in [178].

In this study, since all the REC members are assumed to be equipped with a PV generation unit connected to the same buses we highlighted in Figure 3.2, PV production profiles are required to estimate the impact of distributed generation on the REC. This assumption is the worst-case scenario concerning grid stability studies, since it was proven that PV systems greatly affect the voltage stability of the electric system by simultaneously injecting power in the central hours of the day, as explained in Section 2.1.1. The PV production was computed by making use of OpenDSS's built-in tool for PV production, PVsyst [5]. The irradiance and temperature data profiles were measured at the Bolzano-Dolomiti airport (Bolzano, Italy) in 2017 (further details are reported in [179]). Specifically, the performance ratio of the PV modules never goes below 77%, and its median is around 91%, meaning that for 50% of the simulated time instants, the loss due to the temperature and inverter-driven losses is around 9%. As far as the PV capacity installed by each REC member is concerned, a rule of thumb was followed, specifically prescribing that the target for self-sufficiency should be around 30% without considering any storage systems [180, 181]. Furthermore, there exists a limitation to the installed PV power on the grid related to the voltage constraint from (1b), which for this study is around 45% PV penetration, without considering storage. Table 3.1 summarises the main load and production features, from a power perspective.

As explained in Section 3.2, one of the features of the proposed algorithm is the possibility to exclude from the BESS sizing optimisation any user, in case there is no willingness to purchase a storage system. In this work, three scenarios

[5] PVsyst Element Model, OpenDSS by EPRI, `http://svn.code.sf.net/p/electricdss/code/trunk/Distrib/Doc/OpenDSS%20PVSystem%20Model.pdf`

Scenarios		Present (no heat pumps)		Future (with heat pumps)	
		min. [kW]	max. [kW]	min. [kW]	max. [kW]
Loads	Winter	39.1	363.6	72.9	422.8
	Summer	25.6	377.4	25.8	623.2
Peak PV	Winter	18.8	373.6	22.7	449.8
	Summer	245.4	410.2	295.5	493.9

TABLE 3.1: Minimum and maximum values of the load consumption profiles synthesised with LPG and of the actual daily PV power generation peaks used to simulate present and future load scenarios (i.e., without and with widespread electrical heat pumps, respectively) in winter and summer and with either energy energy sharing policy (i.e., P2G or P2P).

	Parameters	Values
Problem-specific settings	Number of REC members N	90
	Number of buses B	906
	Initial time t_0	Jan. 1 or Aug. 1
	Time interval duration T	31 days (2976 15-min. time steps)
	Min. BESS capacity C_{min}	1 kW h
	Max. BESS capacity C_{max}	60 kW h
	Lower acceptable voltage V_L	0.9 p.u.
	Upper acceptable voltage V_U	1.1 p.u.
	Prob. of not exceeding voltage limits q_α	95% (per week)
	Matrix U of REC members' sites excluded from BESSs installation	Diagonal matrix with $N/2$ elements $\neq 0$ ($P50 - F50$) All-zero matrix ($P100 - F100$)
NSGA-II	Min. BESS capacity increment	1 kW h
	Number of chromosomes M	100
	Crossover probability	50%
	Mutation probability	Decreasing linearly from 25% to 10%
	Number of generations	50

TABLE 3.2: Problem-specific and NSGA–II parameter settings for optimal BESS sizing in the six scenarios $P25 - P75$, $F25 - F75$ described in Section 3.3

were identified, and will hereby be referred to as *conservative* (25% of users with a BESS), *neutral* (50%) and *aggressive* (75%), based on the growing number of users purchasing a BESS. The users deciding to install a BESS are assumed to be uniformly spread over the grid, and each battery is considered to be a modern lithium-ion one. The round-trip efficiency of the batteries is considered to be around 90% and the SOC is constrained between 10% and 90% to avoid excessive battery wear, as in [182, 183].

Six joint-scenarios emerge from the combination of the aforementioned choice of parameters, and they will be henceforth denoted as $P25$, $P50$, $P75$, $F25$, $F50$ and $F75$, where P and F stand for "present" and "future" scenarios, based on the presence of HPs, whereas 25, 50 and 75 refer to the percentage of REC members equipped with a BESS. For each of these scenarios, four different configurations are considered, stemming from the combination of the seasonality choice (winter/summer) and the energy sharing policy/battery control. The former distinction is needed to consider the worst and best scenarios for PV production, which greatly influence G_A and grid voltage stability issues. The latter, instead, is needed to analyse how a centralised BESS control (P2P) modifies the battery sizing results, compared to the business-as-usual control (P2G).

3.3.1 Simulation and optimisation settings

Two groups of parameters (whose values are reported in Table 3.2) have to be set to run the genetic algorithm.

The first group is problem-specific and it is used to compute objective functions (3.2) - (3.3) and/or constraints (1a) - (1c) for each scenario of interest. The meaning of these parameters has been already defined in Section 3.2.1, but some of the values reported in Table 3.2 deserve some further explanation. In particular, the minimum BESS capacity C_{min} that can be assigned to every REC member is 1 kW h. This is the size of a very small battery [184], which can be used to extend the results of this analysis close to the case in which no BESSs are used. The maximum capacity C_{max} per REC member is instead 60 kWh. This is the maximum BESS capacity that can be regarded as acceptable in terms of size at

a residential level, considering that its volume is about 1 m^3 based on the technical specifications of several manufacturers. The values of parameters V_L, V_U and q_α in (1b) ensure that the bus RMS voltage levels lie within $\pm 0.1 p.u.$ of the nominal value with 95% probability, in compliance with the requirements of the EN Standard 50160:2009 [11]. A further parameter, not explicitly defined in Section 3.2.1, but essential to run the optimisation algorithm, is the time step of grid-level simulations. As highlighted in Section 3.1, the time step is set to 15 minutes because it provides a reasonable trade-off between computational burden and temporal resolution of the power flow analysis. In addition, 15 minutes is also the sampling period duration of the experimental irradiance and temperature patterns used for PV power profile generation and the reporting period length of second-generation smart meters currently deployed in Italy [185].

The second group of parameters in Table 3.2 refers specifically to NSGA-II settings. The first parameter in this group is the minimum BESS capacity increment. This is set equal to C_{min} and affects the quantization of the possible solutions space, as well as the minimum variations of the values that can assigned to each gene. The value of M was tuned heuristically and it corresponds to the lowest possible number of chromosomes that ensure a trustworthy convergence of the Pareto fronts in all scenarios. Finally, the crossover and mutation probabilities are set as recommended in [175] to minimise the risk that the algorithm gets stuck in local minima.

The following subsection describes more in detail the BESS control algorithms, in order to provide an easier understanding of the optimisation results.

3.3.2 P2G and P2P energy sharing policies

The P2G sharing approach relies on the following basic rules:

1. The instantaneous local PV generation and load consumption values are compared to determine if the battery has to be charged (overproduction) or discharged (underproduction).
2. In the former case, the available PV power is charged into the BESS till reaching the maximum SOC. Once reached, the surplus power is injected into the grid and handled directly by the DSO.
3. In the case of PV power local underproduction, the missing power is first taken from the BESSs till reaching the minimum SOC level. Once the stored energy is over, the power missing at a given time is drawn from the main distribution grid.

The P2G sharing policy is quite simple to implement as it does not require a dedicated monitoring and communication infrastructure, and can be regarded as the "business as usual" one. The main rules underlying the P2P sharing policy are instead summarised below, and a flowchart is presented in Figure 3.3 to clarify the main steps.

1. The instantaneous PV production and load consumption values are aggregated to compute the difference between power supply and demand for the whole REC.
2. The available BESSs try to cover the residual power demand/production at a given time on the basis of their SOC.
    - In the case of a local *overproduction* of PV power, the surplus is charged into multiple BESSs proportionally to their instantaneous depth-of-discharge (DOD). This way, the BESSs with the highest DOD values are charged more than the others.
    - In the case of a PV power local *underproduction*, the missing power is taken from multiple BESSs, proportionally to their SOC. Hence, the BESSs with the highest SOC values are discharged more than the others.

The P2P sharing policy is more difficult and expensive to implement, as it requires a more complex communication infrastructure and an aggregator with full knowledge of the power supply, demand situation and BESSs SOC for all REC members.

3.4 Optimisation Results

Fig. 3.4(a)-(f) shows the obtained Pareto fronts of optimal solutions obtained for scenarios $P25 - F25$, $P50 - F50$ and $P75 - F75$, respectively.

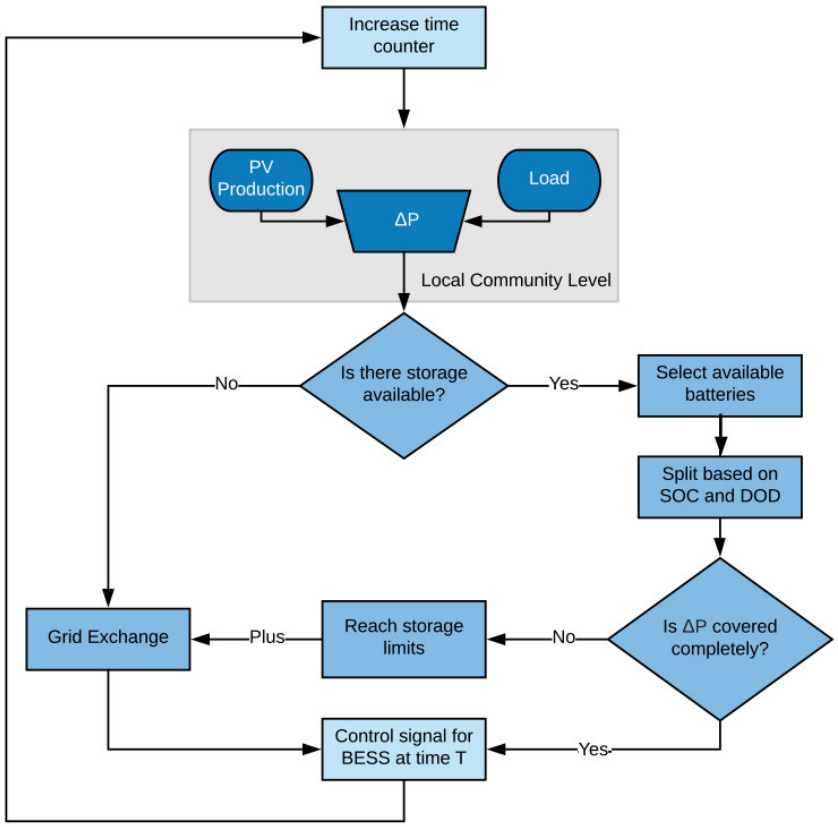

FIGURE 3.3: Flowchart of the P2P control algorithm.

The Pareto fronts confirm the expectations, since an increase in the installed BESS capacity (C_T) within the REC level produces a reduction in the dependence from the main grid (G_A). However, this reduction is sizeable only when the percentage of users equipped with a BESS increases by more than 25%. Furthermore, G_A in winter is always greater than summer, due to the lower availability of the solar resource.

The most relevant general remarks are henceforth summarised:

- The definition of G_A in (3.3) implies that, when the installed BESS capacity is small, the amount of energy purchased by the REC from the main grid depends on seasonal factors only. This is clearly visible from the fact that when C_T tends to 0, all winter or summer Pareto fronts start approximately from the same G_A level. The maximum G_A values are obviously lower in summer (around 50%) than in winter (70% to 75% depending on the presence of HPs). A minor difference exists between the G_A values at $C_T = 0$ in scenarios $P25$, $P50$, $P75$ and those in scenarios $F25$, $F50$, $F75$. This happens because even if in the "future" scenarios the loads are 40% higher, their impact on G_A is mitigated by the PV systems that are sized as a function of the nominal load, as explained in Section 3.3.

- There exists a C_T threshold over which the installed storage capacity is not exploited, due to a number of possible reasons depending on the daily load-production mismatch. Indeed, if the balance is heavily tilted towards one of the two sides, the available storage capacity or stored energy will gradually decrease and the system will be less able to flexibly handle the mismatch. When this C_T threshold value is surpassed, an asymptotic G_A value is reached which tends to decrease as the BESS penetration grows. This happens because a high number of batteries is less likely full when they need to be charged or empty when power absorption is needed. Table 3.3 summarises the threshold C_T values for scenarios $P25 - F25$, $P50 - F50$ and $P75 - F75$ when either the P2G or P2P energy sharing policies are used. It can be noticed that the C_T threshold values are quite independent of the load conditions subsumed by the presence of HPs. Thus, a single common threshold C_T value is shown for each pair of "present" and "future" scenarios. As the BESS penetration grows, so do the threshold C_T values and the gaps between the values obtained in P2G and P2P. The former consideration stems from the fact that a higher number of batteries ensures that the threshold C_T BESS capacity previously described is reached at a higher total

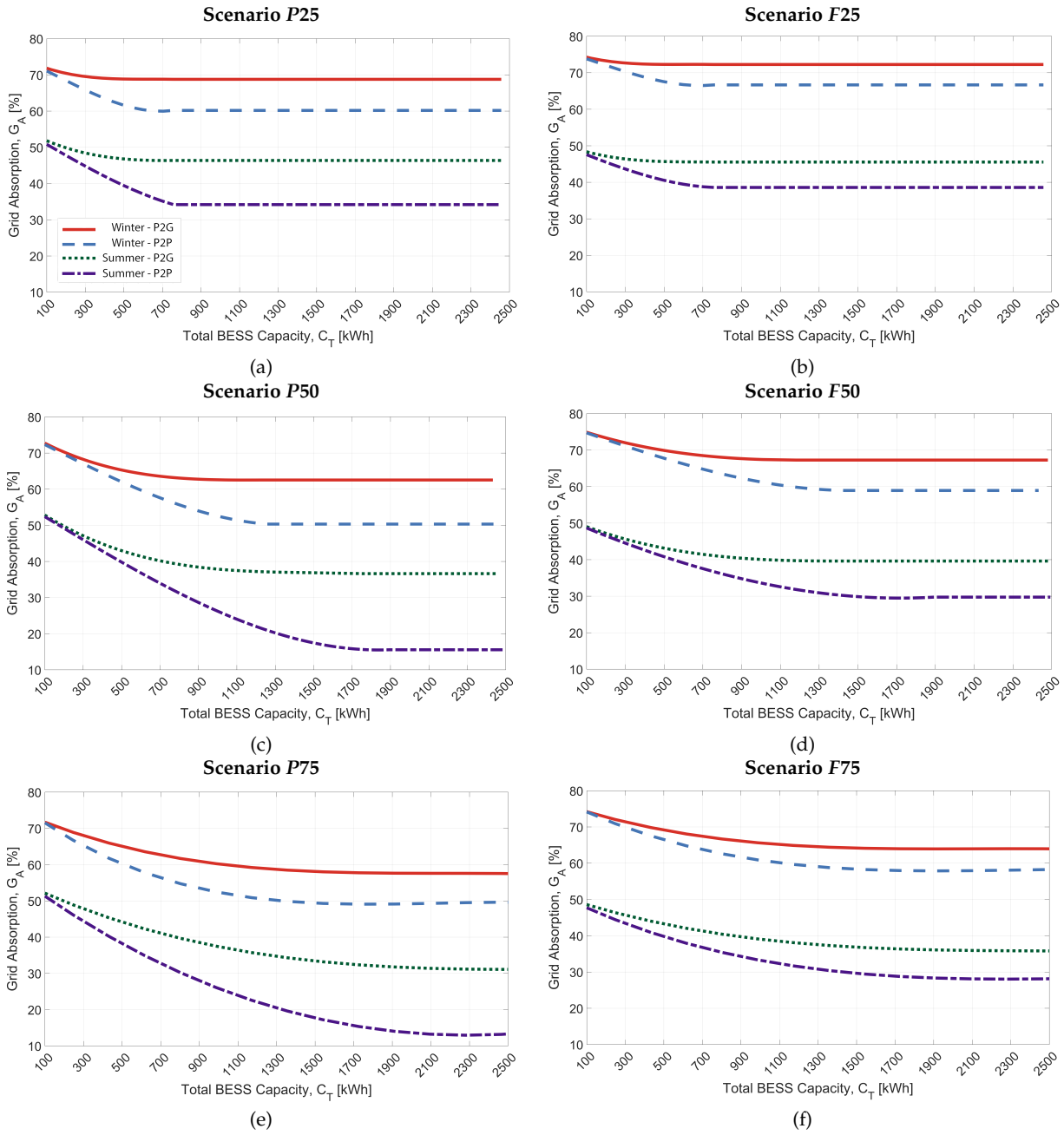

FIGURE 3.4: Pareto fronts resulting from BESS sizing optimisation in scenarios *P*25 (a), *F*25 (b), *P*50 (c), *F*50 (d), *P*75 (e) and *F*75 (f). For each of them, four operating conditions are analysed, i.e. in winter or summer and by using a P2G or a P2P energy sharing policy within the REC.

installed BESS capacity. The second instead, depends on how the P2P algorithm works. Since in P2P all the users pool their storage resources to respond to a power mismatch in the system, generally a more efficient exploitation of the available BESS capacity is ensured. As a consequence, the P2P G_A profile keeps decreasing after the P2G C_T threshold is surpassed.

- It is important to highlight that the main benefit of the P2P energy sharing policy is the ability to achieve the same G_A level with a lower installed capacity C_T. Indeed, even if only 25% of the REC members owns a BESS, the others can still benefit from the installed storage capacity. In the case of P2G instead, since the batteries are singularly managed, each user can only self-consume their production (if possible). Therefore, an evident gap can be highlighted between P2G and P2P, and its value tends to increase while the percentage of users equipped with a BESS does. Interestingly enough, this only happens until the *P*50 scenario. After that, the gap decreases, and if all the users were equipped with a BESS, the gap would disappear. The latter consideration is explained by the fact that all the users become independent not only from the main grid, but also from their neighbours,

		P25 − F25	**P50 − F50**	**P75 − F75**
P2G	**Winter**	500	1100	1800
	Summer	500	1300	2100
P2P	**Winter**	800	1400	1800
	Summer	800	1800	2300

TABLE 3.3: Winter and summer threshold C_T BESS capacity values (expressed in kWh) in scenarios $P25 - F25$, $P50 - F50$ and $P75 - F75$ when either the P2G or the P2P energy sharing policy are used.

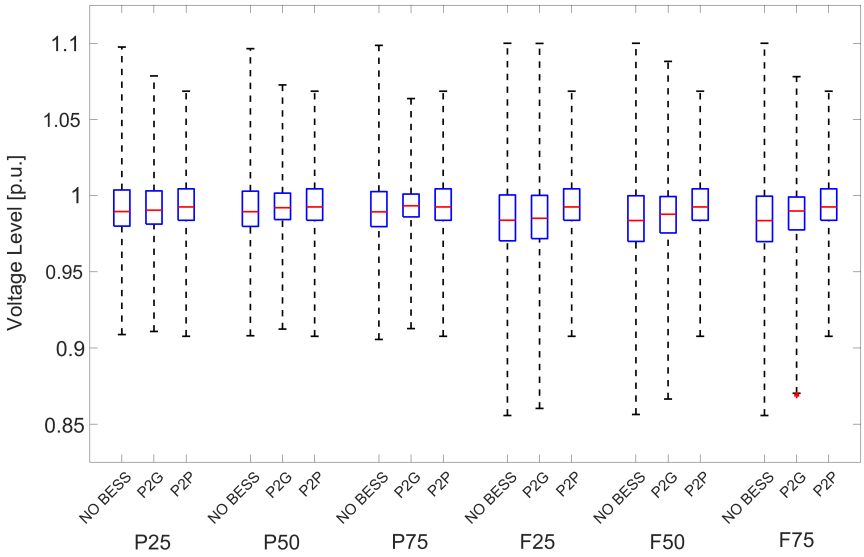

FIGURE 3.5: Box-and-whiskers plot of the normalised voltage levels at all buses of the distribution grid under test over 1 year of simulations in scenarios $P25 - F25$, $P50 - F50$ and $P75 - F75$ both without and with BESSs. In the latter case, either a P2P or P2G energy sharing policy are used. The BESS capacity values assigned to REC members in each scenario correspond to the C_T critical thresholds of the P2P and P2G summer Pareto fronts beyond which no significant reduction of G_A is observed.

thus eroding the margin that the P2P policy has over P2G at low BESS penetration levels.

- Comparing the "present" scenarios with the respective "future" ones, it is clear that both for P2G and P2P the G_A values are higher (from a few % points, up to 10%) due to the higher share of the daily energy demand that is not covered by BESS or directly provided by PV systems.

Quantitatively, the maximum reduction of the REC dependence from the main grid due to the installation of PV and BESS is around 50% in winter and 80% in summer

3.5 Impact Analysis

What follows is an analysis of the broader impacts of the installation of optimal BESS on voltage levels, losses, CO2 emissions and the economic return-on-investment for the users. Since it is not possible to provide all the results for all the points, we selected the C_T threshold values as the most representative ones for each scenario among those of the Pareto fronts provided by the algorithm. This assumption is valid because it combines the highest REC independence levels (lowest G_A values) with the best exploitation of BESSs, since increasing C_T further does not produce any sizeable effect on G_A. In addition, only the BESS sizing solutions obtained in the summer scenarios are presented, since sizing the batteries should be done for the period with the highest solar resource availability.

3.5.1 Voltage Levels

Figure 3.5 uses the box-plot representation to represent the voltage levels in the 906 buses of the grid at the critical threshold C_T levels.

It is noticeable how the voltage levels are all under the 1.1 p.u threshold, while some values are under the 0.9 p.u. threshold in the F scenarios. The violation frequencies however, are very low (1% maximum), and way below the maximum allowed value of 5% [11], as imposed by constraint (1b). Moreover, the probability of voltage violation decreases as C_T grows due to the voltage stabilisation effect of the batteries, in accordance with other studies on the same topic (check 2.2). Interestingly enough, the voltage fluctuations are independent from the battery penetration level, meaning that if only a small percentage of the users have a battery, the algorithm will oversize their storage capacity to reach the same flexibility that a higher BESS share allows for. P2P sharing is preferable to P2G in almost all the scenarios, since both the interquartile and the maximum voltage ranges are reduced. If we consider "present" scenarios only instead, the two energy sharing policies have a comparable impact on voltage fluctuations. Finally, in future scenarios ($F25$, $F50$ and $F75$), the probability of violation is slightly higher than present ones. This increment is mainly in the "lower" threshold of 0.9 p.u., since the inclusion of larger loads decreases the RMS voltage at certain moments of the day.

3.5.2 Relative energy losses

The energy losses are estimated as the ratio between the total energy dissipated in the network lines or in the BESS charging/discharging over the total gross energy required by the REC users in a $[t_0, t_0 + T]$ time interval. Equation (3.5) quantifies the relative losses as follows

$$REL(t_0, T, \mathbf{x}) = \frac{E_L(t_0, T, \mathbf{x})}{E_L(t_0, T, \mathbf{x}) + \sum_{n=1}^{N} E_{D_n}(t_0, T)} \tag{3.5}$$

where $E_L(t_0, T, \mathbf{x})$ and $E_{D_n}(t_0, T)$ are the total energy losses and the electrical energy consumption of the $n-$th REC member, as defined in Section 3.2.

Fig. 3.6 shows the results of this analysis for one-year long power flow simulations. The REL values are presented as a percentage of the total yearly energy demand for both the P2G and P2P sharing policies, and compared to the "no-storage" scenario, in which the PV generators are used without the BESS support. The hatched bars represent the line losses due to the resistance in the conductors, whereas the other bars represent the losses for charging/discharging the batteries. It is immediately visible that using the batteries reduces the total energy losses by 20 to 40%, and only minor differences can be observed between the total relative losses with the P2G and P2P policies, if the same scenarios are considered. Breaking up the total losses into components, the line losses are higher in P2G, since the amount of electricity circulating in the system is higher due to the lower single-user self-consumption values. The charging and discharging losses instead, grow when the P2P is considered, and this is due to the higher exploitation of the storage resources by the centralised coordinated charging algorithm. If the battery penetration is low, a higher number of power exchanges between users is likely, thus the line losses are higher. As the number of deployed BESSs increases, the line losses decrease, while the battery ones increase. In order to provide the reader with a quantitative idea, in scenarios $P75 - F75$, the amount of electrical energy exchanged between REC members using the P2P policy is 1.75 times more than the P2G case, while in $P25 - F25$ this ratio is close to 1.

3.5.3 CO2 emissions

In the following subsection, the results of the BESS sizing algorithm on the related CO2 emissions following the approach presented in [186] is shown, i.e. without a full life-cycle assessment of the environmental impacts of PV generators and BESSs. In equation (3.6), only the emissions related to the residual net energy demand in the REC $E_G(t_0, T, \mathbf{x})$ are considered, i.e.

$$EM_{CO_2}(t_0, T, \mathbf{x}) = k_{\mathrm{CO}_2} \cdot E_G(t_0, T, \mathbf{x}) \tag{3.6}$$

where k_{CO_2} is the equivalent CO2 emission factor for the Italian electricity mix, around 0.344 t/MWh [186].

Using P2P instead of P2G reduces the emissions by 25% to 50% in P scenarios, whereas this reduction is lower (10% − 30%) if the heating sector is electrified with HPs. The P2G policy is less efficient than P2P but still improves the situation

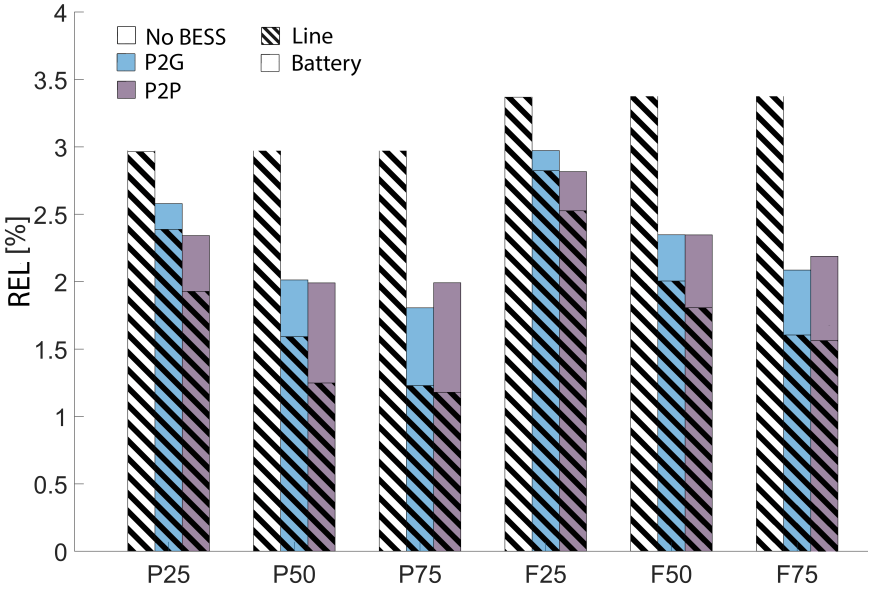

FIGURE 3.6: Yearly relative energy losses (due to both electricity distribution and BESS charging/discharging) either with or without BESSs, and by choosing P2P or P2G as the sharing policies.

over the base "no BESS" scenario, providing a 25% reduction in scenario $P75$ and a reduction by 5% in scenario $F25$. Thus, widespread deployment of BESSs is beneficial in terms of CO_2 emissions reduction for all scenarios.

3.5.4 Simplified Investment Analysis

Two complementary performance indicators are considered to provide the reader with an idea of how the BESS sizing algorithm impacts the return-on-investment of the user: the Internal Rate of Return (IRR) and the Payback Period (PP). Both indicators require the estimation of the so-called Net Present Value (NPV) [187]. Let DR be the average discount rate and Y is the number of years after the initial investment. The IRR and the PP associated with the $n-$th REC member are defined as in equation (3.7)

$$\begin{aligned} IRR(x_n, Y) &= \left\{ DR \quad | \quad NPV = CAPEX_n + \sum_{y=1}^{Y} \frac{MS(y,x_n)}{(1+DR)^y} = 0 \right\} \\ PP(x_n, DR) &= \left\{ Y \quad | \quad NPV = CAPEX_n + \sum_{y=1}^{Y} \frac{MS(y,x_n)}{(1+DR)^y} = 0 \right\} \end{aligned} \tag{3.7}$$

where

- $CAPEX_n$ is the CApital EXpenditure (CAPEX) of the $n-$th REC member for the installation of a PV generator with a BESS of capacity x_n;
- $MS(y, x_n)$ represents the annual savings achieved in the $y-$th year resulting from the difference between the energy bill reduced by the self-consumption or the valorisation of the grid-injected energy, and the bill in the purely passive consumer scenario (i.e., without PV generator and BESS). The OPerative EXpenses (OPEX) are included too, and may reduce the value of $MS(y, x_n)$

The energy sold to the grid is remunerated at the wholesale market price p_{sell}, while the electricity absorbed from the main grid is bought at the retail price p_{buy}, where normally $p_{sell} < p_{buy}$. If the P2G energy sharing policy is used, the difference between p_{sell} and p_{buy} depends just on external factors driving the market. In the P2P case instead, the economic value is computed on the basis of the so-called supply-to-demand ratio (SDR) method [188], [126]. Following this approach, the electricity buying and selling prices between REC members (labelled as $p_{buy,REC}$ and $p_{sell,REC}$, respectively) change dynamically within the REC as a function of the actual power demand and supply at a given time. In the following, an explanation of the SDR methodology is offered.

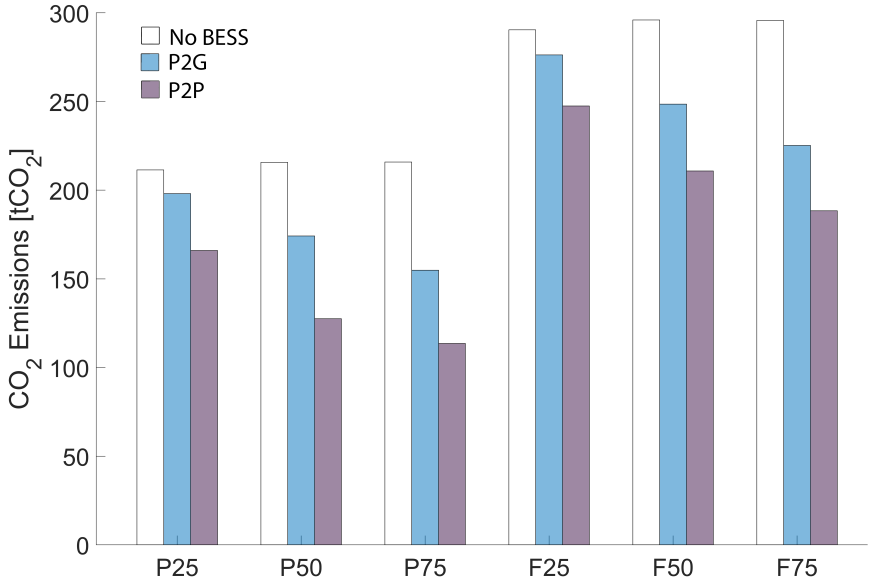

FIGURE 3.7: Yearly total CO_2 emissions either with or without BESSs, and by choosing P2P or P2G as the sharing policies.

3.5.4.1 SDR method for dynamic energy price computation

As already introduced in Sections 3.5 and 3.3.2, the adopted P2P energy sharing policy relies on the assumption that a single aggregator for the whole REC trades the energy with an electricity retailer.

Let $SDR(t) = \frac{\Delta E_S(t)}{\Delta E_B(t)}$ be the supply-to-demand ratio within the REC at time t [126, 188], namely the ratio between the total energy sold and bought by all REC members (denoted with symbols $\Delta E_S(t)$ and $\Delta E_B(t)$, respectively) within a given time slot (e.g., 15 minutes in the case study at hand). Starting from the basic economic principle that the selling price of any good is inversely proportional to its availability on the market, the electricity selling price within the REC is given by

$$p_{sell,REC}(t) = \frac{1}{a \cdot SDR(t) + b} \tag{3.8}$$

where, in the case at hand, parameters a and b can be determined under two specific conditions, i.e. when $SDR(t) = 0$ and when $SDR(t) = 1$. In the former case, all of the energy required by the REC must be bought from the main grid at a price p_{buy} through the aggregator. Therefore, the buying price within the REC $p_{buy,REC}$ is equal to p_{buy} and must be in turn equal to the internal selling price, since the aggregator should not generate net incomes. Hence, for $SDR(t) = 0$, $b = \frac{1}{p_{buy}}$.

If $SDR(t) \geq 1$, the energy balance of the REC is positive and the surplus of energy can be injected into the grid at a price p_{sell}. Thus, the internal selling and buying prices between REC members can also be set to the same minimum allowed value, i.e. p_{sell}. In particular, if $SDR(t) = 1$, it follows from (3.8) that $b = \frac{1}{p_{sell}}$ and $a = \frac{p_{buy} - p_{sell}}{p_{buy} \cdot p_{sell}}$. Thus, the electricity selling price within the REC is given by

$$p_{sell,REC}(t) = \begin{cases} \frac{p_{sell} \cdot p_{buy}}{(p_{buy} - p_{sell}) \cdot SDR(t) + p_{sell}} & 0 \leq SDR(t) < 1 \\ p_{sell} & SDR(t) \geq 1 \end{cases} \tag{3.9}$$

The buying price within the REC is based instead on a simple economic balance for $0 \leq SDR(t) < 1$, which is described by the following equation, i.e.

$$[\Delta E_B(t) - \Delta E_S(t)] \cdot p_{buy} = \Delta E_B(t) \cdot p_{buy,REC}(t) - \Delta E_S(t) \cdot p_{sell,REC}(t) \tag{3.10}$$

		P25	P50	P75	F25	F50	F75
IRR [%]	**P2G**	8	7	5	8	9	11
	P2P	9	7	6	7	9	10
PP [yrs]	**P2G**	8	10	12	9	9	7
	P2P	8	10	12	9	8	7

TABLE 3.4: IRR and PP values for an aggregator purchasing PV generators and BESSs for all REC members in scenarios *P*25, *P*50, *P*75, *F*25, *F*50 and *F*75 if either the P2G or the P2P energy sharing policy are used.

Therefore, by replacing the definition of $SDR(t)$ into (3.10) and recalling that if $SDR(t) \geq 1$ the buying price must be equal to p_{sell} for the aforementioned reasons, the result is that

$$p_{buy,REC}(t) = \begin{cases} p_{sell,REC}(t)SDR(t) + p_{buy}(1 - SDR(t)) & 0 \leq SDR(t) < 1 \\ p_{sell} & SDR(t) \geq 1 \end{cases} \tag{3.11}$$

Equations (3.9) and (3.11) are finally used to determine the monetary savings needed to compute (3.7).

3.5.4.2 Investment Analysis Results

The power exchanges between REC members are managed by a single legal entity (shortly referred to as "aggregator" in the following), which collects information about the BESSs state, PV systems and loads at every time instant. In the analysis we assessed the IRR and PP both when the aggregator purchases the batteries and when the REC members pay the upfront cost.

Since a lot of parameters need to be considered to perform the analysis and univocal results can hardly obtained due to the multiple uncertainty sources affecting the NPV computation, the following assumptions were made:

- The CAPEX costs for PV are proportional to the installed PV generation (1200 €/kWp) and BESS (600 €/kW h) capacities [189]. The OPEX costs instead, are about 2.1% and 1.5% of their CAPEX values per year, as in [189].
- No incentives are in place for the installation of PV units or BESS, which qualifies this analysis as the worst-case scenario.
- A simplified model for PV efficiency decrease is implemented. As a result, the amount of generated PV energy is supposed to decrease linearly by 0.5% per year due to degradation [190].
- In the P2G case, the average values of p_{sell} and p_{buy} are 0.052 €/kWh and 0.21 €/kWh respectively, in accordance with the Italian market data for 2019 [191].
- When the P2P policy is considered instead, $p_{sell,REC}$ and $p_{buy,REC}$ change as a function of time (as explained in Section 3.3.2), but their values are constrained within the interval $[p_{sell}, p_{buy}]$, in order to increase the economic value of energy exchanges between REC members, as prescribed by the EU commission [192].
- For IRR calculation, the time horizon Y is 20 years, which is the typical lifetime of modern PV systems. When calculating PP instead, the discount rate DR is assumed to be 0%, since we suppose that the user purchases the PV systems without comparing its profitability to other investments.
- The battery systems are replaced after 10 years of use, which is in line with the results of several papers estimating the lifetime expectancy of Lithium-ion stationary home storage systems [193, 194].
- Since it is difficult to estimate the yearly increase in the retail prices for buying electricity in the next years [195], we assumed them to be constant. Again, this represents a worst-case scenario, since the economic benefits of installing a PV system with a BESS increase as the gap between the electricity buying and selling prices grows.

If the analysis is performed from the perspective of the aggregator purchasing the BESSs (see Table 3.4), the "future" scenarios are more profitable than the "present" ones. Indeed, electrifying the heating system with a HP increases the base-load consumption and the savings due to a higher exploitation of a PV+BESS system. Choosing P2P policy over

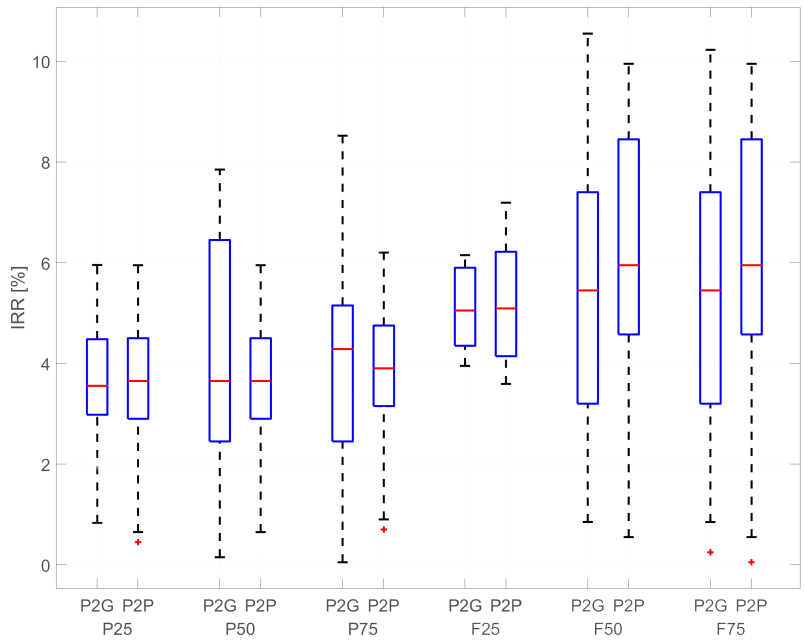

(a)

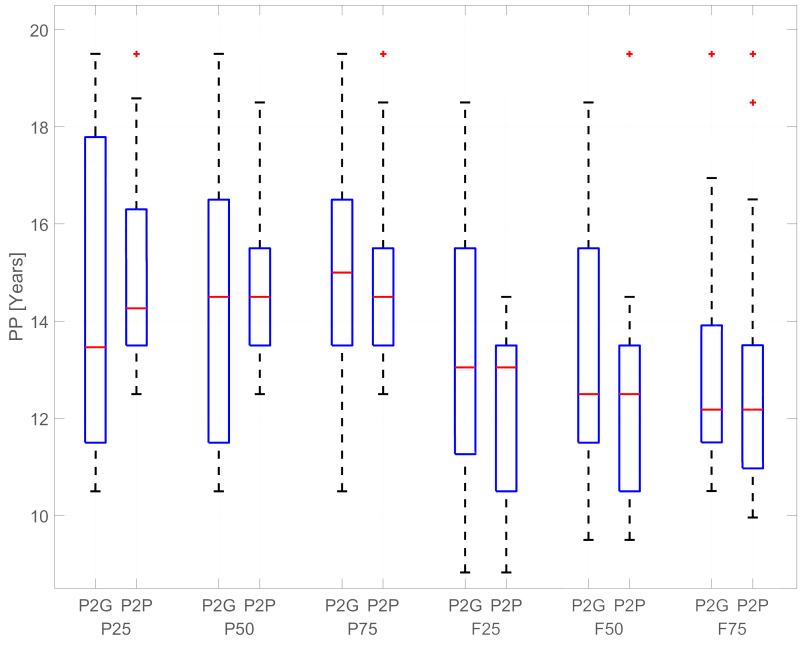

(b)

FIGURE 3.8: Box-and-whiskers plots of the IRR (a) and PP (b) values of individual REC members purchasing a PV generator with a BESS in different scenarios by using either the P2G or the P2P energy sharing policy. In practice, only the results related to the REC members with $PP \leq 20$ and $IRR \geq 0\%$ are represented here, i.e. the vast majority.

P2G one instead, has little impact only on the IRR and PP values. This is explained by the fact that the main economic driver for the installation of the PV+BESS systems is the PV unit, whose generation capabilities do not depend on the sharing policy. If the impact of an increased number of deployed BESSs is analysed instead, we realised that it is positive in "future" scenarios only, when the electricity demand is supposed to be higher. This highlights once more the importance of growing the installed BESS capacity along with the energy demand.

Figure 3.8 shows instead a box-plot representation of the IRR and PP values of the users whose $PP \leq 20$ and $IRR \geq 0\%$, i.e. the majority. The results are consistent with those presented in Table 3.4, though some minor differences can be noted. For example, in "future" load scenarios, the IRR median values for the same energy sharing policy tend to grow by about 1.5-2% on average, while the PP values decrease by 1-2 years. Moreover, the BESS penetration does not strongly affect the median values, but has contrasting effects on the variability of IRR and PP. Interestingly enough, the IRR and PP interquartile ranges in the P2P case are narrower than in the P2G case in almost all scenarios. This means the PV+BESS benefits are more equally spread among REC members than in the P2G case. In this scenario, REC members are supposed to trade power directly between themselves rather than relying on the distribution grid, which tends to equalise the disparities between users.

3.6 Conclusions

In this Chapter, the BESS sizing problem applied to the case of RECs was analysed by adapting a well-known genetic algorithm to the particular features of this problem. The joint minimisation of both the share of electricity purchased from the grid G_A and the total installed BESS capacity C_T stems from the main purpose of RECs, which is to reduce the dependence of users from the main grid. Since the participation of users to a REC is voluntary, the optimisation strategy automatically excludes the members that do not want or cannot purchase a BESS, while still considering them in the simulations as prosumers. The DSO perspective is also considered, since the algorithm discards the solutions that violate the voltage levels regulatory limits. Finally, two different BESS control strategies are considered: a business-as-usual P2G one and a REC-oriented P2P one.

From a quantitative standpoint, G_A decreases by 5%-80%, compared to the no-storage scenario. Such a reduction depends on the season of the year, the energy sharing policy, the number of prosumers installing a BESS (with a total installed capacity of C_T) and the load conditions. The REC-oriented P2P algorithm is able to exploit the storage capacity more efficiently than the P2G one, especially when the BESS penetration is low (many users do not install a BESS) and when the electric demand grows (e.g. due to the deployment of HPs). A simplified economic analysis was also presented, and the P2P benefit is further confirmed by a more equal distribution of the PV+BESS benefits. From a broader system-view perspective, the proposed BESS sizing algorithm may significantly reduce both the energy losses (by 20-40 % in the considered case studies) and the CO_2 emissions (by 10%-50%).

The results show that, for each scenario, a "critical" installed BESS capacity value is reached, beyond which the installation of additional storage capacity is useless for reducing G_A. In order to understand why this happens, we need to highlight that, in order to maximise the usage of the storage systems, the mismatch between power production and demand has to be limited.

For example, Figure 3.9 shows what happens when the mismatch is leaning towards the "production" side, i.e. when an excessive amount of PV power is generated. In this case, two scenarios consisting of two different P2P-controlled BESS capacities $C_{T,A}$ and $C_{T,B}$ installed on the REC are considered. Note that these results are presented for the $P50$ scenario, so half of the REC members are equipped with a BESS and there are no HPs.

As shown in Figure 3.9(a) for a three-day time horizon, the cumulative SOC increases when the REC's net-power at the transformer is positive (overproduction), whereas the cumulative SOC decreases in the opposite scenario. Below the threshold PV penetration level, if the battery size is increased from $C_{T,A}$ to $C_{T,B}$, the SOC grows more slowly and, by the end of the third day the maximum SOC is still not reached. In this case, the amount of PV-produced energy does not saturate the BESS capacity, thus increasing the battery capacity from $C_{T,A}$ to $C_{T,B}$ significantly reduces G_A. Conversely, if the installed PV power is over the maximum PV penetration level (around 45% in the current case study, as previously mentioned), both the battery capacities $C_{T,A}$ and $C_{T,B}$ are saturated by the end of the third day. In that scenario, the total G_A just slightly improves when the larger total $C_{T,B}$ capacity is used, as shown in Figure 3.9(b). Therefore, in this case, further increasing the total BESS capacity of a REC is unnecessarily expensive.

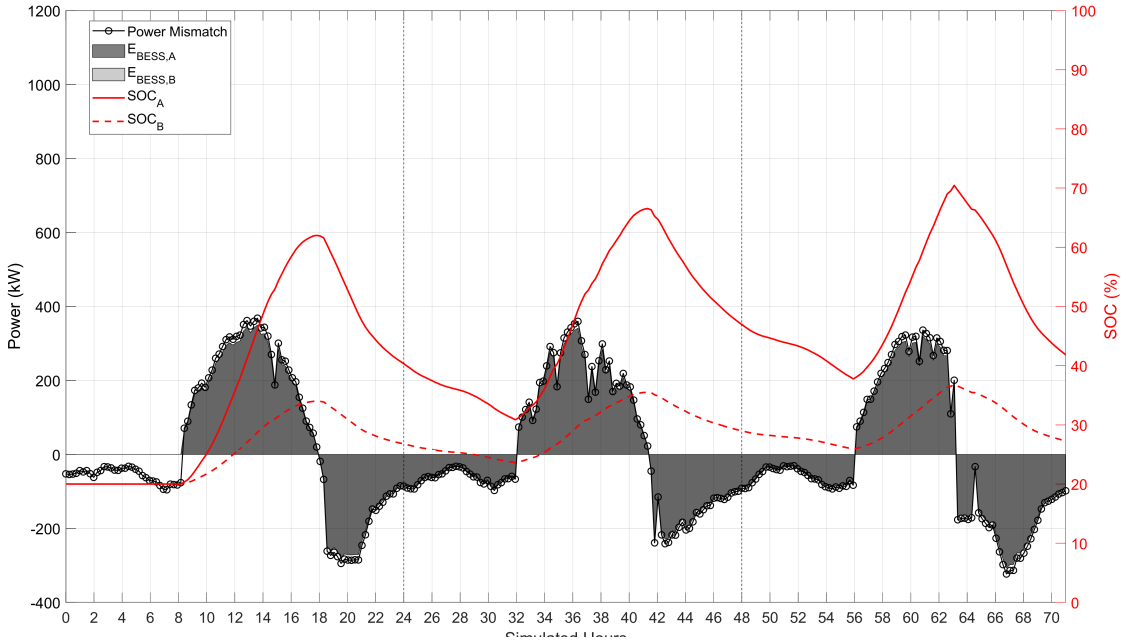

(a)

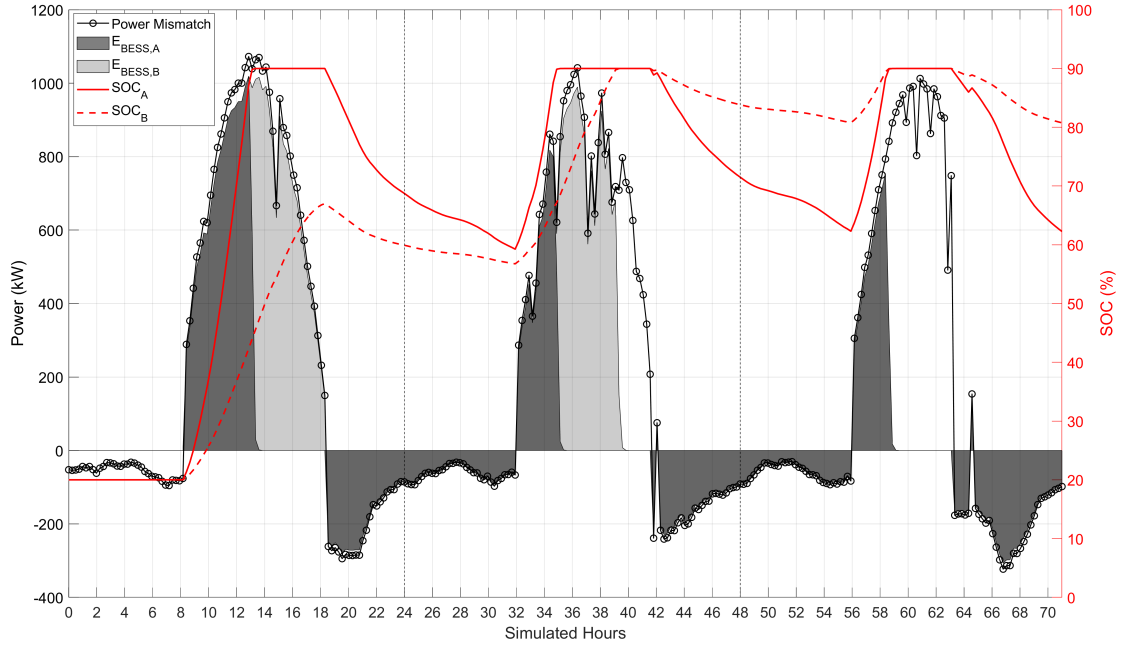

(b)

FIGURE 3.9: Effect of a $C_{T,A}$ to $C_{T,B}$ total storage capacity increase on the district-level SOC when PV penetration is under (a) or over (b) the maximum penetration level for the case study.

Since the economic compensation for selling electricity is generally much lower than the electricity buying price (check the price difference between p_{sell} and p_{buy} in 3.5), this study reveals that a careful and balanced sizing of BESSs with respect to the actual power generation and demand is essential to avoid a waste of both energy and hardware resources. Also, some help in this direction may come from the use of flexible loads able to reduce the mismatch between power supply and demand throughout the day. An example of this strategy, albeit based on EV smart charging instead of BESSs control, is going to be presented in Chapter 4.

Chapter 4

EV charging impact mitigation

In this Chapter[1], a centralised coordinated smart charging algorithm for EVs is presented. The objective of the algorithm is to perform active power support, i.e. peak-shaving and valley-filling the active power profile of a LV/MV transformer. The analysis considers different penetration levels of PV and EV stations, and analyses the impact of smart charging not only on the transformer, but also on the voltage levels of a test LV grid, the energy independence of the district from the main electric grid and the battery wear caused by the higher cycling the battery undergoes.

4.1 Introduction

The European Union's (EU) target for 2050 greenhouse gases emissions reduction is 55%, compared to the levels recorded in 1990 [196]. For this purpose, it is essential to reduce the environmental impact of the mobility sector, which, per se, accounts for around 20% of the total worldwide carbon dioxide emissions in the atmosphere [197]. The conversion of a sizeable number of internal combustion engine vehicles (ICEVs) into fully electric vehicles (EVs) would definitely contribute to solve to this problem [198, 199], provided the electricity mix used to charge their batteries is mainly based on renewable energy sources. However, in order to meet the aforementioned goals, both the number of EVs and generation units (typically PV systems) has to considerably grow in the next years. A large-scale deployment of EVs [200] and PVs [201] may pose a variety of business and technical challenges, especially at the distribution level, where large daily fluctuations of power demand and supply may jeopardize grid stability but also require new grid state estimation techniques [202]. From a Distribution System Operator (DSO) perspective, the technical challenges are the most important ones, but their solution cannot be detrimental to the quality of service and the profitability expected by EV owners. Several studies found that one of the parameters highly affected by an increasing EV penetration is the Medium-Voltage/Low-Voltage (MV/LV) transformer loading at the secondary substations (SS) [46, 54]. Moreover, it is well-known that EVs simultaneously charging may cause voltage fluctuations [46–48], lines overloading [46, 48, 54] and/or power quality problems, such as frequency deviations [46, 48, 54], voltage imbalances [46, 69, 78], harmonics [85, 87] and flicker [91, 93]. As a consequence, it is difficult to comply with the requirements of local, national or international regulations, such as the ones specified in the EN Standard for LV electricity distribution EN 50160:2010 [11]. The additional power demand peaks due to EVs could be mitigated through smart charging. This can be achieved by using a variety of scheduling algorithms conceived not only to change the absorbed power depending on the actual urgency of battery charging, but also, whenever possible, to exploit possible *bidirectional* vehicle-to-grid (V2G) control schemes. Indeed, modern power electronics converters allow EVs to either absorb or inject electrical power in the grid if suitable control techniques are implemented. As a result, the EV batteries can be regarded not only as loads, but also as additional, dynamic storage elements supporting the peaks of electrical power demand, thus maximising the utilisation of the distributed energy resources (DERs) capacity [144, 145, 203]. In this context, the distinction between a "centralised" V2G algorithm (where the charging is entirely demanded to a central control unit, the so called "aggregator") and a "decentralised" V2G scheme (where EV owners can decide whether to charge the battery or not in a pre-defined time-slot) is crucial. Usually, the active power support to shave the power demand peaks at the transformer is more effective if all the EV charging stations are able to cooperate. Therefore, in this case, a *centralised* V2G scheme (in which EV charging or discharging is entirely managed by the aggregator) is preferable, especially if the power fluctuations are further increased by the power absorption of a large EV fleet. The problem of centralised V2G control becomes even more important if not only the EV load profiles, but also the power generation ones change as a function of time, e.g., as a result of the increasing photovoltatic (PV) penetration. In this paper, an automated strategy

[1] Part of this chapter was submitted for publication on Sustainable Energy Grids and Networks

Objective	Methodology	Type	Examples
Maximising PV Utilisation	PSO+Real-Time	Centralised	[171]
	PSO+Model-Predictive Control	Decentralised	[169]
	Linear Programming or Real-Time	Centralised	[131]
	Mixed-Integer Linear Programming	Centralised	[135]
	Non-Linear Programming	Decentralised	[137]
	Mixed-Integer Quadratic Programming	Centralised	[145]
Minimising NLV	Model-Predictive Control	Centralised	[167, 168]
	Real-Time Control	Centralised	[204–207]
	Fuzzy Control+Weighted Sum	Decentralised	[208]
	Particle Swarm Optimisation	Centralised	[150–152]
	Genetic Agorithm	Centralised	[160]
	Quadratic Programming	Decentralised	[47, 141–143]
	Quadratic Programming	Centralised	[140, 141, 144]

TABLE 4.1: Relevant literature overview on smart EV charging techniques.

for EV charging with V2G capability is proposed and analysed in-depth, considering the EV-PV interaction as well. The proposed approach aims at minimising the net load variance at the substration transformer.

The main elements of novelty presented in this work are summarised below:

- Even if initially we assume perfect knowledge of both load profiles and EV availability for active power support, the effect of possible deviation between the expected scenario and the real one in subsequent days is evaluated, showcasing the good robustness of the proposed approach in realistic scenarios.
- The interaction between EVs and PV systems is analysed in a broad set of operating conditions, ranging from current (in which the PV and EV penetration levels are low) to future ones, when PV and EV penetrations are instead supposed to be much higher.
- A repeated power low analysis with a 15-minute time step is performed to assess to what extent the proposed centralised V2G-based optimisation strategy is beneficial in terms of voltage stability.
- Finally, a preliminary study on battery wear (one of the most debated aspects of V2G-based charging schemes) is presented.

The rest of the paper is structured as follows. In Section 4.2, the specific contribution of this paper in the context of the related work is briefly presented. In Section 4.3, the optimisation problem and the underlying methodology are formalised. Section 4.4 describes the key features of the case study considered for testing along with the main simulation settings. Section 4.5 reports a quantitative performance evaluation of the proposed optimal smart EV charging approach. Finally, Section 4.6 provides an overview of the broader impact of the proposed technique on: users' energy requirements for self-sufficiency, grid voltage stability and EV battery wear. Finally, Section 4.7 concludes the paper.

4.2 Related Work

Some of the most significant methodologies proposed in the literature to perform smart EV battery charging (possibly empowered by V2G) are listed in Table 4.1. Due to the broad variety of possible objective functions and considering the scope of this work, we will mainly focus on two classes of problems, i.e. those aimed at maximizing the exploitation of PV resources (usually to reduce the investment payback period or the overall CO2 emissions) and those reducing the aggregated Net-Load Variance (NLV) at the transformer substation.

In the first group, Liu et al. in [171] use a centralised Particle Swarm Optimisation (PSO) algorithm combined to a real-time EV charging control to maximise PV utilisation, whereas El-Naggar et al. combined PSO and model-predictive control [169] for the same purpose. Some other Authors used linear [131] or mixed-integer linear programming [135] to maximise the PV utilisation and, in [135] to maximise the economic revenues as well. Alternatively, Ioakimidis et al. [137] and Cortes-Borray et al. [145] relied on non-linear and quadratic programming respectively, to minimise the

share of energy produced by PV and injected into the grid. Most of these solutions (with the exception of those in [137, 169]) rely on a centralised approach, so the energy exchanges between the users are encouraged.

The inherent difference between the smart EV charging techniques listed above and the methodology adopted in this paper is that the former ones tend to minimise the amount of PV energy sold to the grid by maximising its local exploitation for EV charging. In this paper instead, the smart EV charging is applied both when the PV generators are not producing and when they overproduce. This is indeed essential for NLV minimisation, especially when many EVs and PV systems are actively connected to the grid at the same time.

The meaning of NLV and the related optimisation policy, however, considerably depend on the problem definition. For instance, if the goal is to perform real-time smart EV charging, the NLV can only be minimised over the timestep duration, using centralised optimal control algorithms. For example, Jian et al. [205, 206] minimised the NLV by using a centralised algorithm that also discharges the EV batteries when the electricity demand grows. This approach was also adopted in [204], by including the charging costs in the optimisation algorithm. Hashim et al. [207] minimised the NLV of a high-voltage/medium-voltage (HV/MV) transformer, so the V2G-based mitigation capability of the EV charging stations increase due to the higher number of connected EVs. These controls, although very effective in practice and powerful when paired to forecasting techniques, cannot, per se, be used to investigate the potential benefits of centralised V2G-based policies over a time horizon of several hours or days, since they only optimise the NLV at a given timestep. Conversely, the charging scheduling solutions based on NLV minimisation over long time intervals can hardly be implemented in the real world because forecasting the activities of many users' is very difficult and may lead to EV charging schedules considerably different from the reality.

The methodology presented in this paper lies in between these two extreme visions outlined above. It does not address a real-time optimal scheduling problem, but at the same time it provides an *a-posteriori* solution that, with a reasonable lag, can be used to define a temptatively realistic EV charging schedule. In fact, the information collected over a full day can be used to find the globally optimal EV charging schedule minimising the NLV. Such a global solution can be found by solving a quadratic programming (QP) problem. Even if the actual performance in terms of NLV reduction will be lower than in ideal conditions, due to the differences in load, PV generation profiles and EV usage, the results are still rather good, as it will be clearly shown in Section 4.5. Such a performance evaluation in realistic conditions, as well as the study of the impact of the proposed smart EV charging policy on the LV distribution grid and battery are the key elements of novelty of this paper, compared to other similar centralised strategies, such as [140, 141, 144]. In fact, only a few Authors perform a proper power-flow analysis to assess the combined impact of PV and EV systems on grid voltage stability [152, 208]. However, no analyses on battery wear are however usually reported. A variety of other solutions for NLV minimisation based on a decentralised approach exist [47, 141–143, 208]. In those studies, there is no need to share any information between the EV charging stations but it is very unlikely that the global NLV is minimised, since the smart EV charging algorithm just relies on local information.

4.3 Problem formulation

Given an LV distribution system consisting of a set $\mathcal{U}$ of M users, let $\mathcal{U}_{PV}$ and $\mathcal{U}_{EV}$ be the subsets of $\mathcal{U}$ including the $K \leq M$ and the $N \leq M$ users equipped with a PV system or an EV charging station, respectively. Also, let $PV_{share} = \frac{K}{M}$ and $EV_{share} = \frac{N}{M}$ be the corresponding shares of users. Assuming, for the sake of simplicity, but without loss of generality, that

- each user owns at most one EV;
- no energy storage systems different from the EV batteries are deployed in the grid;
- the users consumption and the EV battery charging process are completely monitored and controlled by an aggregator, as customary in centralised smart EV charging schemes [144, 145];
- each EV is connected to its own proprietary charging station;

the average net power absorbed from or injected into the grid by the $i-$th user within the $t-$th metering time slot of duration Δt is

$$p_{i,t}^{Net} = p_{i,t}^{Load} + p_{i,t}^{EV} - p_{i,t}^{PV}, \quad i \in \mathcal{U} \quad t = 1, \ldots, T \tag{4.1}$$

where T is the number of data collected in a given time interval (e.g., one day), $p_{i,t}^{Load}$ is the user's average load consumption due to seasonal factors, building occupancy and users' activities within the $t-$th time slot, and $p_{i,t}^{EV} \neq 0$, $p_{i,t}^{PV} \neq 0$ are the additional average EV power consumption and the generated average PV power in the same time slot t, if $i \in \mathcal{U}_{EV}$ or $i \in \mathcal{U}_{PV}$, respectively. Of course, if the $i-$th user does not own either a PV system or an EV, both terms $p_{i,t}^{PV}$ and $p_{i,t}^{EV}$ in (4.1) are null. Quite importantly, when a PV system is available, the sequence of $p_{i,t}^{PV}$ values (similarly to those of $p_{i,t}^{Load}$) can be regarded as inputs to the proposed optimisation problem, as they depend on the actual irradiance as well as on the PV capacity installed by each user. On the contrary, all terms $p_{i,t}^{EV}$ can be regarded as the decision variables of the optimisation problem, as they can be actually modified by the adopted smart EV charging policy (if any). As a consequence, the values of $p_{i,t}^{EV}$ are positive when the EV is connected to the charging station and the battery is under charge, while they become negative if a V2G policy for active power support is applied.

If the $p_{i,t}^{Net}$ values of all users in the same time slot t are summed up, it follows from (4.1) that the aggregate net load is

$$P_{i,t}^{Net} = \sum_{i \in \mathcal{U}} p_{i,t}^{Net} = P_t^{Base} + \sum_{j \in \mathcal{U}_{EV}} p_{j,t}^{EV}, \quad t = 1, \ldots, T \tag{4.2}$$

where the sequence of values $P_t^{Base} = \sum_{i \in \mathcal{U}} p_{i,t}^{Load} + \sum_{k \in \mathcal{U}_{PV}} p_{k,t}^{PV}$ for $1, \ldots, T$ is the baseline net load for the considered optimisation problem when no EVs are considered.

If we denote with $i_1, \ldots, i_N$ the indexes of the users in the subset $\mathcal{U}_{EV} \subseteq \mathcal{U}$, by rearranging the terms of the rightmost side of (4.2) for every $t = 1, \ldots, T$ into a single $T \cdot (N+1)-$long column vector

$$\mathbf{P} = [P_1^{Base}, P_{i_1,1}^{EV}, ..., p_{i_N,1}^{EV}, ..., P_T^{Base}, p_{i_1,T}^{EV}, ..., p_{i_N,T}^{EV}]^T \tag{4.3}$$

through a few basic algebraic steps it can be shown that the maximum likelihood estimator of the daily aggregated NLV can be rearranged into a matrix form as follows, i.e.,

$$\sigma_P^2(\mathbf{P}) = \frac{1}{T} \cdot \sum_{t=1}^{T} \left(P_t^{Net} - \frac{1}{T} \sum_{t=1}^{T} P_t^{Net} \right)^2 = \frac{1}{2} \mathbf{P}^T \mathbf{H} \mathbf{P} \tag{4.4}$$

where

$$\mathbf{H} = \frac{2}{T^2} \left[\begin{array}{cccc} (T-1)\mathbf{U}_{N+1} & -\mathbf{U}_{N+1} & ... & -\mathbf{U}_{N+1} \\ \vdots & \vdots & \ddots & \vdots \\ -\mathbf{U}_{N+1} & -\mathbf{U}_{N+1} & ... & (T-1)\mathbf{U}_{N+1} \end{array} \right] \Bigg\} T \text{ blocks}$$

is a square matrix composed by $T \times T$ blocks including the $(N+1) \times (N+1)$ all-ones matrix $\mathbf{U}_{N+1}$, multiplied by either $T-1$ or -1.

If (4.3) is the vector of the decision variables used to schedule the battery charging of all EVs over the considered time interval and (4.4) is the chosen objective function, the corresponding optimisation problem can be easily formalized as follows, i.e.,

$$\min_{\mathbf{P}} \ \sigma_P^2(\mathbf{P}). \tag{4.5}$$

Expression (4.4) confirms that the chosen objective function is inherently quadratic. Therefore, a solution to (4.5) can be found with standard QP solving tools.

Nevertheless, in order to find a correct and realistic EV charging schedule, a number of further constraints must be included. Such constraints are explained and formalised below.

1. **Constraints due to the actual net-load conditions**. The elements P_t^{Base} of (4.3) have to be excluded from the optimisation process, since, as explained above, the aggregate base net-load values are in fact an input to the optimisation problem. Thus, the following equality constraints have to be applied, i.e.,

$$P_t^{Base} = P_t^*, \quad t = 1, \ldots, T \tag{4.6}$$

where P_t^* for $t = 1, \ldots, T$ is the overall net power demand profile (excluding the EVs) measured in each time slot.

2. **Constraints on EV battery charging**. In every metering time slot t, each EV can be either connected to or disconnected from its own charging station, depending on actual users' needs. Assuming that S_j (for $j = 1, \ldots, N$) is the number of the daily charging sessions of the $j-$th EV, and denoting with $\mathcal{T}_{s_j} \subseteq \mathcal{T}$ (where $\mathcal{T} = \{1, \ldots, T\}$) the subset of time slots of the $s-$th charging session of vehicle j (i.e., for $s = 1, \ldots \ldots, S_j$), the following equality constraints on EVs' battery state-of-charge (SOC) must be met to prevent the EV battery charge to deplete during the following scheduled trip, i.e.

$$\sum_{t \in \mathcal{T}_{s_j}} \frac{\eta_j}{C_j} p_{j,t}^{EV} \Delta t = (SOC_{s_j}^{end} - SOC_{s_j}^{init}) \qquad s = 1, \ldots, S_n, \quad j \in \mathcal{U}_{EV} \tag{4.7}$$

In (4.7) constants η_j and C_j represent the battery charging efficiency and the battery capacity of the j-th EV, while $SOC_{s_j}^{init}$ and $SOC_{s_j}^{end}$ are the battery SOC values at the beginning and at the end of the $s-$th charging session, respectively. It is important to emphasize that both $SOC_{s_j}^{init}$ and $SOC_{s_j}^{end}$ are just inputs to the optimisation problem, as they depend on the actual use of each EV. The $SOC_{s_j}^{init}$ values can be measured as soon as the EV is connected to the charging station, while the $SOC_{s_j}^{end}$ values at the end of each charging session are usually close to the maximum attainable SOC.

Besides (4.7), a further set of inequality constraints must be applied during each EV charging session to prevent excessive battery charging or discharging (in V2G mode) i.e.,

$$SOC_{MIN} \leq SOC_{s_j}^{init} + \sum_{\tau} \frac{\eta_j}{C_j} p_{j,t}^{EV} \Delta t \leq SOC_{MAX} \qquad \forall \tau \in \mathcal{T}_{s_j}, \quad s = 1, \ldots, S_j, \quad j \in \mathcal{U}_{EV}. \tag{4.8}$$

This is needed to prevent a faster battery wear, as highlighted in [209, 210]. Note that, even if the lower and upper threshold valus SOC_{MIN} and SOC_{MAX} actually depend on battery type, size and manufacturer, for the sake of simplicity, in the rest of this paper these limits will be assumed to be the same for all vehicles. In fact, they usually do not differ significantly.

3. **Constraints due to EVs unavailability**. When an EV is not connected to the charging station, of course its battery can neither be charged, nor it can be used for V2G-based active power support. Therefore, the following equality constraints have to be applied, i.e.,

$$p_{j,t}^{EV} = 0 \quad t \in \mathcal{T}_{d_j}, \quad j \in \mathcal{U}_{EV} \tag{4.9}$$

where $\mathcal{T}_{d_j} = \mathcal{T} \backslash (\bigcup_{s \in S_j} \mathcal{T}_{s_j})$ includes all time slots in which the $j-$th EV is not connected to the charging station.

4. **Constraints on maximum EV charging and discharging power**. Finally, it is important to recall that, due to contractual restrictions, technology limitations and/or safety reasons, the EV charging and discharging power cannot exceed a given limit $\pm P_j^{LIM}$. Therefore, a further set of inequality constraints to apply when solving the optimisation problem is given by

$$|p_{j,t}^{EV}| \leq P_j^{LIM} \quad t = 1, \ldots T, \quad j \in \mathcal{U}_{EV}. \tag{4.10}$$

It can be observed that constraints (4.6)-(4.10) are all linear and can be easily formalised in a matrix form by using sparse matrices. Therefore, they are simple to implement and the memory requirements are reasonable. As a consequence, the QP optimisation problem based on (4.5) and subject to constraints (4.6)-(4.10) converges to a solution within a reasonable time. As a consequence, the scalability of the optimisation problem is also acceptable.

4.4 Case Study Description

This Section describes the features of the LV distribution grid used as a case study, the baseline load profiles, the way in which both the EV usage profiles and the PV generation patterns are generated. A summary of the general simulation settings and scenarios that were considered to evaluate the performance of the proposed optimisation strategy is presented as well.

4.4.1 Grid Model

The distribution system used as a case study is the IEEE 906-bus LV Test Feeder[2], which is an example of a typical 240 V European LV grid, with a 800 kV A transformer and conductors' ampacities ranging between 200 and 500 A for the main lines and between 50 and 80 A for the secondary ones [211].

4.4.2 Baseline Load Profiles

The daily power consumption profiles of 297 households were synthesized through LPG[3], a bottom-up software application that mimics the domestic electricity demand of different kinds of users depending on their daily activities. The power consumption profiles of different users, taken from the database created for [212], were aggregated into 90 load profiles associated to as many buildings, in order to replace the 90 non-zero-injection buses of the original IEEE 906-bus LV Test Feeder. Such baseline power demand profiles keep into consideration the building stock composition and the age distribution of the city of Bolzano/Bozen, Italy, based on ASTAT[4] data. As a result, the building stock consists of single-family (i.e., detached) houses and buildings with four or six flats. The contractual power demand of each household is assumed to be 4.5 kW, rather than 3 kW (although this is currently the most common case in Italy for residential users) in order to safely accommodate the additional load due to EV charging (see Section 4.4.3). The power factors values are randomly chosen between 0.95 and 1.

4.4.3 Baseline EV Usage Profiles

The baseline EV consumption and charging patterns based on their supposed usage were generated with the RAMP-mobility[5] software tool [213], by setting the shares of plug-in hybrid EVs (PHEVs), battery EVs (BEV) and their battery capacity. The shares of PHEV and BEVs are assumed to be 60% and 40%, respectively[6], while the battery capacity is around 8-10 kW h for PHEVs and between 30 and 100 kW h for BEVs[7]. The maximum EV charging and discharging power P_j^{LIM} was set to 3.7 kW for $nj \in \mathcal{U}_{EV}$, as assumed in other research works [47, 214], while the EV charging-discharging efficiency η_{EV} is around 0.9 as in [47, 215]. The resulting average yearly EV energy consumption per charging station is around 1.1 MW h, in good agreement with the Eurostat data on vehicular mobility in Italy, where each vehicle travels 11.4 km per day on average[8], and the EV consumption is assumed to be around 0.23 kWh/km [216]. In the rest of this paper the simulations are based on the generated EV profiles, assuming that each EV drains the maximum allowed power when it is connected to the charging station, till the target SOC (usually maximum) is reached.

4.4.4 PV Generation Profiles

Due to the limited geographical area of the considered LV distribution grid, for the sake of simplicity, all users are assumed to share the same irradiation and panel temperature patterns. In the considered case study, such data are

[2] IEEE LV Test Feeder: https://site.ieee.org/pes-testfeeders/

[3] LPG: A Bottom-Up Customizable Load Generator, Noah Pflugradt, `https://www.loadprofilegenerator.de`

[4] ASTAT: Statistics Institute for the Autonomous Province of South-Tyrol

[5] RAMP-mobility: a RAMP application for generating bottom-up stochastic electric vehicles load profile `https://github.com/RAMP-project/RAMP-mobility`

[6] Motus-E Market Analysis for Italy, `https://www.motus-e.org/analisi-di-mercato/gennaio-2022-i-primi-segnali-dellassenza-di-incentivi`

[7] EV Database Org, `https://ev-database.org/cheatsheet/useable-battery-capacity-electric-car`

[8] EUROSTAT: "Passenger Mobility Statistics 2021", `https://ec.europa.eu/eurostat/statistics-explained/index.php?title=File:Average_distance_per_person_per_day_(kilometres)_v3.png`

experimental, as they were collected at the Airport Bolzano Dolomity, Bozen (Italy) every 15 minutes in 2019. Of course, the installed PV capacity (if any) differs from user to user. In particular, the PV systems are sized in such a way that the amount of energy produced in the average day of each season and the corresponding energy consumption approximately coincide [217]. As a consequence, the resulting installed PV capacities per household generally range between 1.5 and 4 kW, in steps of 250 W, which is the size of a typical PV module [217].

4.4.5 Simulated Scenarios

The main used settings are briefly summarized below:

- The profiles of $M = 297$ users are aggregated to be connected to the 90 non-zero-injection buses of the LV test distribution system;
- The simulation time step is set to 15 minutes, which provides a good tradeoff between computational complexity and simulation accuracy [218]. As a result, $T = 96$. This is a realistic choice also because the last-generation smart meters (including those recently deployed in Italy) can measure and trasmit the power/energy consumption values every 15 minutes.
- To explore the joint impact of different levels of EV and PV penetration, the values of parameters EV_{share} and PV_{share} are increased from 10% to 90% and from 0% to 90%, respectively. In all cases, the users equipped with a PV system and/or with an EV charging station are selected randomly so that the results are comparable (i.e. a user equipped with a PV system retains it in higher PV penetration scenarios).

To keep the overall computation time within reasonable limits, the optimal EV charging schedules for each pair of EV_{share} and PV_{share} values were computed day-by-day over an average week in summer and winter, respectively, namely when the solar irradiation is close to its maximum and its minimum, respectively.

4.5 Optimisation Results

The proposed optimisation algorithm for EV smart charging was implemented in Matlab. The weekly scenarios were simulated using the High Performance Cluster (HPC) of the University of Trento. Each optimal daily EV charging schedule is computed using one of the available cores the cluster, belonging to a 2.8-3.4 GHz Intel Xeon Gold/E5 CPU (up to 30 cores are used in parallel). The parallelisation of the optimisation problem allows for a rapid estimate of all the EV charging schedules, even the ones where the EV penetration is very aggressive, so that the simulation times are always under one day. This result allows for the application of our methodology in a "day-ahead" context, optimising the EV charging for one day, and then applying the obtained profiles to the following one.

The overall weekly net-load profiles at the substation transformer computed without including the EVs and with the additional EV loads assuming a significant EV_{share} value (i.e., 60%) both without (lines with circles) and with the proposed V2G-based smart charging policy (dashed lines) are shown in Fig. 4.1a-4.1b. The figures are presented for both the summer and winter scenarios respectively, assuming that either no PV systems at all are installed (plots on the left) or about 30% of users are equipped with PV generation units (plots on the right).

In all cases, the effect of smart EV charging is twofold, i.e., power consumption peak shaving and reverse power flow prevention. This is especially visible when the PV penetration is higher and in the summer season, and confirms the correct operation of the smart EV charging optimisation algorithm. Interestingly, the reverse power flows are much less efficiently managed by the smart EV charging policy (the negative net-load peaks are shaved much less than the positive ones), due to the limited storage capability of EV batteries in the case of large PV overproduction. As it will be shown in Section 4.6, this issue will affect the voltage fluctuations as well.

The efficiency of the proposed V2G-based smart EV charging policy is assessed in terms of relative NLV reduction (NLVR) with respect to the no smart EV charging scenario.

Figs. 4.2b and 4.2a show the contour lines of the NLVR surfaces as a function of both PV_{share} and EV_{share} in the summer and winter scenarios, respectively. These diagrams quantify the joint effect of EV and PV penetration in ideal conditions (i.e., when a perfect schedule is possible), thus highlighting the operating conditions for which a maximum NLVR can be achieved. The analysis reveals that NLVR values exceeding 60% can be potentially reached in both summer

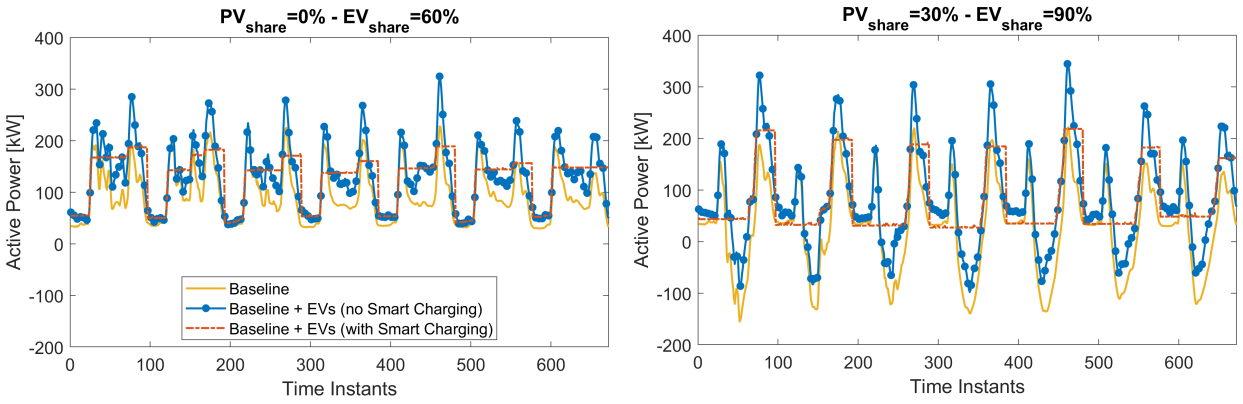

(A) Summer scenario

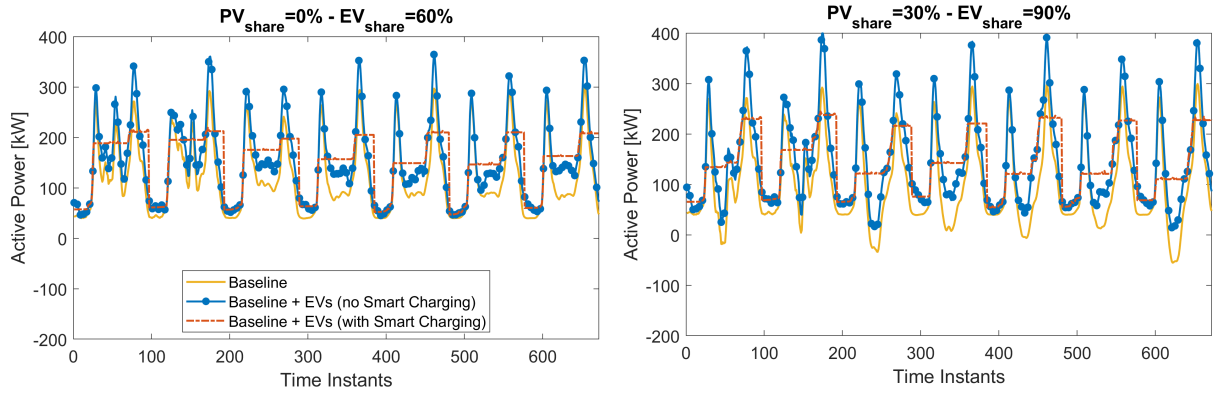

(B) Winter scenario

FIGURE 4.1: Active net-load power profiles at the substation transformer without EVs and with 60% of users provided with EVs both without and with adopting the proposed V2G-based smart charging policy. The plots in (a) and (b) refer to the summer and winter scenarios, respectively, assuming that the shares of users equipped with PV systems are 0% (left) or 30% (right).

and winter scenarios although the best conditions for the joint use of PV production for EV charging depend on the total amount of available solar energy. The curves in the winter scenario look like a zoomed view of the contour lines on the left side of the summer case. This is simply due to the fact that in winter a much larger number of PV generators is needed to reach the same total amount of PV energy which can be achieved in summer with $PV_{share} \leq$ 20%. Quite interestingly, if no PV generators at all are deployed, the maximum NLVR (between 50% and 55% in the case at hand) is reached realistically if EV_{share} ranges between 35% and 45%. While these numbers depend on the specific case study considered, this result is very important because it confirms that the optimal V2G-based EV charging scheme is potentially very effective, regardless of whether the distributed generators are installed or not. The effect of PV generators is twofold. To a certain extent (e.g., with PV_{share} up to 30%), the deployment of PV generators and the resulting solar energy, support the net-load variance reduction achieved through the V2G-based charging even if the share of users with an EV grows. This results is simply due to the fact that the PV units contribute to meet the increasing power demand due to EVs, thus reducing the supply-demand mismatch. However, if PV_{share} increases excessively (especially if the number of EVs stays the same) the summer NLVR sharply decreases, since the net-load at the substation transformer is so heavily affected by the reverse power flows that the EVs are no longer able to consume enough energy.

Figs. 4.3a and 4.3b show the NLVR contour lines computed when the optimal V2G-based EV charging schedule computed a posteriori using the data of a full day is applied to the following day. These curves are qualitatively similar to those in Figs. 4.2b and 4.2a, but they refer to a much more realistic situation, since in this case, the load, PV generation and EV usage conditions differ from the expected ones. As a consequence, the daily-ahead EV charging profiles will be locally overridden by the new day constraints (e.g., due to EV unavailability) and the obtained results are of course suboptimal. It is worth noticing that the peak reduction is about 15%-18% lower than in the ideal case in both summer and winter. Indeed, the NLVR value never exceeds 50%, which is however a remarkable improvement, especially because it can be achieved over a broad range of PV_{share} and EV_{share} values. The presented analysis clearly shows that, in

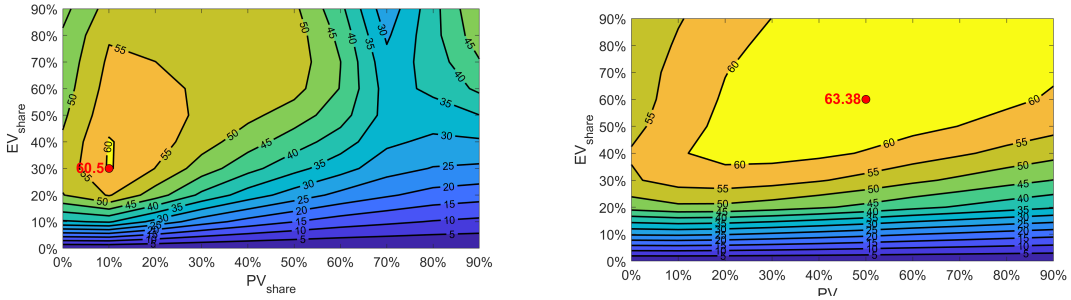

(A) Summer (B) Winter

FIGURE 4.2: Ideal contour curves of the NLVR surfaces as a function of increasing shares of users equipped with PV systems and/or EVs in summer (a) and winter (b), respectively. Results are computed in ideal conditions, i.e. assuming that the user behaviour's and profile is exactly the same as expected.

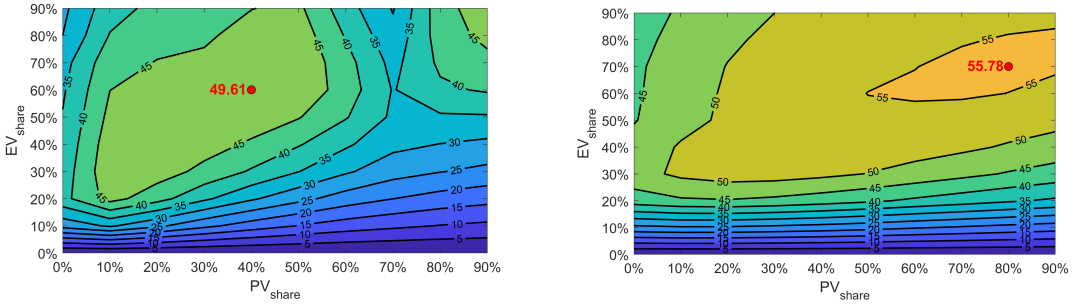

(A) Summer (B) Winter

FIGURE 4.3: Day-ahead contour curves of the NLVR surfaces as a function of increasing shares of users equipped with PV systems and/or EVs in summer (a) and winter (b), respectively. In this case the EVs V2G charging profile computed with the data over a given day is applied to the following day, but the constraints due to actual EVs unavailability override the expected EV charging schedule.

all cases, a good mitigation of the net-load variance can be obtained if at least 20% of users own an EV and that such the net-load variance is dominated by the PV reverse power flows when PV_{share} exceeds about 50%, and EV_{share} is instead lower than 50%.

4.6 Impact Analysis

Since the implications of smart EV battery charging are wider than active power support, this Section will present the results of multiple analyes on: district-level energy independence, grid voltage stability and transformer loading, and EVs' battery wear.

4.6.1 Energy Independence Analysis

Several Authors found that smart EV charging is useful to increase the self-consumption (SC) and self-production (SP) of the district [140, 141]. SC expresses how efficient a system is in consuming the self-generated energy whereas SP represents how much of the total consumption is covered by the users own production. The ideal scenario would see them both at their maximum, in accordance with the concept of net-zero energy districts [219]. The total relative increments in SC and SP at the district level caused by the proposed smart EV charging policy are shown in Fig. 4.4(a)-(b) in the summer scenario. The results in winter are qualitatively similar, but milder. Therefore, they are omitted for the sake of brevity.

Not surprisingly, the highest SC and SP increments are obtained for (PV_{share}, EV_{share}) values significantly different from those of the maxima in Figs. 4.3a and 4.3b, i.e. about (40%,70%) in 4.4(a) and (50%,80%) in 4.4(b). In fact, there is no reason why an algorithm aimed at minimising the overall load variance should also maximise the exploitation of the available solar energy. Nevertheless, the benefits of jointly and properly increasing PV and EV penetration to a certain extent are evident.

Interestingly enough, if $PV_{share} \approx 45\%$ and $EV_{share} \approx 75\%$, then $SC = 42\%$ and $SP = 50\%$. This means that about half of the PV energy is consumed or stored into the EVs's batteries, while half of the total energy demand is covered by the PV generation.

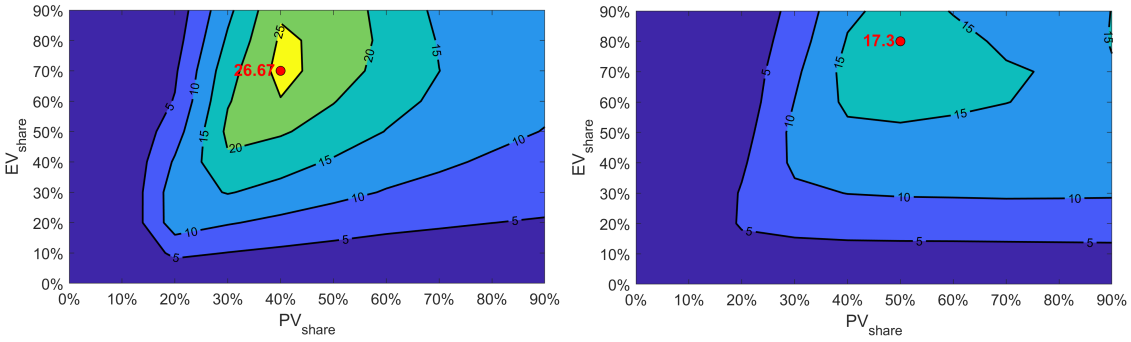

FIGURE 4.4: Increments of the district-level self-consumption (SC) (a) and self-production (SP) values (b) due to the proposed EV smart charging policy in the summer scenario.

4.6.2 Grid Voltage Stability

The correct and stable operation of the IEEE 906-bus LV distribution system under test for increasing values of PV_{share} and EV_{share} with and without running the smart EV charging algorithm was verified through repeated power flow analyses (with a 15 minutes time step) based on the well-known software tool EPRI OpenDSS (v9.0.0). The bar diagrams in Fig. 4.5 show the weekly bus voltage variations range with 99% probability in the summer scenario (i.e., in the worst case) in the baseline case (i.e., without considering the EVs) and with the additional EV load, with and without the proposed V2G-based smart charging algorithm. The groups of bars are plotted for different EV_{share} values and assuming an increasing share of users equipped with PV generators.

As it can be easily seen, the bus voltage levels without smart EV charging exceed the upper bound boundary of 1.1 p.u. reported in [11] only if $PV_{share} = 90\%$. However, this is due mainly to the reverse power flows caused by the surplus of PV-based power and not by the EVs. In any case, the V2G-based smart EV charging tend to better exploit the available distributed PV-power, with an evident benefit in terms of voltage fluctuations reduction. This benefit is more and more evident as the EV_{share} and PV_{share} values grow. The additional load due to the EVs has a strong impact on the undervoltages and, even in the case of $EV_{share} = 30\%$ may significantly exceed the 0.9 p.u. reported in [11]. However, also in this case the smart EV charging algorithm clearly reduces the risk and the amount of such events.

The simulated transformer loading (not shown for the sake of brevity) exhibits of course an increasing stress due to the higher EV and PV penetration. However, the EV smart charging policy of course greatly mitigates such fluctuations, as expected. In any case, the saturation of the transformer is far from being reached, because its 800 kVA capacity is more than enough for 297 households. The peak lines loading and the related losses were evaluated too, but there is no significant improvement on those parameters, since centralised V2G incentivizes the energy exchanges between users.

4.6.3 Battery Wear Analysis

One of the strongest criticisms to V2G-based smart EV charging schemes is the actual stress for EVs' batteries, whose lifetime could be reduced due to a higher number of charging and discharging cycles. For this reason, an estimate of the battery lifetime reduction is provided in this Section. The total relative reduction of the battery capacity of the $j-$th EV after y years of use can be estimated by following the procedure in [194, 220] as $\frac{\Delta C_j}{C_j}(y, T_K) = \frac{\Delta C_j^{CAL} + \Delta C_j^{CYC}}{C_j}$, where $\frac{\Delta C_j^{CAL}}{C_j}$ and $\frac{\Delta C_j^{CYC}}{C_j}$ are the capacity reductions due to the pure calendar-time aging and to the charging-discharging cycling effect, respectively. Both contributions can be estimated by using the following empyrical expressions [220]:

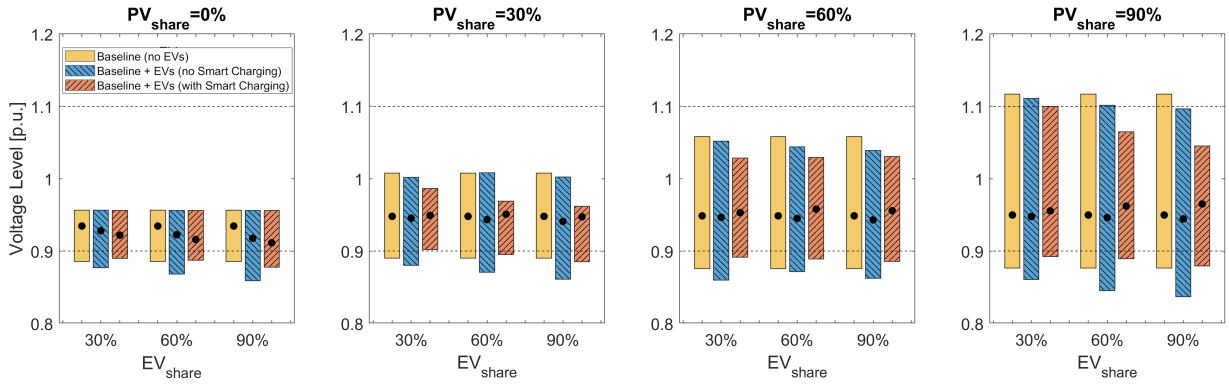

FIGURE 4.5: Range of weekly bus voltage fluctuations with 99% probability over the whole LV distribution system under testing in the summer scenario.

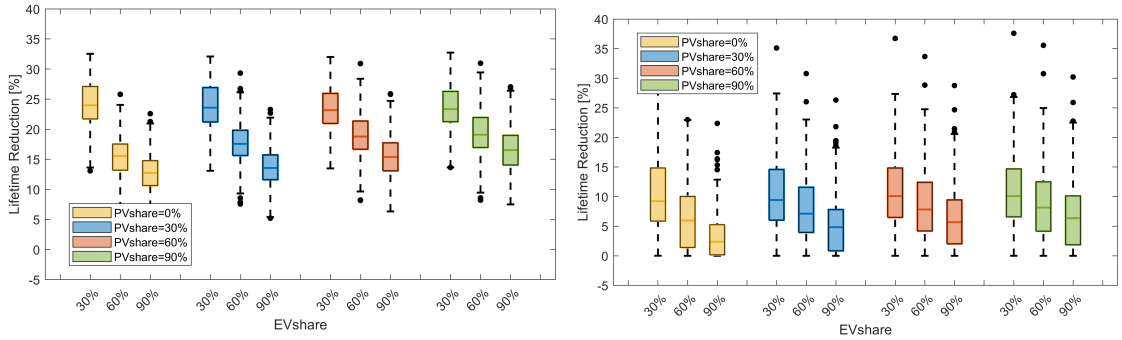

(A) PHEVs

(B) BEVs

FIGURE 4.6: Distribution of the relative lifetime reduction of PHEVs (a) and BEVs (b) batteries due to the application of the proposed V2G-based smart EV charging algorithm.

$$\frac{\Delta C_j^{CAL}}{C_j} = \alpha_{CAL} \cdot e^{\beta_{CAL} \cdot T_K} \cdot (y \cdot 12)^{0.5} \tag{4.11}$$

$$\frac{\Delta C_j^{CYC}}{C_j} = \alpha_{CYC} \cdot e^{\beta_{CYC} \cdot T_K} \cdot (NC_j^{EQ})^{0.5} \cdot y \tag{4.12}$$

where

- the coefficients $\alpha_{CAL} = 1.985 * 10^{-7}$, $\beta_{CAL} = 0.0510$, $\alpha_{CYC} = 4.42 * 10^{-5}$ and $\beta_{CYC} = 0.02676$ were derived from tests on EV Li-ion batteries [194].
- C_j is the nominal battery capacity of the $j-$th EV;
- T_K is the battery pack temperature in Kelvin degrees (set to 40°C as in [194]);
- NC_j^{EQ} is the number of equivalent "full" charging and discharging cycles, estimated by using the Palmgren-Miner rule as in [194];

The battery lifetime is estimated from (4.6.3) by computing the y value for which $\frac{\Delta C_j}{C_j} = 20\%$, which is a conservative, but realistic assumption [194]. Fig. 4.6(a)-(b) shows the box-and-whiskers plots of the relative EV battery lifetime reduction produced by the V2G-based smart charging policy. Since the number of full charging and discharging cycles highly depends on the battery capacity, the results for PHEVs (8-10 kW h) and BEVs (30-80 kW h) are separately presented in Fig. 4.6(a) and (b). Both box-and-whiskers plots are reported for increasing values of EV_{share} and PV_{share}, assuming that the parameter NC_j^{EQ} is set to the typical value estimated in the summer season, which, based on the available simulated data set, is the highest one. Therefore, it is likely that the mean values of the battery lifetime reductions shown in Fig. 4.6(a)-(b) are higher than the real ones.

A first noticeable difference between PHEVs and BEVs is that, for the same values of EV_{share} and PV_{share}, the battery lifetime reduction of the majority of PHEVs is much higher than in the BEVs case, with the median values being roughly twice as large. This is due to the much smaller size of PHEVs' batteries, which causes a larger number of full charging-discharging cycles NC_j^{EQ}, when the V2G-based smart EV charging policy is applied. Interestingly enough, the battery lifetime reduction variability range is quite larger in the BEVs case, because of the broader range of simulated C_j values, that produces a lower NC_j^{EQ} count.

It is also easy to see from both the box-and-whiskers plots in Fig. 4.6(a)-(b), that there are two contrasting trends when EV_{share} and PV_{share} increase. In the former case, a larger EV fleet allows the optimiser to use each vehicle less to perform V2G-based smart EV charging. Therefore, the battery wear is milder. In the latter case instead, when the PV production grows, a slightly higher battery wear effect is noticeable, and this happens because a higher availability of PV production pushes the algorithm to exploit the EV flexibility more and more, thus producing a higher count of equivalent full cycles NC_j^{EQ}. Hence, the higher battery wear. In absolute values, the peak battery capacity reductions are quite high, around 35-40%, meaning that the EV battery lifetime is about 1/3 shorter than in the case when no active power support is performed.

4.7 Conclusions

In this work, the efficiency of a V2G-based centralised smart charging algorithm aimed at reducing the net-load variance at the transformer level was assessed, under an increasing number of users with EV stations and PV systems. The problem was solved with a quadratic programming approach, to fully explore the capabilities of bidirectional centralised V2G for active power support (e.g. minimising NLV). The optimisation results show there are sizeable benefits in simultaneously increasing both the number of EV owners and PV systems, since the NLVR values peak at around 60% and follow an optimal trajectory if an increase in PV systems is supported by more EV charging stations. The analysis in a more realistic day-ahead operation shows that losses in NLVR of up to 15% could happen: increasing the PV penetration reduces the day-ahead estimation error, while increasing the EV penetration produces the opposite effect. Due to the presence of smart charging, 27% increases in district self consumption and 17% in self production are attainable. In those scenarios, the district produces around 50% of its demand and consumes around 50% of its PV production. Smart charging also impacts the the grid-level simulations, since a sizeable reduction of both the over and under-voltage frequencies are noticeable. Results of a simplified economic analysis show that, even if centralised smart charging is an economic loss for the user, a small compensation for the extra purchased electricity greatly reduces the economic losses, and may even produce a net annual gain in some cases. Finally, the battery wear analysis shows that a reduction in the battery lifetime could happen due to smart charging, ranging from 5 to 35% for PHEVs and from 1.5 to 35% for BEVs, with the BEVs suffering much less than PHEVs due to the larger battery size. A reduction this large has to be considered one of the main results of this analysis, and further work should include the battery lifetime in the objective function to minimise. Note that, in this work, the battery wear was not included because the equations in 4.12 are empirical, and can hardly be included in a quadratic programming formulation. We suggest that a more specific analysis should be performed regarding the battery wear issues, since they seem to be the most limiting factor for the widespread diffusion of smart V2G-based charging on the grid. In perspective, future research should combine the best of perfect-foresight and real control algorithms, including forecasting techniques. That would allow to optimise the EV behaviour considering a daily time horizon, while still allowing for an easy implementation of the control algorithm in modern power controllers. This solution could also allow for the consideration of the interaction between stationary storage systems (outside of the scope of this work) and EVs, since a priority system could easily prioritise the EVs for active power support, and use the batteries as a backup to further increase the independence of the district from the grid. Eventually, this solution could reduce the required BESS capacity to install, providing economic incentives to the users.

Chapter 5

EV Impact Scenarios on a Real Distribution Grid

The last Motus-E report on the state of the EV charging infrastructure in Italy[1] states that at present there are 26000 charging stations spread over 10000 locations in the country, 57% of which is found in the northern regions. The steep increase in the number of stations per year, i.e. 6700 in 2021 (+37% of the total stations) indicates that the government and the companies are investing a lot of money in the development of the charging infrastructure. The vast majority, around 94% of the total, is in AC, while the remaining 6% are fast-charging DC stations. Around 17% of the AC stations are slow chargers (<7 kW), while 77% are fast ones (between 7 and 50 kW). Among that 6% DC charging stations, 3.6% is up to 50 kW, 1.4% up to 150 kW and 1% over 150 kW. Both the government energy and climate plan (PNIEC) and the charging infrastructure plan (PNIRE) for 2030 suggest that, even if nowadays the owners tend to drive in the city only thus home EV charging is preferred, in the future, as the battery technology will allow for longer travelled distances, a widespread enough network of public charging stations will be vital. In highways, for example, it is possible to find 1.2 charging points every 100 km. The Motus-E report concludes that the state of the charging infrastructure is good, since other countries with a higher share of EVs have a lower penetration of charging stations. All things considered, supplying the electricity required by the charging stations and safeguarding the network from possible disruptions are still very important aspects. In that regard, as mentioned in Chapter 2, the simultaneous charging of a high number of EVs poses multiple threats to the stability of distribution systems. Hence, since the number of installed EV stations will increase in the next years, addressing the grid-related issues will be more important then ever.

In the framework of the Stardust H2020 project[2], we quantified the future impact of EV charging on the distribution grid of Trento, Italy. The main objective of this work was understanding when EV charging will start to significantly impact the analysed distribution grid, and to quantify its magnitude by considering future EV uptake scenarios. Moreover, the analysis of the V2G-based smart charging mitigation capabilities was performed.

5.1 Methodology

In order to clarify the approach adopted for the Stardust project, the performed steps are shown in Figure 5.1. Firstly, the *power system* was modelled in OpenDSS and *validated* by considering the available measured net-load profiles. Secondly, the EV penetration scenarios in the municipality were analysed, and a charging profiles generator for EVs was used to create a *realistic database* of charging *profiles*. Thirdly, those stations were then *distributed on the grid* as loads and the *EV impact analysis* was performed. Finally, the possibility of *smart EV-charging* was also analysed.

In the following sections, each of these stages will be described in detail, and the main conclusions will be drawn.

5.1.1 Power Grid Model

For the creation of a power system model in OpenDSS[3], the *topology* of the distribution network of Trento was provided by the local DSO. We considered the location and electric parameters of the aerial and underground cables, secondary (SSs) and primary substations (PSs), LV/MV and MV/HV transformers. Moreover, the main electric properties of the power conversion elements (loads/generators) were also considered, along with their type (domestic/commercial/lighting).

[1] "Le infrastrutture di ricarica pubbliche in Italia: III edizione", Motus-E, https://www.motus-e.org/wp-content/uploads/2022/01/Le-infrastrutture-di-ricarica-pubbliche-in-Italia-1.pdf

[2] Part of this chapter is featured in the final report for the WP4 "Smart Community Trento" of the H2020 Stardust project, under the Grant Agreement 774094, https://stardustproject.eu/

[3] OpenDSS: Open Distribution System Simulator v9.0.0, R.Dugan, D.Montenegro, A.Ballanti, https://www.epri.com/pages/sa/opendss

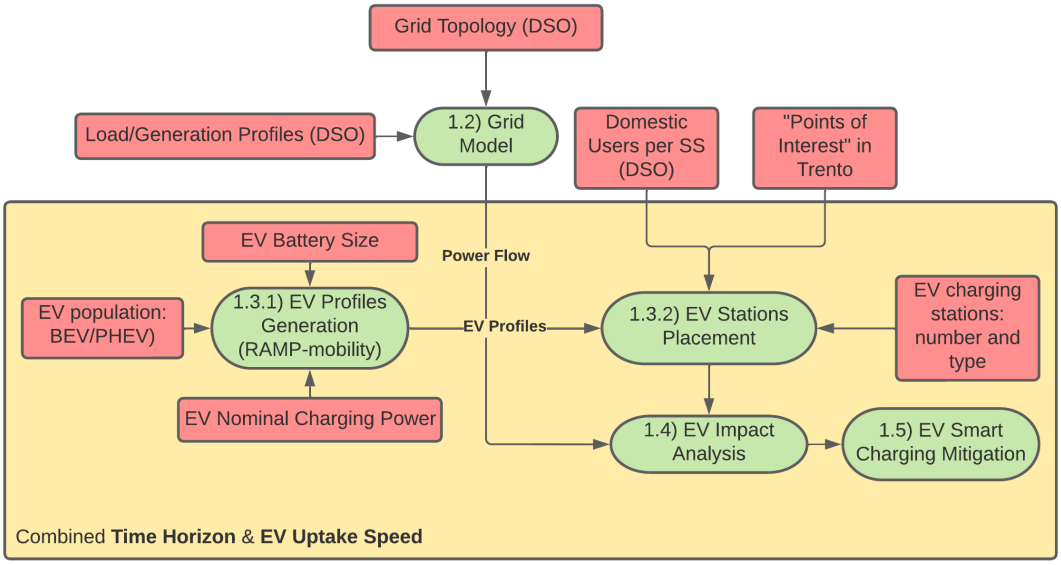

FIGURE 5.1: Flowchart of the adopted analysis approach.

	$N_{FEEDERS}$	S_{TR}	N_{SS}	N_{LV}^{USERS}	N_{MV}^{USERS}
PS_1	12	80 MVA	274	19955	83
PS_2	16	80 MVA	285	32473	92
PS_3	12	103 MVA	248	31383	58

TABLE 5.1: Main characteristics of the analysed distribution grid.

Firstly, the grid was divided into three sub-networks, each one referring to an HV/MV transformer located at a PS, and hereafter dubbed as PS_1, PS_2 and PS_3. The reason behind this choice is that the voltage levels and transformer set-points for the different PSs are slightly different. Secondly, each bar was subdivided into a variable number of feeders, each serving a number of secondary substations (SSs), hereafter referred to as $SS_1, \ldots, SS_{807}$. Figure 5.2 gives an overview of the grid topology by highlighting the extension of the feeders and the placement of the SSs.

A summary of the main features of each PS is presented in Table 5.1 instead, where $N_{FEEDERS}$ is the number of feeders, S_{TR} is the HV/MV transformer apparent power rating (MVA), N_{SS} is the number of secondary substations, N_{LV}^{USERS} is the number of LV-connected loads, and N_{MV}^{USERS} is the number of MV-connected ones.

5.1.2 Model Validation

The RMS values of the line to neutral voltage V_{LN} and phase current I_{PH} averaged over 10 minutes were available for a period of three years, from 2016 to 2018. The profiles were measured at each of the 40 feeders, in close proximity to the PS connection point. Since the PF was unknown, the apparent power consumption profiles at each feeder were estimated based on the voltage and current profiles and redistributed on the different SSs. Since no information was available on the simultaneity factors for the different SSs (i.e. the maximum concurrent absorbed power at each SS), a simplified approach was chosen. As such, the apparent load consumption profiles of the m-th feeder at time t, was split based on the nominal power of the loads on each SS, to obtain the apparent power flow at the i-th SS.

A power factor (PF) is then assumed for each type of load, based on values found in the scientific literature: $PF \simeq 0.95$ and $PF \simeq 0.9$ are typical values for domestic and commercial loads respectively [221], whereas $PF \simeq 0.85$ is appropriate for neon-lights used in public lighting [4]. The apparent power flow at the i-th SS at time "t" is thus the sum of three components, each with a different PF.

As reported in the international regulation EN50160:2010 for LV electricity distribution systems [11], all the loads with nominal power over 6 kW have to be considered as three phase, whereas the others as one-phase. The latter group

[4] ABB, "Guida all'illuminazione", 2020, `https://library.e.abb.com/public/a5bc26ccdd713781c1257db00058f331/2CSC004070B0901.pdf`

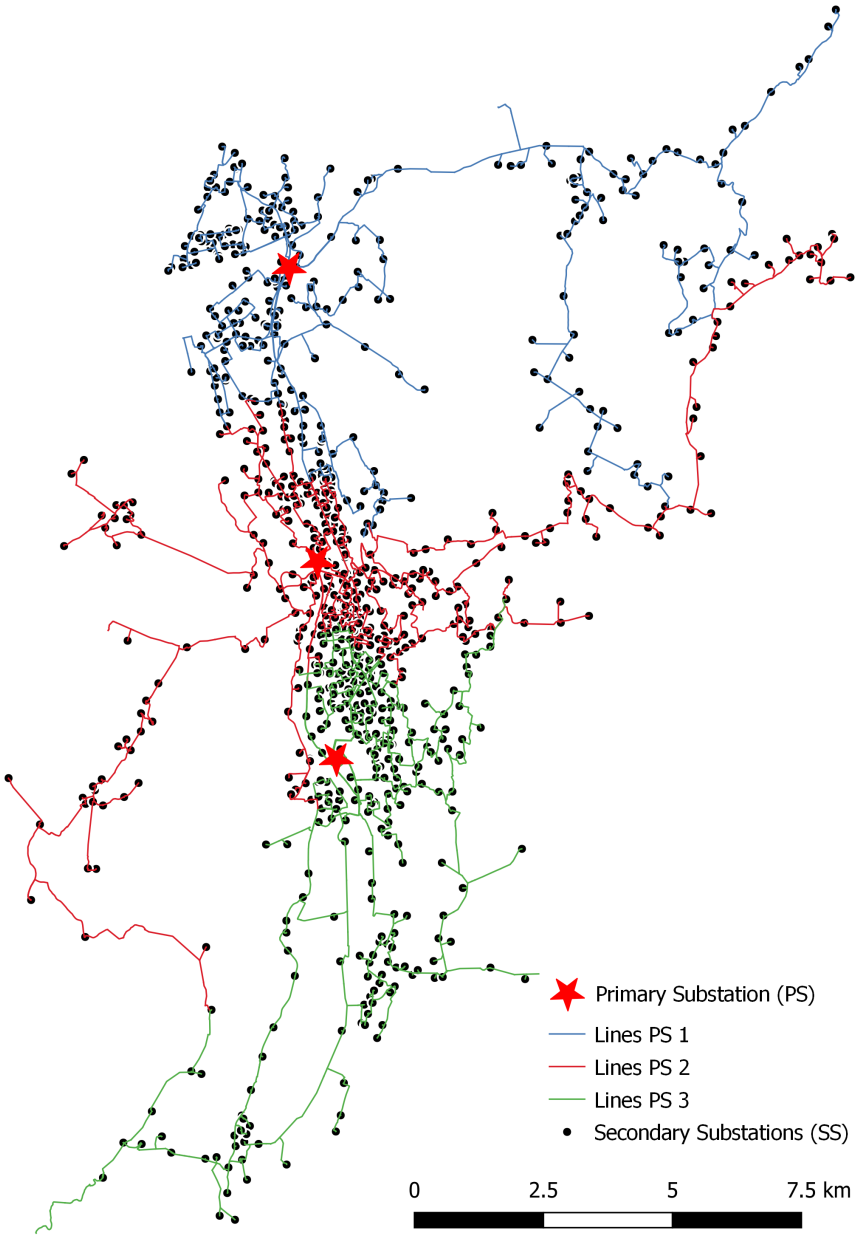

FIGURE 5.2: GIS representation of the 807 SSs and of the three PSs.

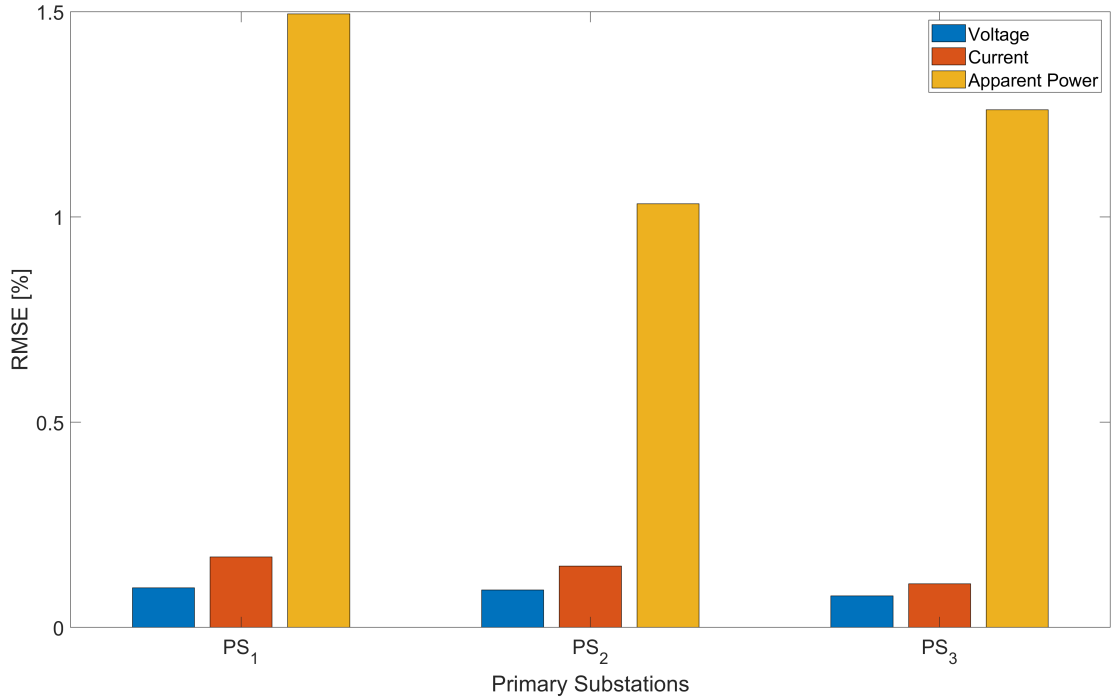

FIGURE 5.3: RMSE values for the grid validation on the different PSs bars.

	Max./Min. Violation Magnitude	**Max. Violation Duration**	**Violation Frequency**
MV/HV Transformer Overload	105%	1 h 40 min	2%
LV/MV Transformer Overload	110%	3 h	4-5 %
MV Bus Undervoltage	0.89 p.u.	2 h 30 min	<0.225 %
MV Bus Overvoltage	N.A.	N.A.	0%
MV Lines Overcurrent	N.A.	N.A.	0%

TABLE 5.2: Baseline scenario results, negligible EV impact on the grid.

of loads was equally distributed on the grid phases to attenuate voltage unbalance. The MV loads are instead all three-phase ones, since their nominal power is always higher than 6 kW.

Once the grid model was assembled, we checked how different the measured values were from the time-dependent profiles of the same electric same parameters but obtained through the OpenDSS simulation. Those parameters were the voltage magnitude V_{LN}, phase current magnitude I_{PH} and apparent power S_{TR} profiles a each feeder's end (i.e. close to the PS they are connected to). The relative root-mean square error (RMSE) was used to estimate the validation error for the x-th PS (5.1):

$$RMSE_{V_{LN}}[\%] = \frac{\sqrt{\sum_{t=1}^{T} \frac{\left(V^{PS_x}(t) - \hat{V}^{PS_x}(t)\right)^2}{T}}}{\overline{V^{PS_x}}} \cdot 100 \tag{5.1}$$

where $\hat{V}^{PS_x}(t)$ is the L-N voltage profile resulting from the OpenDSS simulation, $V^{PS_x}(t)$ is the corresponding measured value at time t, T is the number of considered time instants, and $\overline{V^{PS_x}}$ is the mean voltage profile at PS_x: $\overline{V^{PS_x}} = \frac{\sum_{t=1}^{T} V^{PS_x}(t)}{T}$. An Equation similar to (5.1) can be used to calculate the RMSE values of I_{PH} and S_{TR}. Figure 5.3 shows the results of the validation performed at the HV/MV transformer bar level.

It is possible to conclude that the model is accurate enough to perform an EV impact analysis.

5.1.3 Baseline Impact Analysis

Once the grid model was validated, power flow simulations were performed on the analysed grid for the baseline scenario (no EVs), and the main results of the violations analysis are presented in Table 5.2.

Type	2020	2030	2040	2050	
Residential	16	33	39	40	**REF**
Workplace	4	9	10	10	
Public	4	9	10	10	
Residential	56	1567	3724	4626	**CPI**
Workplace	14	392	931	1157	
Public	14	392	931	1157	
Residential	78	4959	17125	26933	**TECH**
Workplace	20	1240	4282	6734	
Public	20	1240	4282	6734	
Residential	100	8886	22333	28103	**RAPID**
Workplace	25	2222	5584	7026	
Public	25	2222	5584	7026	

TABLE 5.3: Number of EV charging stations of different types for the multiple considered time horizons.

The considered threshold values were obtained from the available international regulation EN50160:2010 [11] for the voltage levels (0.9 p.u. lower limit, 1.1 p.u. upper limit), while the Italian CEI64-8:2021 [12] was adopted for overcurrents (max 145% overcurrent). Since the violation frequency for transformers is usually provided by the manufacturer, we adopted a maximum transformer loading equal to 100% which represents a very restrictive value, since oil-immersed transformers are allowed to overload by 10-50% of the total simulation time, considering the average previous loading level and the peak magnitude of the overload event [5], and the selected threshold is quite restrictive. These results are however coherent with the local DSO reports, which confirmed that the grid has no significant issue at present.

After the baseline was calculated, the EV penetrations scenarios were analysed, as explained in the following section.

5.2 EV Modelling

Once the grid model was finalised, the EV modelling task was performed based on a three-steps methodology. First, the *EV penetration scenarios* from a local report were considered. Then, a charging profiles generator was used to generate a *database of EV charging profiles* for the quasi-steady state simulations. Finally each EV station was associated to a charging profile and then *placed on the grid* based on different rules for domestic and public charging.

5.2.1 EV Penetration Scenarios

In the framework of the Stardust project, different *EV uptake speeds* were considered for the different *time horizons* spanning the 2020-2050 period. The following case scenarios, elaborated starting from the Fuelling Italy's Future report[6], were analysed:

- **REF ("Reference")**: the EVs share on the circulating car fleet will not change in the future, thus e-mobility will not be an important part of future mobility scenarios.
- **CPI ("Current Policy Initiatives")**: a modest increase in sales of PHEVs/BEVs is recorded, in agreement with the European targets for global CO2 emissions reduction by 2030.
- **TECH**: a smooth transition to PHEVs/BEVs happens until 2030, then a lower adoption of EVs is predicted, in favour of fuel-cell EVs.
- **RAPID**: a faster transition to PHEVs/BEVs and fuel cell EVs than the one in TECH scenario is envisioned. By 2030, the market will be dominated by electric mobility.

From the combination of the four presented EV uptake speeds and time horizons, 16 scenarios are obtained. The predicted *number of EV charging stations* in Trento is shown in Table 5.3, along with their assigned use.

[5] "What is the permissible overload percent for oil-immersed transformers?", Schneider Electric, https://www.se.com/eg/en/faqs/FA335947/

[6] "Fuelling Italy's Future: How the transition to low carbon mobility strengthens the economy", European Climate Foundation, 2018, https://europeanclimate.org/content/uploads/2019/12/fuelling-italys-future-how-the-transition-to-low-carbon-mobility-strengthens-the-economy-summary.pdf

	PHEV	BEV			
	2020-2050	**2020**	**2030**	**2040**	**2050**
Small	6	35	45	60	70
Medium	8	50	60	75	85
Large	10	80	90	100	115

TABLE 5.4: EV battery sizes [kWh] in the EV pools created for the different time-horizon scenarios.

Table 5.3 shows that the low number of EVs until 2030 will probably produce a mild impact for all uptake speeds, especially because, as it will be shown later in this chapter, simultaneous charging of all the stations is a very rare occurrence, i.e. the simultaneity factor decreases as the number of considered EVs increase (check Figure 5.9). After that, the impact should increase more and more, due to the higher number of installed charging stations. It is generally possible to distinguish between the number of "domestic" and "public" stations for each combined scenario. For the purpose of this study, "workplace" stations are merged with the "residential" ones. In fact, both those types are not publicly available and their charging power is in the range 3.7-22 kW. Moreover, the typical charging session lasts up to 7-8 hours for a full charge, which is acceptable for users that can charge their EVs while working or staying at home, and thus also allow for V2G-based smart charging. "Public" stations instead, are the ones available in parking lots, and whose nominal charging power is much higher (50-350 kW). Moreover, they typically do not work in V2G-mode, because their users generally just want to charge their EVs in the shortest amount of time and then leave the station.

5.2.2 EV Profiles Generation

The software RAMP-mobility, which was already introduced in Section 4.4, was used again to create one realistic pool of EV charging profiles for every scenario combining an EV uptake speed and a time horizon. The database was created following some assumptions, listed below:

- *EV Battery Size:* classified as small/medium/large; each group covers a share of the total EV fleet. For the purpose of this work, these values were kept constant at the present level for Italy, i.e. 24%, 68% and 7%, as suggested in [213]. Moreover, since the battery capacity has increased in the past few years together with the EV driving range, different battery sizes were adopted for the the time horizons after 2020, as in Table 5.4.

  Since no data was available about future trends after 2030, the PHEVs batteries size were assumed to not increase after 2020, since the plug-in hybrid technology is considered as a "transition" between internal combustion engines and BEVs. For this last category instead, the size of the battery in the future can be estimated through a linear extrapolation of the battery increase in the last 10 years, as available in the literature [222] and online [7].

- *Charging Power Frequency:* since EV charging at a domestic stations is less expensive than charging at a public one, it is reasonable to assume each EV will have a domestic charging station, where most of the charging sessions will happen (we assumed around 75% in line with the Motus-E report for the EV charging habits in Italy in 2030[8]). As seen in Figure 5.4a, representing the frequency for each EV to charge at a certain nominal power level, the vast majority of the sessions currently happens at 3.7 kW domestic stations. However, by 2040 and 2050, the newly installed domestic charging points will gradually switch from 3.7 kW to 7 kW or more, so in Figure 5.4b the 7 kW charging sessions are prevalent, at the domestic level.

  The remaining 25% of the sessions will be split between the available public charging stations. In order to estimate the probability of charging at a specific nominal power level, the OpenCharge Map[9] database for public EV stations and Motus-E mobility report 2020[10] were analysed and cross-checked to derive the distribution of public charging stations in Italy for 2020 and 2030. An example of the current situation can be seen in figure 5.5 for the provinces of Trento and Bolzano.

[7] Electric Vehicles Database, https://ev-database.org/cheatsheet/useable-battery-capacity-electric-car

[8] "Il futuro della mobilità elettrica: l'infrastruttura di ricarica in Italia nel 2030", Motus-E, https://www.motus-e.org/wp-content/uploads/2020/10/Il-futuro-della-mobilit%C3%A0-elettrica-linfrastruttura-di-ricarica-in-Italia-2030-2.pdf

[9] OCM (OpenCharge Map) Database https://openchargemap.org/site/

[10] Motus-E EV Charging Infrastructure Report (December 2020) https://www.motus-e.org/wp-content/uploads/2021/01/Report-IdR_Dicembre_2020-2.pdf

(A) RAPID 2020 Scenario

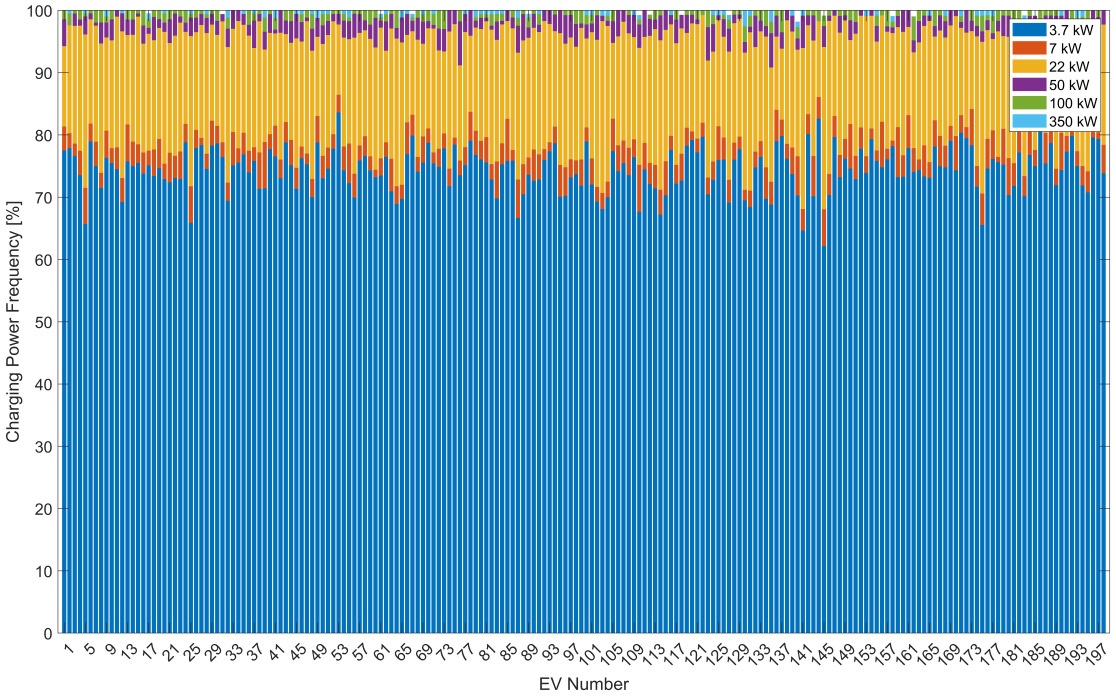

(B) RAPID 2050 Scenario

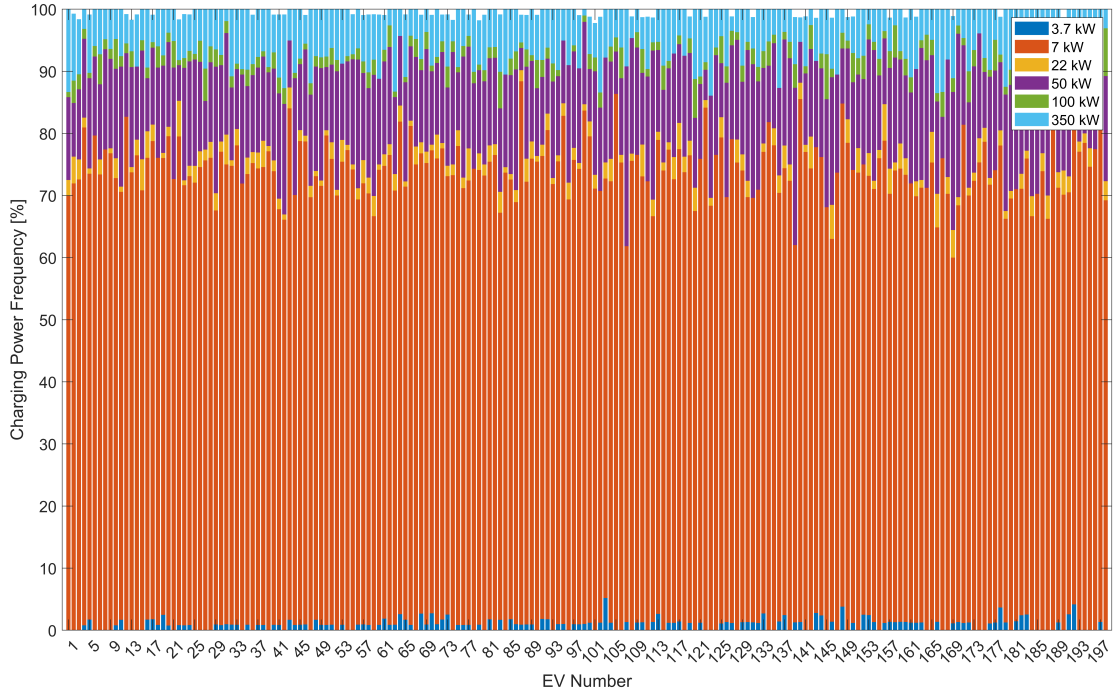

FIGURE 5.4: Nominal charging power frequency for two EV profiles pools for the RAPID 2020 and RAPID 2050 scenarios.

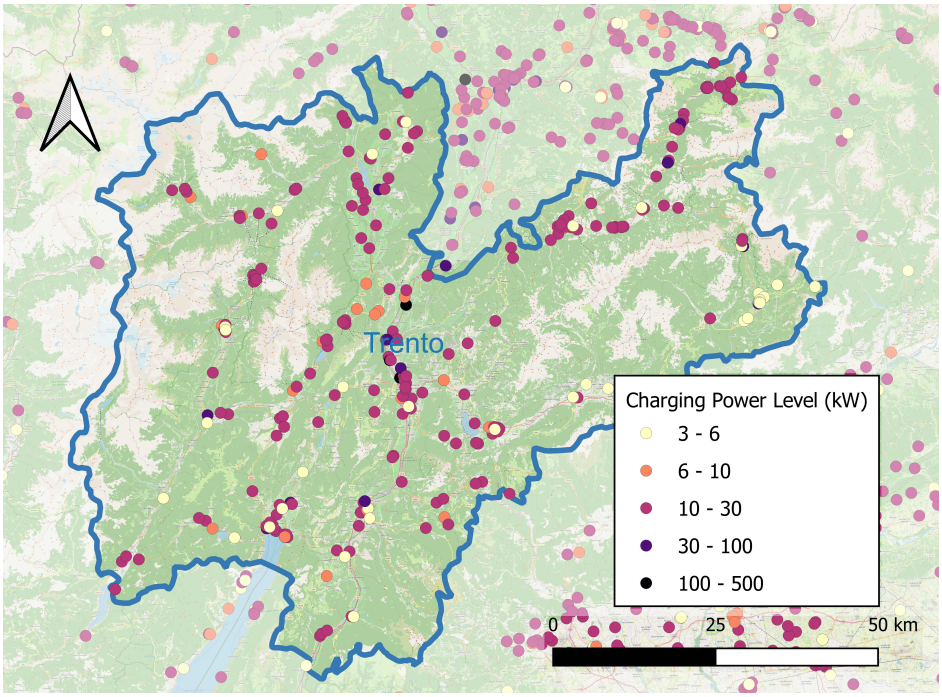

FIGURE 5.5: Public charging points positioning for the province of Trento, Italy.

After 2030, we assumed that the domestic charging will happen at 7 kW instead of 3.7, and that the public charging will switch from 22 kW to a mix of 50-350 kW. No information was found regarding the charging levels in the future, but these assumptions seem to be in agreement with the Motus-E report for Italy.

- *Type of EV*: each pool of EV profiles features either PHEVs (6-10 kWh) or BEVs (35-115 kWh), thus the data from the aforementioned Fuelling Italy's Future Report was used to derive the share of either category in each different combined scenarios. These percentages are the last input parameter required to run RAMP-mobility.

Once the 16 pools of EV charging profiles (one per combined speed+horizon scenario) were generated, we had to understand how many stations are required for each pool. The number *domestic EV stations* N^{ST}_{DOM} was obtained by assuming it equal to the number of EVs in the pool. This assumption holds because the home charging stations are nowadays cheaper and more widespread than public ones, so it is reasonable to assume that every EV has its own home charging wallbox. The number of *public stations* N^{ST}_{PUB} charging at a specific power level was instead obtained by

- cumulating the sessions with the same nominal charging power P^{ST}_{NOM}
- estimating the minimum required number of stations to feed that maximum power
- sorting the sessions of the cumulative profile on the N^{ST}_{PUB} public stations, so that only one EV is charged at a time

The total energy absorbed per year and the number of charging sessions for each station were checked to make sure the profiles are realistic, the aggregated power required for the RAPID scenario is reported in figure 5.6, as an example.

Finally, a random extraction of the number of EV charging profiles required by each scenario (from Table 5.3) was performed. Those profiles were then placed on the 807 SSs of the grid following the logic explained in the following section.

5.2.3 EV Stations Placement

The total number of stations assigned to the i-th SS, i.e. $N^{ST}_i = N^{ST}_{i,DOM} + N^{ST}_{i,PUB}$ requires the knowledge of the number of domestic $N^{ST}_{i,DOM}$ and public $N^{ST}_{i,PUB}$ charging stations assigned to the i-th SS. For that reason, two weights were estimated for the domestic $W_{i,DOM}$ and public $W_{i,PUB}$ charging stations, so that:

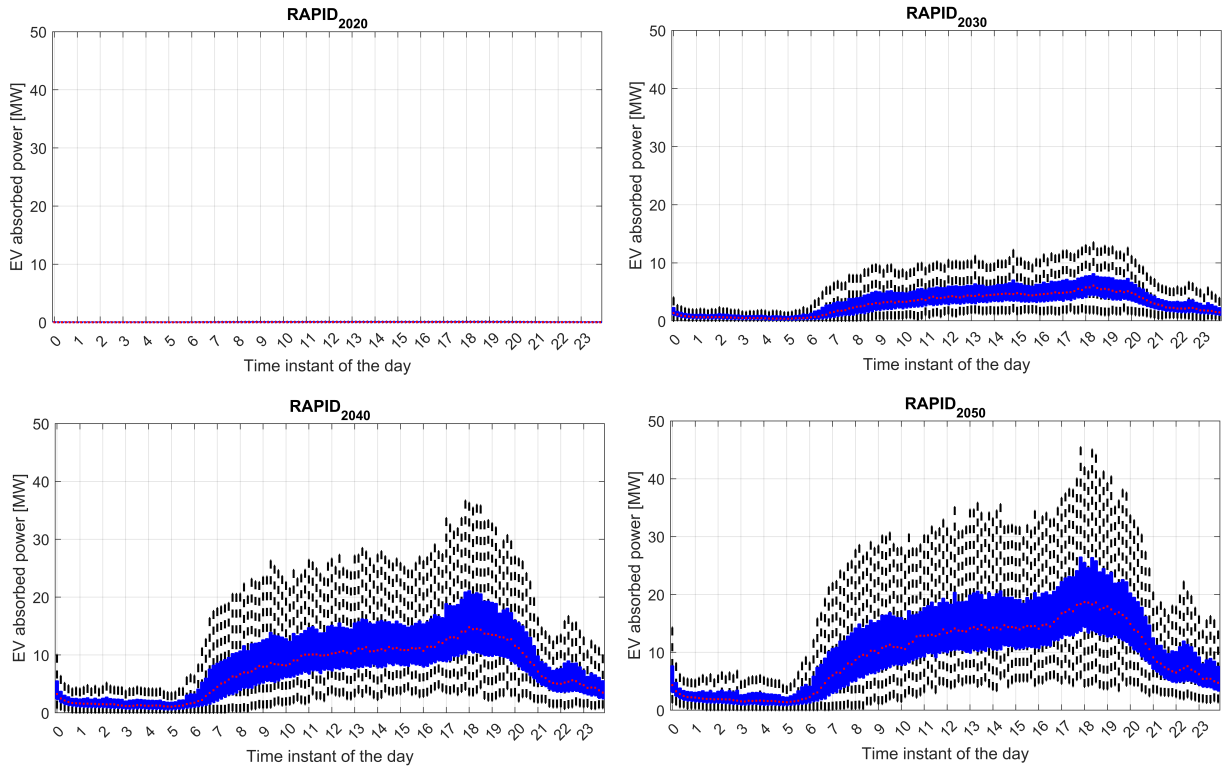

FIGURE 5.6: Daily average EV charging pattern profiles over the entire grid for the RAPID EV uptake speed.

$$\begin{aligned} W_{i,DOM} &= \frac{N_{i,DOM}^{ST}}{N_{DOM}^{ST}} \quad \sum_{i=1}^{N_{SS}} W_{i,DOM} = 1 \\ W_{i,PUB} &= \frac{N_{i,PUB}^{ST}}{N_{PUB}^{ST}} \quad \sum_{i=1}^{N_{SS}} W_{i,PUB} = 1 \end{aligned} \tag{5.2}$$

Since the placement of "domestic" and "public" charging points follows a different rationale, two separate methodologies were used to obtain $W_{i,DOM}$ and $W_{i,PUB}$.

For the *domestic stations*, $W_{i,DOM}$ depends on the number of domestic users $N_{i,DOM}^{USERS}$ each SS serves, as in Equation (5.3):

$$W_{i,DOM} = \frac{N_{i,DOM}^{USERS}}{\sum_{i=1}^{N_{SS}^{TOT}} N_{i,DOM}^{USERS}} \tag{5.3}$$

where N_{SS}^{TOT} is the total number of SSs of the grid. Following this approach, the highest number of EV charging stations is assigned to the SSs serving highly populated areas.

For the *public stations* instead, a spatial multi-criteria assessment of civic, commercial, cultural, and parking points of interest was performed. The chosen methodology, based on an analytic hierarchy process (AHP) produces a score for each pixel of the map (check an example in Figure 5.7).

The higher the score, the higher the number of "points of interest" available at that location. Thus, the weight $W_{i,PUB}$ was calculated so that the EV charging stations are more likely to be placed where the score is high, as in Equation (5.4):

$$W_{i,PUB} = \frac{\omega_i}{\sum_{i=1}^{N_{SS}^{TOT}} \omega_i} \tag{5.4}$$

where ω_i is the score value associated to the i-th SS.

Once this step is performed, a specific charging profile needs to be assigned to each station. Thus, a random extraction is performed from the EV consumption profile pools generated as in Section 5.2.2.

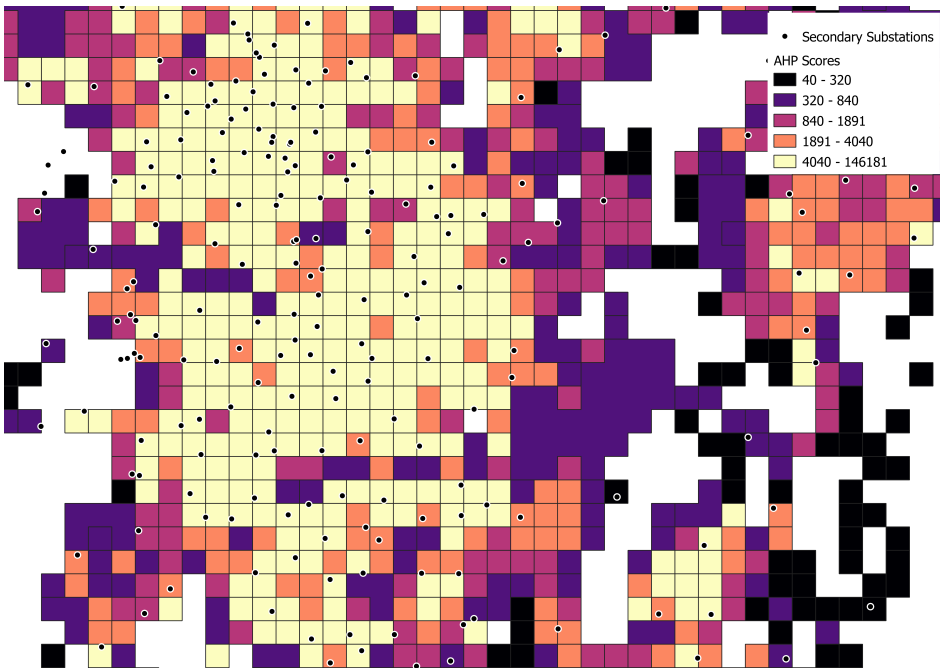

FIGURE 5.7: Example of the results of the AHP Analysis: each SS is included in one pixel of the map, whose score represents the classification obtained by analysing the points of interest of the city.

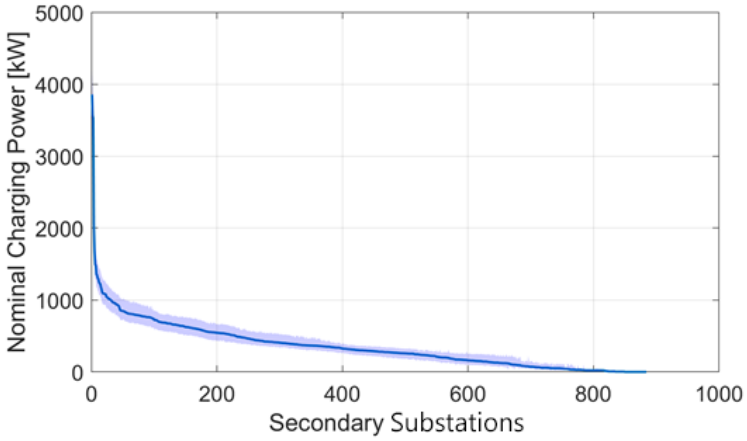

FIGURE 5.8: Variability of nominal EV station installed power along the 807 SSs of the grid fot the RAPID-2050 scenario. The median of the 1000 Monte-Carlo runs is highlighted with a blue line, while the shaded area covers the distance between the 25-th and 75-th percentiles of the distributions.

The random extraction validity was tested by repeating it 1000 times for every SS, and an example of the results is reported in Figure 5.8 for the highest EV penetration scenario (RAPID):

As shown by Figure 5.8, the variability of the aggregated nominal charging power is very limited, which means that a different random placement of the charging stations will probably not strongly affect the grid. The validity of this hypothesis is additionally confirmed by the simultaneity factor values for the different feeders, shown in Figure 5.9 and representing the ratio between the maximum power absorbed by all the EV stations connected to the feeder and the installed one.

It is easy to check that in 2050, the feeders simultaneously absorb around 25-30% of the nominal power, which means that the numbers from Figure 5.8 need to be scaled down approximately by a 4.5 times.

5.3 EV Impact Analysis: Simulation Results

The impact of the different combinations of time horizons and EV uptake speeds on the grid are far more significant than in the baseline scenario, as reported in Table 5.5.

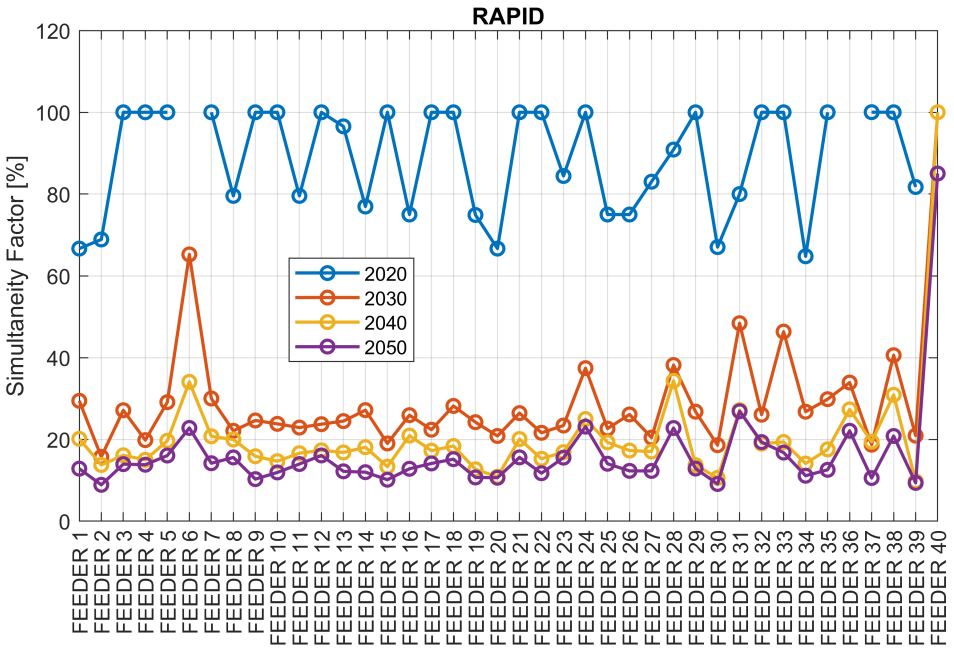

FIGURE 5.9: Simultaneity factors for the RAPID EV speed scenario in 2020-2050.

Horizon	EV Speed	Undervoltage	Overcurrent	LV/MV TR Overload	MV/HV TR Overload
2030	**TECH**	0.28%	0.00%	5.20%	0.10%
	RAPID	0.28%	0.20%	5.20%	0.20%
2040	**TECH**	0.30%	0.12%	13.00%	1.25%
	RAPID	0.35%	0.55%	22.50%	2.00%
2050	**TECH**	0.38%	1.00%	23.00%	3.50%
	RAPID	0.38%	0.90%	27.50%	2.50%

TABLE 5.5: Violation frequencies for the main electric parameters of the grid.

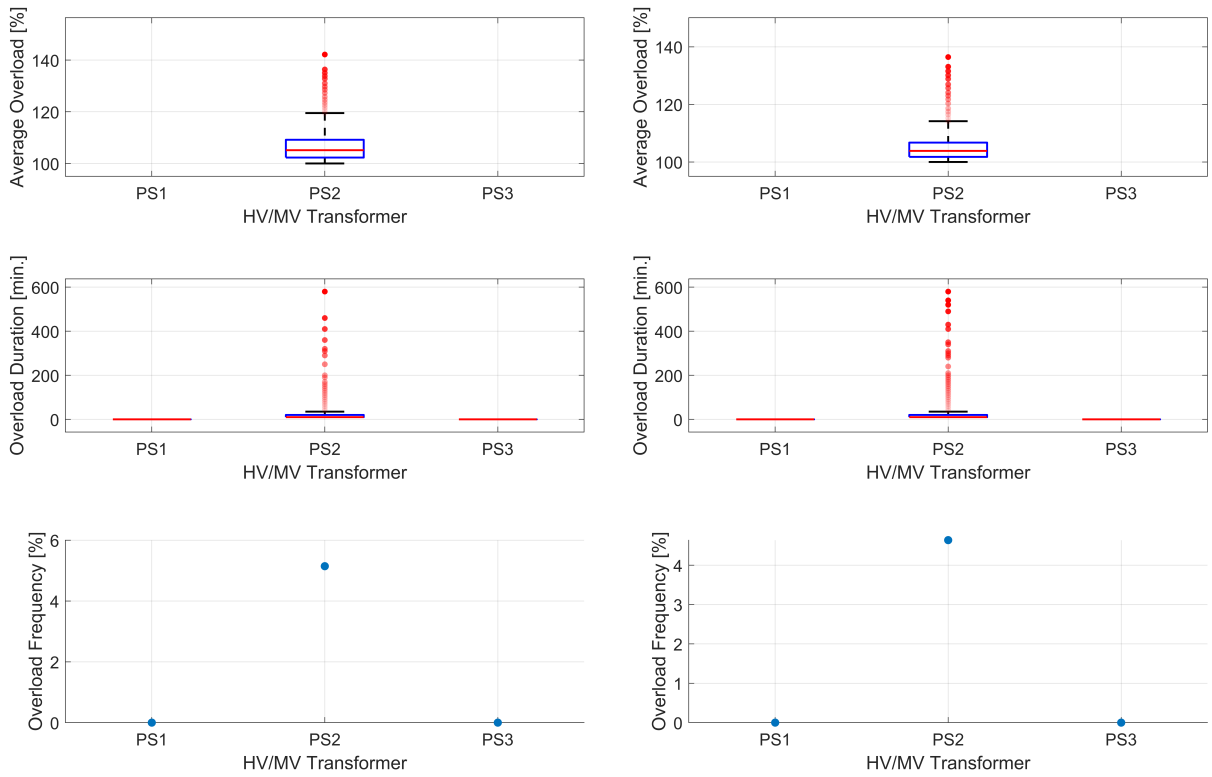

FIGURE 5.10: Overload analysis for MV/HV transformers in the TECH 2050 (left) and RAPID 2050 (right) scenarios.

Note that the REF ("Reference") and CPI ("Current Policy Initiatives") scenarios are not included in the results because their impact on the electric parameters is almost equivalent to the baseline one, given the low number of EV charging stations. Also note that the overvoltage infractions (i.e. when the voltage level exceeds the upper 1.1 p.u. threshold) never happen, due to the low penetration of PV systems. The most impacted parameters are, once again, the LV/MV and MV/HV transformer loading levels, especially in the TECH and RAPID scenarios for 2050. Thus, only the analysis of the transformer overloads for those two scenarios will be expanded.

Figure 5.10 show the results of the analysis of the MV/HV transformer overloads for each of the three PSs

It is possible to see that the overloads are present for PS_2 only, with average overload magnitudes of up to 140%, lasting for up to 10 consecutive hours. The overloading frequency is, however, very low, peaking at around 5%. The overloads are concentrated on PS_2 only because the PSs serving highly populated areas, such as the city centre in this case, usually display the highest overloading frequency due to the high number of domestic users and points of interest (i.e. because $W_{i,DOM}$ and $W_{i,PUB}$ are at their highest). PS_1 and PS_3 instead, are located outside of the city centre, in the northern and southern parts of the city respectively. It can also be noted that PS_2 has the same frequency, average duration, and average violation magnitude in both the TECH and RAPID scenarios. This allows us to conclude that, those two scenarios have almost the same effect in terms of MV/HV transformers overload.

Figures 5.11 and 5.12 instead, show the overloading frequencies for the LV/MV transformers at the each of the SSs, grouped by feeder.

Feeders 1-16 (belonging to PS_2, the "urban" PS), and feeders 17-28, show the highest overload frequencies. The most impacted feeders are number 13, 17, 23 and 25, where the overloading frequency goes up to 11% of the entire simulation time. Deepening the analysis about feeder 13 and 25, which are the most impacted ones, Figures 5.13 and 5.14 show the results of the analysis for SSs of the RAPID 2050 scenario only.

Since transformers on SS8 for feeder 13 and SS1 for feeder 25 have the lowest rated capacities, their overloading values are higher both in magnitude and duration. This happens because, as shown in Section 5.2.3, the placement of the EV stations did not consider the technical limitations of the grid, but rather the population density (for domestic stations) and the urban points of interest (for public stations). The duration of the overload events is generally lower than

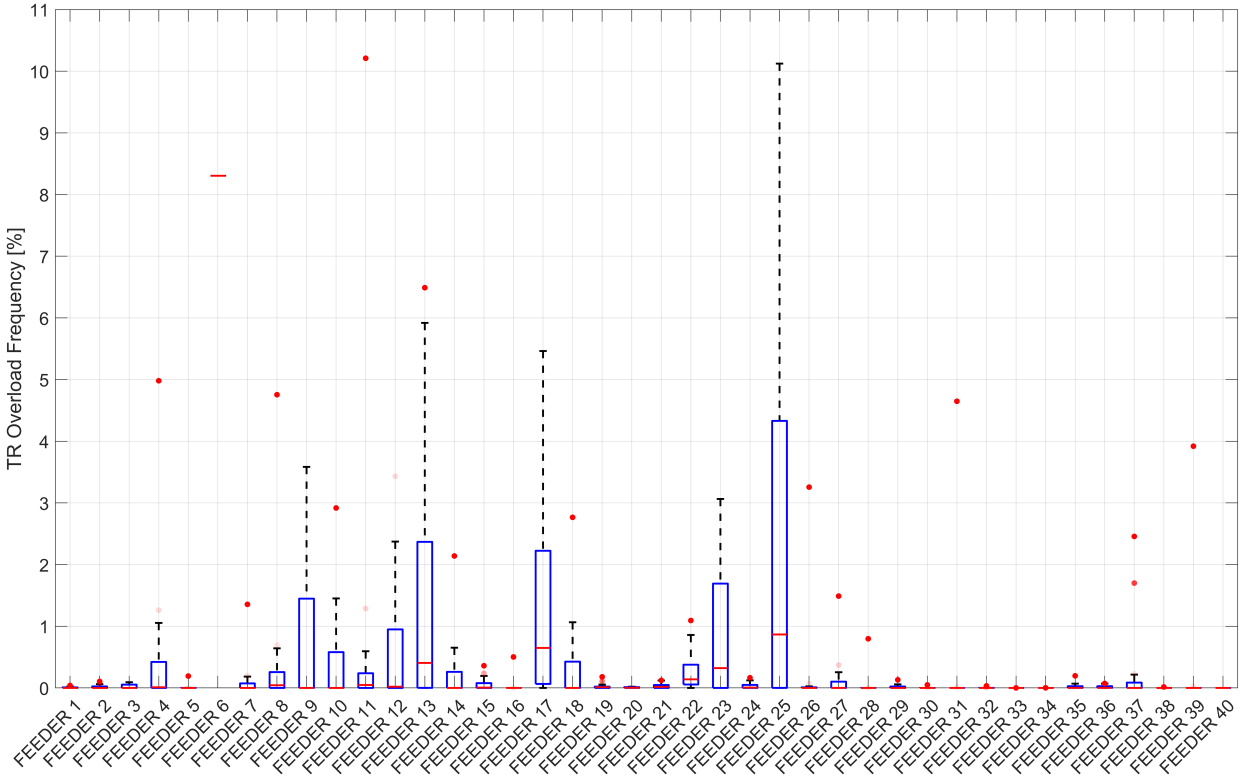

FIGURE 5.11: Feeder overload analysis for LV/MV transformers in the TECH 2050 scenario.

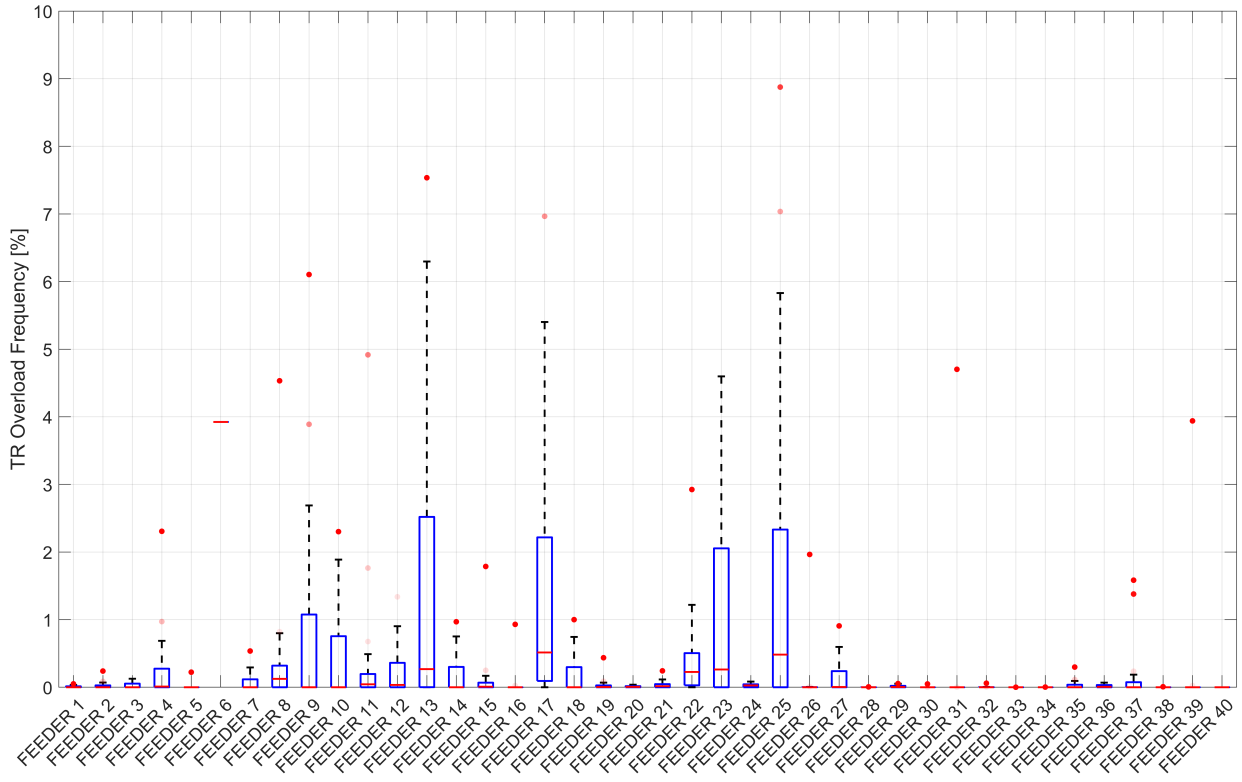

FIGURE 5.12: Feeder overload analysis for LV/MV transformers in the RAPID 2050 scenario.

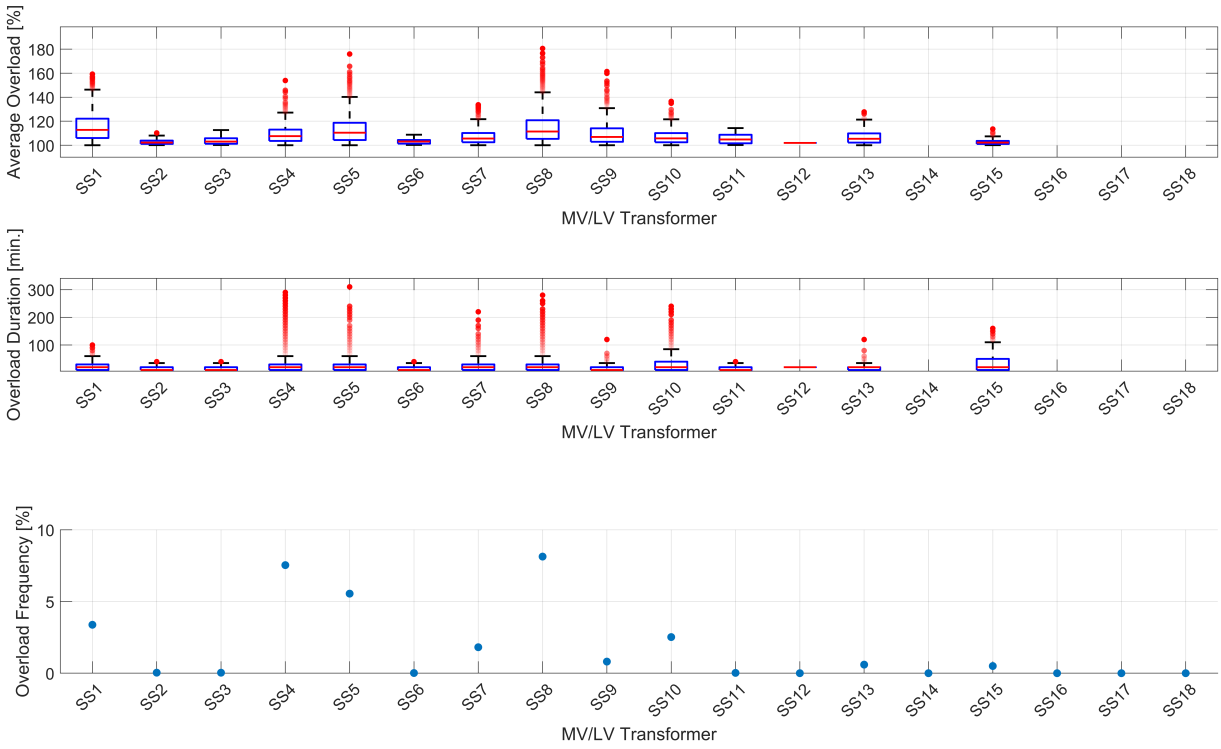

FIGURE 5.13: Secondary substation overload analysis for LV/MV transformers of feeder 13 in the RAPID 2050 scenario.

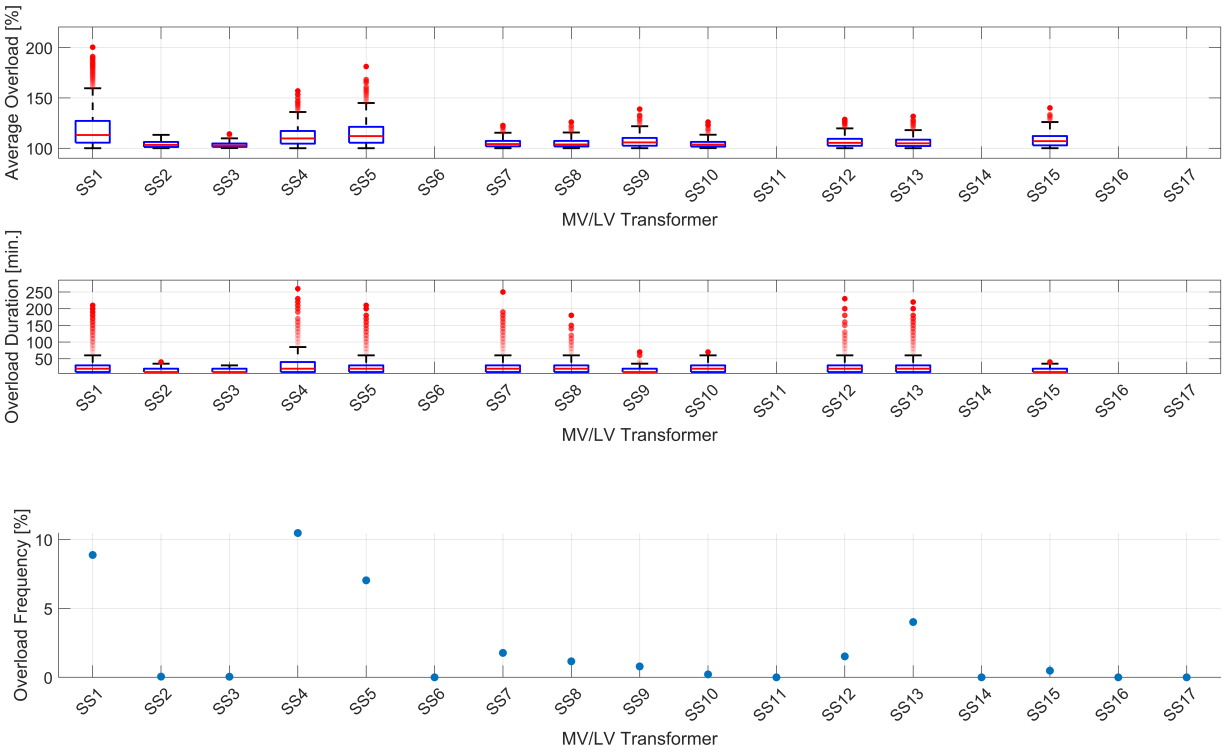

FIGURE 5.14: Secondary substation overload analysis for LV/MV transformers of feeder 25 in the RAPID 2050 scenario.

SS	FEEDER	$P^{NOM}_{EV,LV}$ [kW]	S_{TR} [kVA]	f_{OL} [%]	$f_{OL,V2G}$ [%]	FEEDER	$P^{NOM}_{EV,LV}$ [kW]	S_{TR} [kVA]	f_{OL} [%]	$f_{OL,V2G}$ [%]
1	13	688.3	160	3.5	0.5	25	1058.3	160	9	1
2		991.5	400	0	0		862	400	0	0
3		1017.8	400	0	0		1066.3	400	0	0
4		738.1	160	7.5	1.7		1414.3	250	11	1.7
5		752.1	160	5	1		1368.1	250	7.5	1.5
6		566.7	250	0	0		695.9	400	0	0
7		807.1	250	0	0		826	250	2	0.5
8		786.6	160	9	1.5		1083.4	400	1.5	0
9		534.4	160	0	0		836.1	400	1.25	0
10		1037.3	250	2.5	0.4		516.2	250	0	0
11		658.5	250	0	0		50.4	250	0	0
12		796.7	400	0	0		1242.3	250	2	0
13		402.5	160	0	0		1533.9	400	4.5	0.2
14		374.7	400	0	0		0	250	0	0
15		544.6	250	0	0		801.8	250	0	0
16		304.8	400	0	0		143.8	250	0	0
17		270.6	250	0	0		142.8	400	0	0
18		852	630	0	0					

TABLE 5.6: V2G LV/MV transformer overloads mitigation with V2G.

1h 40 minutes, but some outlier events last almost thrice (300 min = 5 h). The violation frequencies for these smaller transformers are higher than for the MV/HV ones, up to 7.5-10% max., and the average overload magnitude is sizeable as well. Ultimately, we can conclude that the transformer overloading violation events are both high in magnitude and persistent in time.

5.4 Smart EV Charging Mitigation

Since the most impacted parameter is the loading level of the LV/MV transformers, the V2G-based smart EV charging technique described in Section 4.3 is perfect to mitigate the effect of the increasing penetration of EVs.

The aforementioned centralised coordinated EV smart charging algorithm was applied to feeders 13 (140 domestic EV stations) and 25 (93 domestic EV stations) of the RAPID 2050 scenario, and the results are presented in Table 5.6.

When V2G is applied, the overload frequency ($f_{OL,V2G}$) is always much lower than in the case without mitigation (f_{OL}). Indeed, it is often seen that no violations occur.

5.5 Conclusions

Since the analysed grid was designed decades ago based on different requirements, even today some light transformer overloading events may occur.

The network is sufficiently oversized to tolerate EV penetration levels up to 25-30%, in line with the CPI scenario in 2050. The most impacted parameter is, by far, the loading level of the transformers both at the primary and secondary substations. In that regard, the strongest EV charging impact is expected to happen between 2030 and 2040. The violation frequency for LV/MV transformers could increase by 7-17% in both the TECH and RAPID scenarios. The violations are concentrated in urban MV/HV transformers, due to the higher EV charging stations density.

Undervoltage issues at the LV-side of the SS transformers are noteworthy, since the voltage drops down to 0.88 p.u., yet with a very low probability. Nevertheless, it must be highlighted that additional undervoltage violations, alongside with line overloading cases, may occur at the LV side. These issues have not been quantified since the LV grid has not been modelled in the current analysis due to the lack of measured data at the secondary substations and at the electricity points of distribution. Therefore, the simulation results must be regarded as optimistic and this limitation should be considered when performing future grid studies, since most grid issues are expected to arise on the LV grid may anticipate in time the MV grid ones (see Section 2.1.5).

The observability of the distribution grid should be increased by means of additional real-time measurement devices, which currently are limited to the primary substations. By increasing the number of real-time, high-frequency measurement, it could be possible to obtain more representative and trustful data. An additional source of uncertainty in

the model is associated with the EV charging profile generation, since the impact analysis strongly depends on synthetic profiles generation. If real measurement were available, clustering techniques could be used to define a "typical" charging profile for every power level, thus increasing the statistical significance of the results.

Finally, the EV penetration scenarios should be updated frequently, since they are not only dependent on market conditions, but also on incentives and policy makers decisions, which are nowadays rapidly changing.

Centralised V2G-based smart charging can relieve the stress on the SSs transformers, especially when many EVs are idling at domestic charging stations for long hours. However, an important aspect to consider is the willingness of the users to let an external agent, such as an aggregator, determine the charging schedule of their EVs. Since the transition to electric mobility is not only a technical one, but also requires a change in how people make use of their vehicles, studies on social acceptance of this technology are more important than ever and should be incentivised at the European level.

Chapter 6

Conclusions

As mentioned in Chapter 1, a key strategy to meet the requirements of the main climate change mitigation agreements is being able to accommodate larger and larger quantities of distributed energy resources in the power grid. Those resources can either be renewable-based generation units, such as photo-voltaic systems, or consumption ones, such as electric vehicles. A large increase in the number of installed PV systems and EV charging stations poses some threats to the electric distribution system, which needs to be flexible enough to sustain rapid variations of power supply and demand without producing reliability and safety issues for the users. In this context, this thesis firstly analyses the impact of photovoltaic generation (one of the most common sources of clean energy production at the LV side) and proposes possible mitigation strategies based on the use of BESS or smart EV charging strategies.

In Chapter 3, an analysis of the specific case of PV and BESS deployment in renewable energy communities is performed. The latter concept, firstly introduced by the European Commission in 2018, acts as an incentive for the domestic users to purchase a PV+BESS system by compensating them for the amount of energy produced and consumed in the community. In order to make the community as independent from the main grid as possible, BESSs are required, and usually purchased by either the users themselves or an aggregator. In both cases, it is required to minimise the total installed capacity and check that the investment is economically viable for the single users. A multi-objective optimisation genetic algorithm minimising both the dependence of the community on the grid and the total installed battery capacity is thus presented. The main novelty elements include the analysis of the grid impact, in order to make sure that the increase in PV production does not destabilise the voltage levels and produce high electric losses, and the consideration of user willingness to install a BESS. This aspect was considered in the formalisation of the optimisation problem, because the participation to a community is on a voluntary basis, and the users may not want to or have the possibility to also purchase an expensive storage system. Additionally, two different algorithms were tested: a classic peer-to-grid (P2G) one, where each user manages its own battery, and a centralised peer-to-peer (P2P) one, where the batteries are centrally controlled by the aggregator. Results show that, the centralised algorithm performs generally better in terms of energy independence from the grid, since it makes a more efficient use of the available storage capacity. Both losses and CO2 emissions are reduced by the use of storage systems, with P2P showing a slight edge over P2G. Economically wise, the payback period of the investment for each user could be an issue, since not all of them reach payback in 20 years. It has to be noted, however, that in this work no incentives for the participation to an energy community were considered, since the regulation for Italy was still unclear at the time.

A more realistic economic analysis could be performed in this case, since a recent regulatory development in Italy allows for the compensation of the energy shared between the community members. This would provide an additional income source to further reduce the investment payback period for the users. With the current economic incentives for energy communities, the payback problem could be solved if the members shared the cost of the battery, thus benefiting from the scale economy CAPEX reduction. Moreover, the inclusion of flexible demand in the case study, for example to charge electric vehicles or house appliances, could further improve the energy situation.

The impact of electric mobility on a test LV grid is instead analysed in Chapter 4, and a possible smart-charging mitigation strategy with V2G capabilities is proposed. The deployed smart EV charging strategy tries to mitigate the active power fluctuations at the MV/LV transformer level by charging and discharging the EV fleet in a centralised fashion. While the optimisation problem is formulated as a quadratic programming one (a very well known methodology in the literature), there are several novelty aspects that are not so commonly considered in the literature. Firstly, since the

charging algorithm relies on a perfect production-demand mismatch forecast, we analysed to which extent this solutions is robust enough to be applied in real-world conditions (i.e. when the load, generation and EV usage profiles are not the expected ones). Results of the application of the EV charging profiles optimised for one day to the following one show that the solution could be realistic in a day-ahead scheduling scenario, when there is no perfect forecast of the load and demand mismatch of the day. Secondly, the combined impact of the EV charging stations and PV systems on the grid is also analysed, and the results show that smart charging not only decreases the impact that underproduction has on the grid, but also helps mitigating PV-related overproduction, which is usually far more complicated to manage. Thirdly a detailed power flow analysis of the voltage, lines loading and transformer loading levels is performed. Results show that, even if the algorithm is centralised, all the parameters are improved by the EV smart charging strategy. Moreover, the impact of smart charging on the capacity loss for the EV batteries is particularly relevant for PHEVs, which have the smallest batteries.

Even though this first analysis was enough to show the good performance of the smart EV charging algorithm, there are some shortcomings that need to be addressed to complete the work. Firstly, the analysis should be expanded to consider the payback period for purchasing the EV. Secondly, a complete analysis of the CO2 emissions reduction due to smart charging should be performed, not only including the lower electricity consumption term, but also including a life-cycle assessment of the EV with and without smart charging. Moreover, a real-time version of the algorithm should be implemented, so that the active power mismatch is optimised at each time instant but still considering load and production forecasts to fully exploit the capabilities of smart charging on a longer time horizon (daily). The implementation as a real-time algorithm would allow for the provision of other grid stabilisation services, such as reactive power support, voltage stabilisation and losses minimisation. This solution could also allow for the inclusion of stationary storage systems, which could be prioritised over EVs whenever V2G is not possible, and vice-versa. Finally, the inclusion of battery wear as one of the limitations to smart EV charging will need to be considered, as a reduction of 30% of the battery lifetime could dissuade some users to participate in V2G schemes.

In Chapter 5 instead, the impact of slow and fast EV deployment on a real distribution system located in the northern Italian city of Trento is analysed for the 2020-2050 period. The task included the creation and validation of the feeders model, the generation of a database of realistic EV charging profiles for the different time horizons, and the placement of the stations on the grid. The impact analysis shows that the grid will start suffering mostly from transformer overloads and undervoltage events between 2030 and 2040. This happens whenever the EV uptake speed is considered as "rapid" and "very rapid", i.e. when around 50% of the users have an EV charging station. Even though the analysis was performed only at the MV level, and no measurements were available at the secondary substations to validate the grid model, the EV charging impact can be effectively reduced by applying the same smart charging technique proposed in Chapter 4. Results show that the smart charging technique is very efficient in reducing the transformer overloads and stabilising the grid, allowing for a higher EVs penetration. Some suggestions should be made regarding the main technical and practical challenges which frequently surface when performing this kind of study. Firstly, the lack of measurements at the low-voltage level, which makes it really difficult to validate the results of the simulations. In this particular case, one of the shortcomings of the study lies in the lack of measurements at the secondary substations, which does not allow for a validation of the power flow at the LV level. Secondly, the uncertainty in the determination of the number of EVs circulating in a particular area in the following years, mainly due to the large EV market fluctuations. Thirdly, finding a reliable dataset of EV demand profiles is usually very hard, given the high variability of the users charging behaviour, even inside the same country. Around this last topic, it must be remarked that the transition towards electric mobility is not only a technical and economical change of paradigm, but also requires a change in society, and in the way people use their vehicles. Studies on this topic are, today more than ever, fundamental also from the technical standpoint.

Possible improvements here should include the LV network modelling, which could be used to assess more realistically the impact of both uncontrolled and smart EV charging on the grid, and the creation of additional scenarios with an increasing amount of PV generation or even faster EV uptake speeds.

Journal Publications:

- M.Secchi, G.Barchi, D.Macii, D.Moser, D.Petri (2021) "Multi-objective battery sizing optimisation for renewable energy communities with distribution-level constraints: A prosumer-driven perspective", Applied Energy 297 (Elsevier), p.117171. https://doi.org/10.1016/J.APENERGY.2021.117171
- E. Dalla Maria, M.Secchi, D.Macii (2021) "A Flexible Top-Down Data-Driven Stochastic Model for Synthetic Load Profiles Generation", Energies Vol. 15 (MDPI), p.269, https://doi.org/10.3390/EN15010269
- (submitted) M.Secchi, G.Barchi, D.Macii (2022) "Smart Electric Vehicles Charging with Centralised Vehicle-to-Grid Capability for Net-Load Variance Minimisation under Increasing EV and PV Penetration Levels", Sustainable Energy, Grids and Networks (Elsevier)

Conference Publications:

- M.Secchi, G.Barchi (2019) "Peer-to-peer electricity sharing: Maximising PV self-consumption through BESS control strategies", Proceedings - 2019 IEEE International Conference on Environment and Electrical Engineering and 2019 IEEE Industrial and Commercial Power Systems Europe, EEEIC/I and CPS Europe 2019, https://doi.org/10.1109/EEEIC.2019.8783608

Acknowledgements

Some years ago, someone told me "once you delve deep into a discipline, you start finding connections to many others", and I think that sentence contains both the best and the worst side of research. For me, being a researcher means that you are deeply engaged with what you do, sometimes even forgetting that you do not (and should not) identify with it, and that every day you work is a well spent one. That pushes you to wake up every day, to try and give 100% of what you have. I don't think many other jobs can give you the same feeling and motivation. At the same time, it becomes very difficult to get invested in anything else, or enjoy the things you do outside of work, especially when you are overburdened by a lot of work and feelings. During these three (almost four) years of PhD, some periods were exactly like that, an endless barrage of problems to solve, with no end in sight. Nonetheless, even at those times, I was lucky enough to do the job I want to do, and to try to advance a field, the renewable energy grid integration one, that made me feel, many times, unprepared and unable to do anything meaningful. I think it will take me some time to realise that I am finally done, and that I will now have (maybe), a little bit more freedom to try and find new ways to advance the technology behind battery and electric vehicles smart controls. Now, to the real "acknowledgements" part. I have to be honest, and recognise that the first person I have to thank is myself. Enduring all of these challenges was difficult, but I strongly believe it made me a more resilient person, and I have to thank myself for that, first and foremost. I could not, however, have achieved this result without all of my family, friends and colleagues, who have been part of this journey. My parents, who are a very big part of my inspiration and made me who I am: every day I realise how much I owe you and how lucky I was to have your support, even if you probably still don't exactly understand what is my job and what I did during the last four years! You were unlucky enough to have a wandering son who is moving countries and still trying to find his place in the world, but I hope you are proud of me the same. My uncles and aunts, which were always there when I needed support, and, most of all, food. Because nothing makes you feel at home like food (Italians do it better). My travelling companion, part-time complaints listener and best friend Pesco, which is simply one of the greatest people I know. Hope you are going to survive the PhD and achieve all your life goals. Silvia and Riccardo, for all the times they visited Bolzano and brought a lot of food and warmth in our weekends. Luca and Bellent, for all the long, tiring, but funny evenings spent on DnD, Final Fantasy or Sea of Thieves. I would have not survived two lockdowns without you! My flatmates Nico and Heidi, who shared with me every single day in the last three years and never made me feel weird or insane when I was going mad about work. Thank you, I hope we will still be in each others' lives for a long time. Atlas! Because he is the chunkiest fluffiest boi, and he has been the greatest mental health support ever (seriously people, get a dog!). Giulia, because we are "super-friends" (does it work, in English?), Eric, for all the inspiring talks (?) and the buckets he let me score while playing basketball, Carlotta, for all the time we spent together. All of my friends from Bolzano, especially Mariangela, because they dragged me out of my room to enjoy the mountains, the dinners and all of the things we organised during these years. Finally, all of my colleagues at Eurac, for all their advices and support. In particular all the members of the PVS group: Grazia and David for their mentorship and advices, Valeria because we know better than anyone how difficult it is to debug and make everything work, Elisa for all of the nerd and inspiring politics conversations, Martina because "not everything is about work". At UniTN, I would like to thank my supervisor Dario Petri for this opportunity, and David for all the hard work he poured into the two papers we published. I couldn't have achieved this result without all of the people I mentioned!

Now I am sure I forgot to thank someone, but the space here is over, so thank you to everyone that shared even a small part of this journey with me!

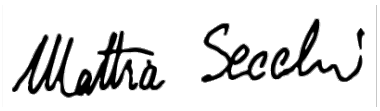

Bibliography

[1] Pörtner et al. *Climate Change 2022: Impacts, Adaptation, and Vulnerability. Contribution of Working Group II to the Sixth Assessment Report of the Intergovernmental Panel on Climate Change*. Cambridge University Press, 2022. URL: https://report.ipcc.ch/ar6wg3/pdf/IPCC_AR6_WGIII_SummaryForPolicymakers.pdf.

[2] Diana María López González and John Garcia Rendon. "Opportunities and challenges of mainstreaming distributed energy resources towards the transition to more efficient and resilient energy markets". In: *Renewable and Sustainable Energy Reviews* 157 (Apr. 2022), p. 112018. ISSN: 1364-0321. DOI: 10.1016/J.RSER.2021.112018.

[3] Juan Caballero-Peña et al. "Distributed energy resources on distribution networks: A systematic review of modelling, simulation, metrics, and impacts". In: *International Journal of Electrical Power and Energy Systems* 138 (June 2022), p. 107900. ISSN: 0142-0615. DOI: 10.1016/J.IJEPES.2021.107900.

[4] *Renewables 2021*. IEA, 2021. URL: https://www.iea.org/reports/renewables-2021.

[5] M. Samper, G. Coria, and M. Facchini. "Grid parity analysis of distributed PV generation considering tariff policies in Argentina". In: *Energy Policy* 157 (Oct. 2021), p. 112519. ISSN: 0301-4215. DOI: 10.1016/J.ENPOL.2021.112519.

[6] Benjamin Pillot, Sandro de Siqueira, and João Batista Dias. "Grid parity analysis of distributed PV generation using Monte Carlo approach: The Brazilian case". In: *Renewable Energy* 127 (Nov. 2018), pp. 974–988. ISSN: 0960-1481. DOI: 10.1016/J.RENENE.2018.05.032.

[7] Hongyang Zou et al. "Large-scale PV power generation in China: A grid parity and techno-economic analysis". In: *Energy* 134 (Sept. 2017), pp. 256–268. ISSN: 0360-5442. DOI: 10.1016/J.ENERGY.2017.05.192.

[8] Nico Goetzel and M. Hasanuzzaman. "An empirical analysis of electric vehicle cost trends: A case study in Germany". In: *Research in Transportation Business & Management* (Apr. 2022), p. 100825. ISSN: 2210-5395. DOI: 10.1016/J.RTBM.2022.100825. URL: https://linkinghub.elsevier.com/retrieve/pii/S2210539522000463.

[9] Zhe Liu et al. "Comparing total cost of ownership of battery electric vehicles and internal combustion engine vehicles". In: *Energy Policy* 158 (Nov. 2021), p. 112564. ISSN: 0301-4215. DOI: 10.1016/J.ENPOL.2021.112564.

[10] Emilio Ghiani and Giuditta Pisano. "Impact of Renewable Energy Sources and Energy Storage Technologies on the Operation and Planning of Smart Distribution Networks". In: *Operation of Distributed Energy Resources in Smart Distribution Networks* (Jan. 2018), pp. 25–48. DOI: 10.1016/B978-0-12-814891-4.00002-3.

[11] "Voltage characteristics of electricity supplied by public distribution networks". In: *CEI/EN 50160:2010* (2010). URL: https://mycatalogo.ceinorme.it/cei/item/0000011266/?sso=y.

[12] "Impianti elettrici utilizzatori a tensione nominale non superiore a 1000 V in corrente alternata e a 1500 V in corrente continua". In: *CEI 64-8:2021* (2021). URL: https://mycatalogo.ceinorme.it/book/item/00M000229?sso=y.

[13] Andrew Dixon. *Modern aspects of power system frequency stability and control*. Elsevier, Jan. 2019, pp. 1–321. ISBN: 9780128161395. DOI: 10.1016/C2017-0-03431-6.

[14] "Ecodesign requirements for light sources and separate control gears." In: *Commission Regulation 2019/2020* (2019). URL: https://eur-lex.europa.eu/legal-content/EN/TXT/?uri=uriserv:OJ.L_.2019.315.01.0209.01.ENG.

[15] Yesbol Gabdullin and Brian Azzopardi. "Impacts of High Penetration of Photovoltaic Integration in Malta". In: *2018 IEEE 7th World Conference on Photovoltaic Energy Conversion, WCPEC 2018 - A Joint Conference of 45th IEEE PVSC, 28th PVSEC and 34th EU PVSEC* (Nov. 2018), pp. 1398–1401. DOI: 10.1109/PVSC.2018.8548256.

[16] Tariq Aziz and Nipon Ketjoy. "PV Penetration Limits in Low Voltage Networks and Voltage Variations". In: *IEEE Access* 5 (Aug. 2017), pp. 16784–16792. ISSN: 21693536. DOI: 10.1109/ACCESS.2017.2747086.

[17] Sa'Adah Daud, Aida Fazliana Abdul Kadir, and Chin Kim Gan. "The impacts of distributed Photovoltaic generation on power distribution networks losses". In: *2015 IEEE Student Conference on Research and Development, SCOReD 2015* (2015), pp. 11–15. DOI: 10.1109/SCORED.2015.7449305.

[18] Nhamo Dhlamini and S. P. Daniel Chowdhury. "Solar Photovoltaic Generation and its Integration Impact on the Existing Power Grid". In: *2018 IEEE PES/IAS PowerAfrica, PowerAfrica 2018* (Nov. 2018), pp. 710–715. DOI: 10.1109/POWERAFRICA.2018.8521003.

[19] Gabriel Tévar-Bartolomé et al. "Network impact of increasing distributed PV hosting: A utility-scale case study". In: *Solar Energy* 217 (Mar. 2021), pp. 173–186. ISSN: 0038-092X. DOI: 10.1016/J.SOLENER.2021.01.066.

[20] Cristina González-Morán, Pablo Arboleya, and Valeria Pilli. "Photovoltaic self consumption analysis in a European low voltage feeder". In: *Electric Power Systems Research* 194 (December 2020 May 2021), p. 107087. ISSN: 03787796. DOI: 10.1016/j.epsr.2021.107087. URL: https://linkinghub.elsevier.com/retrieve/pii/S0378779621000687.

[21] Bryan B. Navarro and Maricar M. Navarro. "A comprehensive solar PV hosting capacity in MV and LV radial distribution networks". In: *2017 IEEE PES Innovative Smart Grid Technologies Conference Europe, ISGT-Europe 2017 - Proceedings* 2018-January (July 2017), pp. 1–6. DOI: 10.1109/ISGTEUROPE.2017.8260210.

[22] N. C. Tang and G. W. Chang. "A stochastic approach for determining PV hosting capacity of a distribution feeder considering voltage quality constraints". In: *Proceedings of International Conference on Harmonics and Quality of Power, ICHQP* 2018-May (June 2018), pp. 1–5. ISSN: 21640610. DOI: 10.1109/ICHQP.2018.8378864.

[23] Anamika Dubey, Surya Santoso, and Arindam Maitra. "Understanding photovoltaic hosting capacity of distribution circuits". In: *IEEE Power and Energy Society General Meeting* 2015-September (Sept. 2015). ISSN: 19449933. DOI: 10.1109/PESGM.2015.7286510.

[24] Oğuzhan Ceylan et al. "Photovoltaic hosting capacity of feeders with reactive power control and tap changers". In: *2017 IEEE PES Innovative Smart Grid Technologies Conference Europe, ISGT-Europe 2017 - Proceedings* 2018-January (July 2017), pp. 1–6. DOI: 10.1109/ISGTEUROPE.2017.8260243.

[25] P. Mohammadi and S. Mehraeen. "Challenges of PV Integration in Low-Voltage Secondary Networks". In: *IEEE Transactions on Power Delivery* 32 (1 Feb. 2017), pp. 525–535. ISSN: 08858977. DOI: 10.1109/TPWRD.2016.2556692.

[26] Hamed Valizadeh Haghi et al. "Feeder Impact Assessment of Smart Inverter Settings to Support High PV Penetration in California". In: *IEEE Power and Energy Society General Meeting* 2019-August (Aug. 2019). ISSN: 19449933. DOI: 10.1109/PESGM40551.2019.8974016.

[27] Andrea Ballanti and Luis F. Ochoa. "On the integrated PV hosting capacity of MV and LV distribution networks". In: *2015 IEEE PES Innovative Smart Grid Technologies Latin America, ISGT LATAM 2015* (Jan. 2016), pp. 366–370. DOI: 10.1109/ISGT-LA.2015.7381183.

[28] Matthew J. Reno and Robert J. Broderick. "Optimal Siting of PV on the Distribution System with Smart Inverters". In: *2018 IEEE 7th World Conference on Photovoltaic Energy Conversion, WCPEC 2018 - A Joint Conference of 45th IEEE PVSC, 28th PVSEC and 34th EU PVSEC* (Nov. 2018), pp. 1468–1470. DOI: 10.1109/PVSC.2018.8547667.

[29] Jian Liu and Hsiao Dong Chiang. "Maximizing Available Delivery Capability of Unbalanced Distribution Networks for High Penetration of Distributed Generators". In: *IEEE Transactions on Power Delivery* 32 (3 June 2017), pp. 1196–1202. ISSN: 08858977. DOI: 10.1109/TPWRD.2014.2359291.

[30] "PV Hosting Capacity Dependence on Harmonic Voltage Distortion in Low-Voltage Grids: Model Validation with Experimental Data". In: *Energies 2018, Vol. 11, Page 465* 11 (2 Feb. 2018), p. 465. ISSN: 19961073. DOI: 10.3390/EN11020465. URL: https://www.mdpi.com/1996-1073/11/2/465/htmhttps://www.mdpi.com/1996-1073/11/2/465.

[31] "Photovoltaic generation penetration limits in radial distribution systems". In: *IEEE Transactions on Power Systems* 26 (3 Aug. 2011), pp. 1625–1631. ISSN: 08858950. DOI: 10.1109/TPWRS.2010.2077656.

[32] Rasmus Luthander, David Lingfors, and Joakim Widén. "Large-scale integration of photovoltaic power in a distribution grid using power curtailment and energy storage". In: *Solar Energy* 155 (Oct. 2017), pp. 1319–1325. ISSN: 0038-092X. DOI: 10.1016/J.SOLENER.2017.07.083.

[33] Gerd Heilscher et al. "Evaluation of PV Hosting Capacities of Distribution Grids with Utilization of Solar-Roof-Potential-Analyses". In: *2017 IEEE 44th Photovoltaic Specialist Conference (PVSC)*. 2017, pp. 2996–3001. DOI: 10.1109/PVSC.2017.8366343.

[34] Falko Ebe et al. "Evaluation of PV hosting capacity of distribuion grids considering a solar roof potential analysis - Comparison of different algorithms". In: *2017 IEEE Manchester PowerTech, Powertech 2017* (July 2017). DOI: 10.1109/PTC.2017.7981017.

[35] Desmond Okwabi Ampofo, Isaac Kofi Otchere, and Emmanuel Asuming Frimpong. "An investigative study on penetration limits of distributed generation on distribution networks". In: *Proceedings - 2017 IEEE PES-IAS*

PowerAfrica Conference: Harnessing Energy, Information and Communications Technology (ICT) for Affordable Electrification of Africa, PowerAfrica 2017 (July 2017), pp. 573–576. DOI: 10.1109/POWERAFRICA.2017.7991289.

[36] K. Balamurugan, Dipti Srinivasan, and Thomas Reindl. "Impact of Distributed Generation on Power Distribution Systems". In: *Energy Procedia* 25 (Jan. 2012), pp. 93–100. ISSN: 1876-6102. DOI: 10.1016/J.EGYPRO.2012.07.013.

[37] Riccardo Carollo, Sanjay K. Chaudhary, and Jayakrishnan R. Pillai. "Hosting capacity of solar photovoltaics in distribution grids under different pricing schemes". In: *Asia-Pacific Power and Energy Engineering Conference, APPEEC* 2016-January (Jan. 2016). ISSN: 21574847. DOI: 10.1109/APPEEC.2015.7380971.

[38] J. W. Smith, R. Dugan, and W. Sunderman. "Distribution modeling and analysis of high penetration PV". In: *IEEE Power and Energy Society General Meeting* (2011). ISSN: 19449925. DOI: 10.1109/PES.2011.6039765.

[39] Robert Joseph Broderick et al. "Time series power flow analysis for distribution connected PV generation." In: (Jan. 2013). DOI: 10.2172/1088099. URL: https://www.osti.gov/servlets/purl/1088099/.

[40] Kalpesh A. Joshi and Naran M. Pindoriya. "Reactive resource reallocation in DG integrated secondary distribution networks with time-series distribution power flow". In: *2014 IEEE International Conference on Power Electronics, Drives and Energy Systems, PEDES 2014* (Feb. 2014). DOI: 10.1109/PEDES.2014.7042111.

[41] Miroslav M. Begovic, Insu Kim, and Mladen Kezunovic. "Impact of stochastically distributed renewable PV generation on distribution network". In: *19th Power Systems Computation Conference, PSCC 2016* (Aug. 2016). DOI: 10.1109/PSCC.2016.7541018.

[42] Fei Ding and Barry Mather. "On Distributed PV Hosting Capacity Estimation, Sensitivity Study, and Improvement". In: *IEEE Transactions on Sustainable Energy* 8 (3 July 2017), pp. 1010–1020. ISSN: 19493029. DOI: 10.1109/TSTE.2016.2640239.

[43] Thomas Stetz et al. "High Penetration PV in Local Distribution Grids - Outcomes of the IEA PVPS Task 14 Subtask 2". In: Sept. 2014.

[44] P. B. Kitworawut, D. T. Azuatalam, and A. J. Collin. "An investigation into the technical impacts of microgeneration on UK-type LV distribution networks". In: Institute of Electrical and Electronics Engineers (IEEE), Nov. 2016, pp. 1–5. DOI: 10.1109/AUPEC.2016.7749321.

[45] Thomas Stetz, Frank Marten, and Martin Braun. "Improved low voltage grid-integration of photovoltaic systems in Germany". In: *IEEE Transactions on Sustainable Energy* 4 (2 2013), pp. 534–542. ISSN: 19493029. DOI: 10.1109/TSTE.2012.2198925.

[46] Ahmed A. Raouf Mohamed et al. "Impact of the deployment of solar photovoltaic and electrical vehicle on the low voltage unbalanced networks and the role of battery energy storage systems". In: *Journal of Energy Storage* 42 (Oct. 2021), p. 102975. ISSN: 2352-152X. DOI: 10.1016/J.EST.2021.102975.

[47] Reza Fachrizal et al. "Combined PV-EV hosting capacity assessment for a residential LV distribution grid with smart EV charging and PV curtailment". In: *Sustainable Energy, Grids and Networks* 26 (Feb. 2021), p. 100445. ISSN: 23524677. DOI: 10.1016/j.segan.2021.100445.

[48] Lucian Ioan Dulau and Dorin Bica. "Effects of Electric Vehicles on Power Networks". In: *Procedia Manufacturing* 46 (Jan. 2020), pp. 370–377. ISSN: 2351-9789. DOI: 10.1016/J.PROMFG.2020.03.054.

[49] P. Papadopoulos et al. "Impact of residential charging of electric vehicles on distribution networks, a probabilistic approach". In: *45th International Universities Power Engineering Conference UPEC2010*. 2010, pp. 1–5.

[50] Amir S. Masoum et al. "Impacts of battery charging rates of plug-in electric vehicle on smart grid distribution systems". In: *IEEE PES Innovative Smart Grid Technologies Conference Europe, ISGT Europe* (2010). DOI: 10.1109/ISGTEUROPE.2010.5638981.

[51] Chris Farmer et al. "Modeling the impact of increasing PHEV loads on the distribution infrastructure". In: *Proceedings of the Annual Hawaii International Conference on System Sciences* (2010). ISSN: 15301605. DOI: 10.1109/HICSS.2010.277.

[52] L. Kelly, A. Rowe, and P. Wild. "Analyzing the impacts of plug-in electric vehicles on distribution networks in British Columbia". In: *2009 IEEE Electrical Power and Energy Conference, EPEC 2009* (2009). DOI: 10.1109/EPEC.2009.5420904.

[53] Justin Schlee et al. "The effects of plug-in electric vehicles on a small distribution grid". In: *41st North American Power Symposium, NAPS 2009* (2009). DOI: 10.1109/NAPS.2009.5484055.

[54] Sylvester Johansson et al. "Investigation of the Impact of Large-Scale Integration of Electric Vehicles for a Swedish Distribution Network". In: *Energies 2019, Vol. 12, Page 4717* 12 (24 Dec. 2019), p. 4717. ISSN: 19961073.

DOI: 10.3390/EN12244717. URL: https://www.mdpi.com/1996-1073/12/24/4717/htmhttps://www.mdpi.com/1996-1073/12/24/4717.

[55] Anamika Dubey and Surya Santoso. "Electric Vehicle Charging on Residential Distribution Systems: Impacts and Mitigations". In: *IEEE Access* 3 (2015), pp. 1871–1893. ISSN: 21693536. DOI: 10.1109/ACCESS.2015.2476996.

[56] Niels Leemput et al. "Impact of electric vehicle on-board single-phase charging strategies on a flemish residential grid". In: *IEEE Transactions on Smart Grid* 5 (4 2014), pp. 1815–1822. ISSN: 19493053. DOI: 10.1109/TSG.2014.2307897.

[57] Mohammed J.M. Al Essa and L. M. Cipcigan. "Effects of randomly charging electric vehicles on voltage unbalance in micro grids". In: *Proceedings of the Universities Power Engineering Conference* 2015-November (Nov. 2015). DOI: 10.1109/UPEC.2015.7339906.

[58] Selcuk Sakar et al. "Increasing PV hosting capacity in distorted distribution systems using passive harmonic filtering". In: *Electric Power Systems Research* 148 (July 2017), pp. 74–86. ISSN: 0378-7796. DOI: 10.1016/J.EPSR.2017.03.020.

[59] Selcuk Sakar et al. "Integration of large- scale PV plants in non-sinusoidal environments: Considerations on hosting capacity and harmonic distortion limits". In: *Renewable and Sustainable Energy Reviews* 82 (Feb. 2018), pp. 176–186. ISSN: 1364-0321. DOI: 10.1016/J.RSER.2017.09.028.

[60] Ricardo Torquato et al. "A Comprehensive Assessment of PV Hosting Capacity on Low-Voltage Distribution Systems". In: *IEEE Transactions on Power Delivery* 33 (2 Apr. 2018), pp. 1002–1012. ISSN: 08858977. DOI: 10.1109/TPWRD.2018.2798707.

[61] Jason Taylor et al. "Evaluations of plug-in electric vehicle distribution system impacts". In: *IEEE PES General Meeting, PES 2010* (2010). DOI: 10.1109/PES.2010.5589538.

[62] Peças J.A. Lopes et al. "Quantification of technical impacts and environmental benefits of electric vehicles integration on electricity grids". In: *2009 8th International Symposium on Advanced Electromechanical Motion Systems and Electric Drives Joint Symposium, ELECTROMOTION 2009* (2009). DOI: 10.1109/ELECTROMOTION.2009.5259139.

[63] Md Rabiul Islam et al. "Compensating Neutral Current, Voltage Unbalance and Improving Voltage of an Unbalanced Distribution Grid Connected with EV and Renewable Energy Sources". In: *2019 22nd International Conference on Electrical Machines and Systems, ICEMS 2019* (Aug. 2019). DOI: 10.1109/ICEMS.2019.8922198.

[64] Junjie Hu et al. "Coordinated voltage control of a decoupled three-phase on-load tap changer transformer and photovoltaic inverters for managing unbalanced networks". In: *Electric Power Systems Research* 131 (Feb. 2016), pp. 264–274. ISSN: 0378-7796. DOI: 10.1016/J.EPSR.2015.10.025.

[65] Michael Emmanuel and Ramesh Rayudu. "The impact of single-phase grid-connected distributed photovoltaic systems on the distribution network using P-Q and P-V models". In: *International Journal of Electrical Power And Energy Systems* 91 (Oct. 2017), pp. 20–33. ISSN: 0142-0615. DOI: 10.1016/J.IJEPES.2017.03.001.

[66] A. Khoshkbar-Sadigh and K. M. Smedley. "The necessity of time-series simulation for investigation of large-scale solar energy penetration". In: *2015 IEEE Power and Energy Society Innovative Smart Grid Technologies Conference, ISGT 2015* (June 2015). DOI: 10.1109/ISGT.2015.7131803.

[67] Daphne Schwanz et al. "Stochastic Assessment of Voltage Unbalance Due to Single-Phase-Connected Solar Power". In: *IEEE Transactions on Power Delivery* 32 (2 Apr. 2017), pp. 852–861. ISSN: 08858977. DOI: 10.1109/TPWRD.2016.2579680.

[68] Luis Pieltain Fernández et al. "Assessment of the impact of plug-in electric vehicles on distribution networks". In: *IEEE Transactions on Power Systems* 26 (1 Feb. 2011), pp. 206–213. ISSN: 08858950. DOI: 10.1109/TPWRS.2010.2049133.

[69] Md Rabiul Islam et al. "Optimal Coordination of Electric Vehicles and Distributed Generators for Voltage Unbalance and Neutral Current Compensation". In: *IEEE Transactions on Industry Applications* 57 (1 Jan. 2021), pp. 1069–1080. ISSN: 19399367. DOI: 10.1109/TIA.2020.3037275.

[70] E. A. Feilat, S. Azzam, and A. Al-Salaymeh. "Impact of large PV and wind power plants on voltage and frequency stability of Jordan's national grid". In: *Sustainable Cities and Society* 36 (Jan. 2018), pp. 257–271. ISSN: 2210-6707. DOI: 10.1016/J.SCS.2017.10.035.

[71] Rudi Darussalam and Iwa Garniwa. "The effect of photovoltaic penetration on frequency response of distribution system". In: *Proceedings - 6th International Conference on Sustainable Energy Engineering and Application, ICSEEA 2018* (Jan. 2019), pp. 81–85. DOI: 10.1109/ICSEEA.2018.8627080.

[72] S. A. Pourmousavi, A. S. Cifala, and M. H. Nehrir. "Impact of high penetration of PV generation on frequency and voltage in a distribution feeder". In: *2012 North American Power Symposium, NAPS 2012* (2012). DOI: 10.1109/NAPS.2012.6336320.

[73] Atik Jawad and Nahid Al Masood. "A systematic approach to estimate the frequency support from large-scale PV plants in a renewable integrated grid". In: *Energy Reports* 8 (Nov. 2022), pp. 940–954. ISSN: 2352-4847. DOI: 10.1016/J.EGYR.2021.12.017.

[74] Md Moktadir Rahman et al. "A new approach to voltage management in unbalanced low voltage networks using demand response and OLTC considering consumer preference". In: *International Journal of Electrical Power and Energy Systems* 99 (July 2018), pp. 11–27. ISSN: 0142-0615. DOI: 10.1016/J.IJEPES.2017.12.034.

[75] Bo Wang et al. "Improving Hosting Capacity of Unbalanced Distribution Networks via Robust Allocation of Battery Energy Storage Systems". In: *IEEE Transactions on Power Systems* 36 (3 May 2021), pp. 2174–2185. ISSN: 15580679. DOI: 10.1109/TPWRS.2020.3029532.

[76] Xiangjing Su, Mohammad A.S. Masoum, and Peter J. Wolfs. "Optimal PV inverter reactive power control and real power curtailment to improve performance of unbalanced four-wire LV distribution networks". In: *IEEE Transactions on Sustainable Energy* 5 (3 2014), pp. 967–977. ISSN: 19493029. DOI: 10.1109/TSTE.2014.2313862.

[77] G. A. Putrus et al. "Impact of electric vehicles on power distribution networks". In: *5th IEEE Vehicle Power and Propulsion Conference, VPPC '09* (2009), pp. 827–831. DOI: 10.1109/VPPC.2009.5289760.

[78] R. Saravanan et al. "A hybrid strategy for mitigating unbalance and improving voltage considering higher penetration of electric vehicles and distributed generation". In: *Sustainable Cities and Society* 76 (Jan. 2022), p. 103489. ISSN: 2210-6707. DOI: 10.1016/J.SCS.2021.103489.

[79] Thongchai Klayklueng and Sanchai Dechanupaprittha. "Impact analysis on voltage unbalance of EVs charging on a low voltage distribution system". In: *2014 International Electrical Engineering Congress, iEECON 2014* (Oct. 2014). DOI: 10.1109/IEECON.2014.6925899.

[80] Ibrahim Cagri Barutcu, Engin Karatepe, and Mutlu Boztepe. "Impact of harmonic limits on PV penetration levels in unbalanced distribution networks considering load and irradiance uncertainty". In: *International Journal of Electrical Power And Energy Systems* 118 (June 2020), p. 105780. ISSN: 0142-0615. DOI: 10.1016/J.IJEPES.2019.105780.

[81] Gianfranco Chicco, Juergen Schlabbach, and Filippo Spertino. "Operation of multiple inverters in grid-connected large-size Photovoltaic installations | IET Conference Publication | IEEE Xplore". In: 2009. URL: https://ieeexplore.ieee.org/document/5255952.

[82] Haitao Hu et al. "Potential harmonic resonance impacts of PV inverter filters on distribution systems". In: *IEEE Transactions on Sustainable Energy* 6 (1 Jan. 2015), pp. 151–161. ISSN: 19493029. DOI: 10.1109/TSTE.2014.2352931.

[83] Zhida Deng, Mihai D. Rotaru, and Jan K. Sykulski. "Harmonic Analysis of LV distribution networks with high PV penetration". In: *Proceedings - 2017 International Conference on Modern Power Systems, MPS 2017* (July 2017). DOI: 10.1109/MPS.2017.7974392.

[84] J. Carlos Gómez and Medhat M. Morcos. "Impact of EV battery chargers on the power quality of distribution systems". In: *IEEE Transactions on Power Delivery* 18 (3 July 2003), pp. 975–981. ISSN: 08858977. DOI: 10.1109/TPWRD.2003.813873.

[85] Jing Guo et al. "Research on Harmonic Characteristics and Harmonic Counteraction Problem of EV Charging Station". In: *2nd IEEE Conference on Energy Internet and Energy System Integration, EI2 2018 - Proceedings* (Dec. 2018). DOI: 10.1109/EI2.2018.8582095.

[86] Lauri Kutt et al. "Harmonic distortions of multiple power factor compensated EV chargers". In: *2014 16th European Conference on Power Electronics and Applications, EPE-ECCE Europe 2014* (Sept. 2014). DOI: 10.1109/EPE.2014.6911035.

[87] C. Biedermann, G.-L. Di Modica, and B. Engel. "Measurement of the Voltage Quality and Load Profiles of Electric Vehicles". In: Institution of Engineering and Technology (IET), Jan. 2022, pp. 891–895. DOI: 10.1049/ICP.2021.2162.

[88] G. K. Ari and Y. Baghzouz. "Impact of high PV penetration on voltage regulation in electrical distribution systems". In: *3rd International Conference on Clean Electrical Power: Renewable Energy Resources Impact, ICCEP 2011* (2011), pp. 744–748. DOI: 10.1109/ICCEP.2011.6036386.

[89] Farzad Ferdowsi, Shahab Mehraeen, and Gregory B. Upton. "Assessing distribution network sensitivity to voltage rise and flicker under high penetration of behind-the-meter solar". In: *Renewable Energy* 152 (June 2020), pp. 1227–1240. ISSN: 0960-1481. DOI: 10.1016/J.RENENE.2019.12.124.

[90] Ammar Arshad and Matti Lehtonen. "Instantaneous Active/Reactive Power Control Strategy for Flicker Mitigation under High PV Penetration". In: *Proceedings - 2018 IEEE PES Innovative Smart Grid Technologies Conference Europe, ISGT-Europe 2018* (Dec. 2018). DOI: 10.1109/ISGTEUROPE.2018.8571855.

[91] Bishoy Basta and Walid G. Morsi. "Probabilistic assessment of the impact of integrating large-scale high-power fast charging stations on the power quality in the distribution systems". In: *2020 IEEE Electric Power and Energy Conference, EPEC 2020* (Nov. 2020). DOI: 10.1109/EPEC48502.2020.9320013.

[92] Anne Blavette et al. "Analysis of the flicker level generated by the grid-connection of a fleet of electric vehicles". In: *IEEE PES Innovative Smart Grid Technologies Conference Europe* (July 2016). DOI: 10.1109/ISGTEUROPE.2016.7856187.

[93] Sami M. Alshareef and Walid G. Morsi. "Impact of fast charging stations on the voltage flicker in the electric power distribution systems". In: *2017 IEEE Electrical Power and Energy Conference, EPEC 2017* 2017-October (Feb. 2018), pp. 1–6. DOI: 10.1109/EPEC.2017.8286226.

[94] Sanchai Dechanupaprittha and Chaowanan Jamroen. "Self-learning PSO based optimal EVs charging power control strategy for frequency stabilization considering frequency deviation and impact on EV owner". In: *Sustainable Energy, Grids and Networks* 26 (June 2021), p. 100463. ISSN: 2352-4677. DOI: 10.1016/J.SEGAN.2021.100463.

[95] Nataly Bañol Arias et al. "Assessment of economic benefits for EV owners participating in the primary frequency regulation markets". In: *International Journal of Electrical Power And Energy Systems* 120 (Sept. 2020), p. 105985. ISSN: 0142-0615. DOI: 10.1016/J.IJEPES.2020.105985.

[96] Mahmoud Elsisi et al. "Model Predictive Control of Plug-in Hybrid Electric Vehicles for Frequency Regulation in a Smart Grid". In: *IET Generation, Transmission and Distribution* 11 (May 2017). DOI: 10.1049/iet-gtd.2016.2120.

[97] Yufeng Guo et al. "Service life of EV batteries used in power grid frequency regulation". In: *2016 UKACC International Conference on Control, UKACC Control 2016* (Nov. 2016). DOI: 10.1109/CONTROL.2016.7737597.

[98] Abhishek Nayak, Rubi Rana, and Sukumar Mishra. "Frequency Regulation by Electric Vehicle during Grid Restoration using Adaptive Optimal Control". In: *IFAC-PapersOnLine* 52 (4 Jan. 2019), pp. 270–275. ISSN: 2405-8963. DOI: 10.1016/J.IFACOL.2019.08.210.

[99] Hui Liu et al. "EV Dispatch Control for Supplementary Frequency Regulation Considering the Expectation of EV Owners". In: *IEEE Transactions on Smart Grid* 9 (4 July 2018), pp. 3763–3772. ISSN: 19493053. DOI: 10.1109/TSG.2016.2641481.

[100] Nozomu Magome and Shigeru Tamura. "A new decentralized control of EVs for load frequency control retaining EV users' convenience". In: *INTELEC, International Telecommunications Energy Conference (Proceedings)* 2018-October (Jan. 2019). ISSN: 02750473. DOI: 10.1109/INTLEC.2018.8612298.

[101] Wei He et al. "Technologies and economics of electric energy storages in power systems: Review and perspective". In: *Advances in Applied Energy* 4 (Nov. 2021), p. 100060. ISSN: 2666-7924. DOI: 10.1016/J.ADAPEN.2021.100060.

[102] Abraham Alem Kebede et al. "A comprehensive review of stationary energy storage devices for large scale renewable energy sources grid integration". In: *Renewable and Sustainable Energy Reviews* 159 (May 2022), p. 112213. ISSN: 1364-0321. DOI: 10.1016/J.RSER.2022.112213.

[103] Yuqing Yang et al. "Battery energy storage system size determination in renewable energy systems: A review". In: *Renewable and Sustainable Energy Reviews* 91 (Aug. 2018), pp. 109–125. ISSN: 18790690. DOI: 10.1016/j.rser.2018.03.047.

[104] Ling Ai Wong et al. "Review on the optimal placement, sizing and control of an energy storage system in the distribution network". In: *Journal of Energy Storage* 21 (Feb. 2019), pp. 489–504. ISSN: 2352152X. DOI: 10.1016/j.est.2018.12.015.

[105] Yu Zheng et al. "Optimal allocation of energy storage system for risk mitigation of discos with high renewable penetrations". In: *IEEE Transactions on Power Systems* 29 (1 Jan. 2014), pp. 212–220. ISSN: 08858950. DOI: 10.1109/TPWRS.2013.2278850.

[106] H. Nazaripouya et al. "Optimal sizing and placement of battery energy storage in distribution system based on solar size for voltage regulation". In: *IEEE Power and Energy Society General Meeting* 2015-September (Sept. 2015). ISSN: 19449933. DOI: 10.1109/PESGM.2015.7286059.

[107] Yu Ru, Jan Kleissl, and Sonia Martinez. "Storage size determination for grid-connected photovoltaic systems". In: *IEEE Transactions on Sustainable Energy* 4 (1 2013), pp. 68–81. ISSN: 19493029. DOI: 10.1109/TSTE.2012.2199339.

[108] Ye Yang et al. "Sizing strategy of distributed battery storage system with high penetration of photovoltaic for voltage regulation and peak load shaving". In: *IEEE Transactions on Smart Grid* 5 (2 Mar. 2014), pp. 982–991. ISSN: 19493053. DOI: 10.1109/TSG.2013.2282504.

[109] Zahnd Alexa et al. "Minimizing the Lead-Acid Battery Bank Capacity through a Solar PV - Wind Turbine Hybrid System for a high-altitude village in the Nepal Himalayas". In: *Energy Procedia* 57 (Jan. 2014), pp. 1516–1525. ISSN: 1876-6102. DOI: 10.1016/J.EGYPRO.2014.10.144.

[110] Peng Li et al. "Data-Based Statistical Property Analyzing and Storage Sizing for Hybrid Renewable Energy Systems". In: *IEEE Transactions on Industrial Electronics* 62 (11 Nov. 2015), pp. 6996–7008. ISSN: 02780046. DOI: 10.1109/TIE.2015.2438052.

[111] Jun Xiao et al. "Determination of the optimal installation site and capacity of battery energy storage system in distribution network integrated with distributed generation". In: *IET Generation, Transmission and Distribution* 10.3 (Feb. 2016), pp. 601–607. ISSN: 17518687. DOI: 10.1049/iet-gtd.2015.0130.

[112] Guishi Wang, Mihai Ciobotaru, and Vassilios G. Agelidis. "Optimal capacity design for hybrid energy storage system supporting dispatch of large-scale photovoltaic power plant". In: *Journal of Energy Storage* 3 (Oct. 2015), pp. 25–35. ISSN: 2352-152X. DOI: 10.1016/J.EST.2015.08.006.

[113] R. Watanabe et al. "Optimal capacity selection of hybrid energy storage systems for suppressing PV output fluctuation". In: *2012 IEEE Innovative Smart Grid Technologies - Asia, ISGT Asia 2012* (2012). DOI: 10.1109/ISGT-ASIA.2012.6303135.

[114] Mostafa Nick, Rachid Cherkaoui, and Mario Paolone. "Optimal allocation of dispersed energy storage systems in active distribution networks for energy balance and grid support". In: *IEEE Transactions on Power Systems* 29 (5 2014), pp. 2300–2310. ISSN: 08858950. DOI: 10.1109/TPWRS.2014.2302020.

[115] R. C. Johnson, M. Mayfield, and S. B.M. Beck. "Optimal placement, sizing, and dispatch of multiple BES systems on UK low voltage residential networks". In: *Journal of Energy Storage* 17 (June 2018), pp. 272–286. ISSN: 2352-152X. DOI: 10.1016/J.EST.2018.03.005.

[116] Philipp Fortenbacher, Martin Zellner, and Göran Andersson. "Optimal sizing and placement of distributed storage in low voltage networks". In: *19th Power Systems Computation Conference, PSCC 2016* (Aug. 2016). DOI: 10.1109/PSCC.2016.7540850.

[117] Mostafa Nick, Rachid Cherkaoui, and Mario Paolone. "Optimal siting and sizing of distributed energy storage systems via alternating direction method of multipliers". In: *International Journal of Electrical Power And Energy Systems* 72 (Nov. 2015), pp. 33–39. ISSN: 0142-0615. DOI: 10.1016/J.IJEPES.2015.02.008.

[118] Wong Ling Ai et al. "Optimal battery placement in photovoltaic based distributed generation using binary firefly algorithm for voltage rise mitigation". In: *Conference Proceeding - 2014 IEEE International Conference on Power and Energy, PECon 2014* (Mar. 2014), pp. 155–158. DOI: 10.1109/PECON.2014.7062432.

[119] Hedayat Saboori and Reza Hemmati. "Maximizing DISCO profit in active distribution networks by optimal planning of energy storage systems and distributed generators". In: *Renewable and Sustainable Energy Reviews* 71 (May 2017), pp. 365–372. ISSN: 1364-0321. DOI: 10.1016/J.RSER.2016.12.066.

[120] Oytun Babacan, William Torre, and Jan Kleissl. "Siting and sizing of distributed energy storage to mitigate voltage impact by solar PV in distribution systems". In: *Solar Energy* 146 (Apr. 2017), pp. 199–208. ISSN: 0038092X. DOI: 10.1016/j.solener.2017.02.047.

[121] Ce Shang, Dipti Srinivasan, and Thomas Reindl. "An improved particle swarm optimisation algorithm applied to battery sizing for stand-alone hybrid power systems". In: *International Journal of Electrical Power And Energy Systems* 74 (Jan. 2016), pp. 104–117. ISSN: 0142-0615. DOI: 10.1016/J.IJEPES.2015.07.009.

[122] Maximilian Schneider et al. "Using inventory models for sizing energy storage systems: An interdisciplinary approach". In: *Journal of Energy Storage* 8 (Nov. 2016), pp. 339–348. ISSN: 2352-152X. DOI: 10.1016/J.EST.2016.02.009.

[123] A. Cervone et al. "Optimization of the battery size for PV systems under regulatory rules using a Markov-Chains approach". In: *Renewable Energy* 85 (Jan. 2016), pp. 657–665. ISSN: 0960-1481. DOI: 10.1016/J.RENENE.2015.07.007.

[124] Tomislav Dragičević et al. "Capacity Optimization of Renewable Energy Sources and Battery Storage in an Autonomous Telecommunication Facility". In: *IEEE Transactions on Sustainable Energy* 5 (4 Oct. 2014), pp. 1367–1378. ISSN: 19493029. DOI: 10.1109/TSTE.2014.2316480.

[125] Meng Yue and Xiaoyu Wang. "Grid Inertial Response-Based Probabilistic Determination of Energy Storage System Capacity Under High Solar Penetration". In: *IEEE Transactions on Sustainable Energy* 6 (3 July 2015), pp. 1039–1049. ISSN: 19493029. DOI: 10.1109/TSTE.2014.2328298.

[126] Chao Long et al. "Peer-to-peer energy sharing through a two-stage aggregated battery control in a community Microgrid". In: *Applied Energy* 226 (April Sept. 2018), pp. 261–276. ISSN: 03062619. DOI: 10.1016/j.apenergy.2018.05.097. URL: https://doi.org/10.1016/j.apenergy.2018.05.097https://www.sciencedirect.com/science/article/pii/S0306261918308146.

[127] Daniel L. Rodrigues et al. "Battery energy storage sizing optimisation for different ownership structures in a peer-to-peer energy sharing community". In: *Applied Energy* 262.January (2020), p. 114498. ISSN: 03062619. DOI: 10.1016/j.apenergy.2020.114498.

[128] Leehter Yao, Zolboo Damiran, and Wei Hong Lim. "A fuzzy logic based charging scheme for electric vechicle parking station". In: *EEEIC 2016 - International Conference on Environment and Electrical Engineering* (Aug. 2016). DOI: 10.1109/EEEIC.2016.7555799.

[129] Masoud Esmaili and Ali Goldoust. "Multi-objective optimal charging of plug-in electric vehicles in unbalanced distribution networks". In: *International Journal of Electrical Power and Energy Systems* 73 (Dec. 2015), pp. 644–652. ISSN: 0142-0615. DOI: 10.1016/J.IJEPES.2015.06.001.

[130] Xiaohua Wu et al. "Optimal integration of a hybrid solar-battery power source into smart home nanogrid with plug-in electric vehicle". In: *Journal of Power Sources* 363 (Sept. 2017), pp. 277–283. ISSN: 0378-7753. DOI: 10.1016/J.JPOWSOUR.2017.07.086.

[131] Mart van der Kam and Wilfried van Sark. "Smart charging of electric vehicles with photovoltaic power and vehicle-to-grid technology in a microgrid; a case study". In: *Applied Energy* 152 (Aug. 2015), pp. 20–30. ISSN: 0306-2619. DOI: 10.1016/J.APENERGY.2015.04.092.

[132] Young Min Wi, Jong Uk Lee, and Sung Kwan Joo. "Electric vehicle charging method for smart homes/buildings with a photovoltaic system". In: *IEEE Transactions on Consumer Electronics* 59 (2 2013), pp. 323–328. ISSN: 00983063. DOI: 10.1109/TCE.2013.6531113.

[133] Alyona Ivanova et al. "Coordinated charging of electric vehicles connected to a net-metered PV parking lot". In: *2017 IEEE PES Innovative Smart Grid Technologies Conference Europe, ISGT-Europe 2017 - Proceedings* 2018-January (July 2017), pp. 1–6. DOI: 10.1109/ISGTEUROPE.2017.8260291.

[134] Gautham Ram Chandra Mouli et al. "Integrated PV charging of EV fleet based on energy prices, V2G, and offer of reserves". In: *IEEE Transactions on Smart Grid* 10 (2 Mar. 2019), pp. 1313–1325. ISSN: 19493053. DOI: 10.1109/TSG.2017.2763683.

[135] Dennis Van Der Meer et al. "Energy management system with pv power forecast to optimally charge evs at the workplace". In: *IEEE Transactions on Industrial Informatics* 14 (7 July 2018), p. 3298. ISSN: 15513203. DOI: 10.1109/TII.2018.2848538.

[136] Kuljeet Kaur, Neeraj Kumar, and Mukesh Singh. "Coordinated Power Control of Electric Vehicles for Grid Frequency Support: MILP-Based Hierarchical Control Design". In: *IEEE Transactions on Smart Grid* 10 (3 May 2019), pp. 3364–3373. ISSN: 19493053. DOI: 10.1109/TSG.2018.2825322.

[137] Christos S Ioakimidis et al. "Peak shaving and valley filling of power consumption profile in non-residential buildings using an electric vehicle parking lot". In: *Energy* 148 (Apr. 2018), pp. 148–158. ISSN: 03605442. DOI: 10.1016/j.energy.2018.01.128. URL: https://doi.org/10.1016/j.energy.2018.01.128.

[138] Adnane Houbbadi et al. "Optimal Scheduling to Manage an Electric Bus Fleet Overnight Charging". In: *Energies 2019, Vol. 12, Page 2727* 12 (14 July 2019), p. 2727. ISSN: 1996-1073. DOI: 10.3390/EN12142727. URL: https://www.mdpi.com/1996-1073/12/14/2727/htmhttps://www.mdpi.com/1996-1073/12/14/2727.

[139] Hassan H. Eldeeb, Samy Faddel, and Osama A. Mohammed. "Multi-Objective Optimization Technique for the Operation of Grid tied PV Powered EV Charging Station". In: *Electric Power Systems Research* 164 (Nov. 2018), pp. 201–211. ISSN: 0378-7796. DOI: 10.1016/J.EPSR.2018.08.004.

[140] Reza Fachrizal and Joakim Munkhammar. "Improved Photovoltaic Self-Consumption in Residential Buildings with Distributed and Centralized Smart Charging of Electric Vehicles". In: *Energies 2020, Vol. 13, Page 1153* 13 (5 Mar. 2020), p. 1153. ISSN: 1996-1073. DOI: 10.3390/EN13051153. URL: https://www.mdpi.com/1996-1073/13/5/1153/htmhttps://www.mdpi.com/1996-1073/13/5/1153.

[141] Reza Fachrizal et al. "Optimal PV-EV sizing at solar powered workplace charging stations with smart charging schemes considering self-consumption and self-sufficiency balance". In: *Applied Energy* 307 (Feb. 2022), p. 118139. ISSN: 0306-2619. DOI: 10.1016/J.APENERGY.2021.118139.

[142] Adnane Houbbadi et al. "A quadratic programming based optimisation to manage electric bus fleet charging". In: *International Journal of Electric and Hybrid Vehicles* 11 (4 2019), pp. 289–307. ISSN: 17514096. DOI: 10.1504/IJEHV.2019.102862.

[143] Mohammad Mominur Rahman et al. "Technical Assessment of Plug-In Hybrid Electric Vehicle Charging Scheduling for Peak Reduction". In: *2019 10th International Renewable Energy Congress, IREC 2019* (Mar. 2019). DOI: 10.1109/IREC.2019.8754588.

[144] F. Palmiotto et al. "A coordinated optimal programming scheme for an electric vehicle fleet in the residential sector". In: *Sustainable Energy, Grids and Networks* 28 (2021), p. 100550. ISSN: 23524677. DOI: 10.1016/j.segan.2021.100550. URL: https://doi.org/10.1016/j.segan.2021.100550.

[145] Andrés Felipe Cortés Borray et al. "Centralised coordination of EVs charging and PV active power curtailment over multiple aggregators in low voltage networks". In: *Sustainable Energy, Grids and Networks* 27 (2021), p. 100470. ISSN: 23524677. DOI: 10.1016/j.segan.2021.100470. URL: https://doi.org/10.1016/j.segan.2021.100470.

[146] Karol Lina López and Christian Gagné. "Optimal Scheduling for Smart Charging of Electric Vehicles Using Dynamic Programming". In: *Lecture Notes in Computer Science (including subseries Lecture Notes in Artificial Intelligence and Lecture Notes in Bioinformatics)* 10832 LNAI (2018), pp. 279–284. ISSN: 16113349. DOI: 10.1007/978-3-319-89656-4_27. URL: https://link.springer.com/chapter/10.1007/978-3-319-89656-4_27.

[147] Yu Wu et al. "Demand side energy management of EV charging stations by approximate dynamic programming". In: *Energy Conversion and Management* 196 (Sept. 2019), pp. 878–890. ISSN: 0196-8904. DOI: 10.1016/J.ENCONMAN.2019.06.058.

[148] Dhananjay M. Anand et al. "A Hierarchical Incentive Arbitration Scheme for Coordinated PEV Charging Stations". In: *IEEE Transactions on Smart Grid* 6 (4 July 2015), pp. 1775–1784. ISSN: 19493053. DOI: 10.1109/TSG.2015.2408213.

[149] Tianjun Zhu, Hongyan Zheng, and Zonghao Ma. "A chaotic particle swarm optimization algorithm for solving optimal power system problem of electric vehicle:" in: *https://doi.org/10.1177/1687814019833500* 11 (3 Mar. 2019), pp. 1–9. ISSN: 16878140. DOI: 10.1177/1687814019833500. URL: https://journals.sagepub.com/doi/full/10.1177/1687814019833500.

[150] Jun Yang, Lifu He, and Siyao Fu. "An improved PSO-based charging strategy of electric vehicles in electrical distribution grid". In: *Applied Energy* 128 (Sept. 2014), pp. 82–92. ISSN: 0306-2619. DOI: 10.1016/J.APENERGY.2014.04.047.

[151] Bo Hu et al. "Power grid peak shaving strategies based on electric vehicles and thermal storage electric boilers". In: *IOP Conference Series: Earth and Environmental Science* 227 (3 Feb. 2019), p. 032026. ISSN: 1755-1315. DOI: 10.1088/1755-1315/227/3/032026. URL: https://iopscience.iop.org/article/10.1088/1755-1315/227/3/032026https://iopscience.iop.org/article/10.1088/1755-1315/227/3/032026/meta.

[152] Sajjad Ahmadi et al. "Optimal use of vehicle-to-grid technology to modify the load profile of the distribution system". In: *Journal of Energy Storage* 31 (October 2019 2020), p. 101627. ISSN: 2352152X. DOI: 10.1016/j.est.2020.101627. URL: https://doi.org/10.1016/j.est.2020.101627.

[153] Hao Wu et al. "A scheduling and control system for electric vehicle charging at parking lot". In: *2017 Asian Control Conference, ASCC 2017* 2018-January (Feb. 2018), pp. 13–18. DOI: 10.1109/ASCC.2017.8287095.

[154] Hao Wu et al. "Dynamic resource allocation for parking lot electric vehicle recharging using heuristic fuzzy particle swarm optimization algorithm". In: *Applied Soft Computing* 71 (Oct. 2018), pp. 538–552. ISSN: 1568-4946. DOI: 10.1016/J.ASOC.2018.07.008.

[155] Abdul Rauf Bhatti and Zainal Salam. "A rule-based energy management scheme for uninterrupted electric vehicles charging at constant price using photovoltaic-grid system". In: *Renewable Energy* 125 (Sept. 2018), pp. 384–400. ISSN: 0960-1481. DOI: 10.1016/J.RENENE.2018.02.126.

[156] Xinhui Lu et al. "Multi-objective optimal load dispatch of microgrid with stochastic access of electric vehicles". In: *Journal of Cleaner Production* 195 (2018), pp. 187–199. ISSN: 09596526. DOI: 10.1016/j.jclepro.2018.05.190.

[157] Yanyu Zhang, Peng Zeng, and Chuanzhi Zang. "Optimization algorithm for home energy management system based on artificial bee colony in smart grid". In: *2015 IEEE International Conference on Cyber Technology in Automation, Control and Intelligent Systems, IEEE-CYBER 2015* (Oct. 2015), pp. 734–740. DOI: 10.1109/CYBER.2015.7288033.

[158] Jorge García-Álvarez et al. "Electric Vehicle Charging Scheduling Using an Artificial Bee Colony Algorithm". In: *Lecture Notes in Computer Science (including subseries Lecture Notes in Artificial Intelligence and Lecture Notes in Bioinformatics)* 10337 LNCS (2017), pp. 115–124. ISSN: 16113349. DOI: 10.1007/978-3-319-59740-9_12. URL: https://link.springer.com/chapter/10.1007/978-3-319-59740-9_12.

[159] Michalis Mavrovouniotis, Georgios Ellinas, and Marios Polycarpou. "Electric Vehicle Charging Scheduling Using Ant Colony System". In: *2019 IEEE Congress on Evolutionary Computation, CEC 2019 - Proceedings* (June 2019), pp. 2581–2588. DOI: 10.1109/CEC.2019.8789989.

[160] Shuangqi Li et al. "Vehicle-to-grid management for multi-time scale grid power balancing". In: *Energy* 234 (2021), p. 121201. ISSN: 03605442. DOI: 10.1016/j.energy.2021.121201. URL: https://doi.org/10.1016/j.energy.2021.121201.

[161] Zhenya Ji et al. "Accelerated Model Predictive Control for Electric Vehicle Integrated Microgrid Energy Management: A Hybrid Robust and Stochastic Approach". In: *Energies 2016, Vol. 9, Page 973* 9 (11 Nov. 2016), p. 973. ISSN: 1996-1073. DOI: 10.3390/EN9110973. URL: https://www.mdpi.com/1996-1073/9/11/973/htmhttps://www.mdpi.com/1996-1073/9/11/973.

[162] Wenhua Li, Tao Zhang, and Rui Wang. "Energy management model of charging station micro-grid considering random arrival of electric vehicles". In: *Proceedings - 2nd IEEE International Conference on Energy Internet, ICEI 2018* (July 2018), pp. 29–34. DOI: 10.1109/ICEI.2018.00013.

[163] Cheng Li et al. "An Electric Vehicle Routing Optimization Model with Hybrid Plug-In and Wireless Charging Systems". In: *IEEE Access* 6 (May 2018), pp. 27569–27578. ISSN: 21693536. DOI: 10.1109/ACCESS.2018.2832187.

[164] Cesar Diaz, Fredy Ruiz, and Diego Patino. "Smart Charge of an Electric Vehicles Station: A Model Predictive Control Approach". In: *2018 IEEE Conference on Control Technology and Applications, CCTA 2018* (Oct. 2018), pp. 54–59. DOI: 10.1109/CCTA.2018.8511498.

[165] Zhaoxi Liu et al. "Two-Stage Optimal Scheduling of Electric Vehicle Charging Based on Transactive Control". In: *IEEE Transactions on Smart Grid* 10 (3 May 2019), pp. 2948–2958. ISSN: 19493053. DOI: 10.1109/TSG.2018.2815593.

[166] Yongmin Zhang and Lin Cai. "Dynamic Charging Scheduling for EV Parking Lots with Photovoltaic Power System". In: *IEEE Access* 6 (2018), pp. 56995–57005. ISSN: 21693536. DOI: 10.1109/ACCESS.2018.2873286.

[167] Rishabh Ghotge et al. "Optimized Scheduling of EV Charging in Solar Parking Lots for Local Peak Reduction under EV Demand Uncertainty". In: *Energies 2020, Vol. 13, Page 1275* 13 (5 Mar. 2020), p. 1275. ISSN: 1996-1073. DOI: 10.3390/EN13051275. URL: https://www.mdpi.com/1996-1073/13/5/1275/htmhttps://www.mdpi.com/1996-1073/13/5/1275.

[168] Bin Wang et al. "Predictive scheduling for Electric Vehicles considering uncertainty of load and user behaviors". In: *Proceedings of the IEEE Power Engineering Society Transmission and Distribution Conference* 2016-July (July 2016). ISSN: 21608563. DOI: 10.1109/TDC.2016.7520018.

[169] Mohammed Fathy El-Naggar and Adel Abdelaziz Abdelghany Elgammal. "Multi-Objective Optimal Predictive Energy Management Control of Grid-Connected Residential Wind-PV-FC-Battery Powered Charging Station for Plug-in Electric Vehicle". In: *Journal of Electrical Engineering and Technology* 13 (2 Mar. 2018), pp. 742–751. ISSN: 1975-0102. DOI: 10.5370/JEET.2018.13.2.742. URL: http://doi.org/10.5370/JEET.2018.13.2.742742.

[170] Bishnu P. Bhattarai et al. "Multi-Time Scale Control of Demand Flexibility in Smart Distribution Networks". In: *Energies 2017, Vol. 10, Page 37* 10 (1 Jan. 2017), p. 37. ISSN: 1996-1073. DOI: 10.3390/EN10010037. URL: https://www.mdpi.com/1996-1073/10/1/37/htmhttps://www.mdpi.com/1996-1073/10/1/37.

[171] Nian Liu et al. "A Heuristic Operation Strategy for Commercial Building Microgrids Containing EVs and PV System". In: *IEEE Transactions on Industrial Electronics* 62 (4 2015), pp. 2560–2570. ISSN: 02780046. DOI: 10.1109/TIE.2014.2364553.

[172] European Parliament. "Directive 2018/2001 on the promotion of the use of energy from renewable sources". In: *Official Journal of the European Union* 2018.L 328 (2018), pp. 82–209.

[173] M. Corrá et al. "A System Based on IoT Platforms and Occupancy Monitoring for Energy-Efficient HVAC Management". In: *2019 IEEE 5th International forum on Research and Technology for Society and Industry (RTSI)*. Florence, Italy, Sept. 2019, pp. 347–352.

[174] Mattia Secchi and Grazia Barchi. "Peer-to-peer electricity sharing: Maximising PV self-consumption through BESS control strategies". In: *Proceedings - 2019 IEEE International Conference on Environment and Electrical Engineering and 2019 IEEE Industrial and Commercial Power Systems Europe, EEEIC/I and CPS Europe 2019* 1042 (2019), pp. 0–5. DOI: 10.1109/EEEIC.2019.8783608.

[175] Kalyanmoy Deb et al. "A fast elitist non-dominated sorting genetic algorithm for multi-objective optimization: NSGA-II". In: *Lecture Notes in Computer Science (including subseries Lecture Notes in Artificial Intelligence and Lecture Notes in Bioinformatics)* 1917 (2000), pp. 849–858. ISSN: 16113349. DOI: 10.1007/3-540-45356-3_83.

[176] Joseph A. Azzolini et al. "Implementation of Temporal Parallelization for Rapid Quasi-Static Time-Series (QSTS) Simulations". In: *Conference Record of the IEEE Photovoltaic Specialists Conference*. Institute of Electrical and Electronics Engineers Inc., June 2019, pp. 2942–2949. ISBN: 9781728104942. DOI: 10.1109/PVSC40753.2019.8980591.

[177] ASTAT - Istituto Provinciale di Statistica. *Dati demografici provincia autonoma di Bolzano, 2018*.

[178] Chiara Dipasquale et al. "Database of energy, environmental and economic indicators of renovation packages for European residential buildings". In: *Energy and Buildings* 203 (Nov. 2019), p. 109427. ISSN: 03787788. DOI: 10.1016/j.enbuild.2019.109427.

[179] K. Rath et al. *IEA PVPS Task 13-ST2.5: PLR Determination Benchmark Study*. 2020. DOI: 10.17605/OSF.IO/YN5DE.

[180] Rasmus Luthander et al. "Photovoltaic self-consumption in buildings: A review". In: *Applied Energy* 142 (Mar. 2015), pp. 80–94. ISSN: 0306-2619. DOI: 10.1016/J.APENERGY.2014.12.028.

[181] Sylvain Quoilin et al. "Quantifying self-consumption linked to solar home battery systems: Statistical analysis and economic assessment". In: *Applied Energy* 182 (Nov. 2016), pp. 58–67. ISSN: 0306-2619. DOI: 10.1016/J.APENERGY.2016.08.077.

[182] Jianxiao Wang et al. "Incentivizing distributed energy resource aggregation in energy and capacity markets: An energy sharing scheme and mechanism design". In: *Applied Energy* 252.September 2018 (2019), p. 113471. ISSN: 03062619. DOI: 10.1016/j.apenergy.2019.113471.

[183] Sahban W. Alnaser et al. "Residential community with PV and batteries: Reserve provision under grid constraints". In: *International Journal of Electrical Power and Energy Systems* 119.February (2020), p. 105856. ISSN: 01420615. DOI: 10.1016/j.ijepes.2020.105856.

[184] SunWatts. *Modular Solar Battery Cells Catalogue*.

[185] Alessandro Pitì et al. "The Role of Smart Meters in Enabling Real-Time Energy Services for Households: The Italian Case". In: *Energies* 10 (Feb. 2017), p. 199. DOI: 10.3390/en10020199.

[186] G.Janssens-Maenhout B. Koffi, A.Cerutti, M.Duerr, A.Iancu, A.Kona. "Council of Mayors Default Emission Factors for the Member States of the European Union Dataset". In: *European Commission, Joint Research Centre (JRC)* (2017), p. 13.

[187] Ondřej Žižlavský. "Net Present Value Approach: Method for Economic Assessment of Innovation Projects". In: *Procedia - Social and Behavioral Sciences* 156 (Nov. 2014), pp. 506–512. ISSN: 18770428. DOI: 10.1016/j.sbspro.2014.11.230.

[188] Nian Liu et al. "Energy-Sharing Model with Price-Based Demand Response for Microgrids of Peer-to-Peer Prosumers". In: *IEEE Transactions on Power Systems* 32.5 (2017), pp. 3569–3583. ISSN: 08858950. DOI: 10.1109/TPWRS.2017.2649558.

[189] Matteo Giacomo Prina et al. "Transition pathways optimization methodology through EnergyPLAN software for long-term energy planning". In: *Applied Energy* 235 (Feb. 2019), pp. 356–368. ISSN: 03062619. DOI: 10.1016/j.apenergy.2018.10.099.

[190] Sascha Lindig et al. "Performance Loss Rates of PV systems of Task 13 database". In: *Conference Record of the IEEE Photovoltaic Specialists Conference*. Institute of Electrical and Electronics Engineers Inc., June 2019, pp. 1363–1367. ISBN: 9781728104942. DOI: 10.1109/PVSC40753.2019.8980638.

[191] GME. *Italian Electricity Market Prices Archive, Gestore Mercato Elettrico*.

[192] European Parliament. "Directive 2019/944 on Common Rules for the Internal Market for Electricity". In: *Official Journal of the European Union* L 158 (2019), p. 18. DOI: http://eur-lex.europa.eu/pri/en/oj/dat/2003/l_285/l_28520031101en00330037.pdf.

[193] Didier Farinet et al. "Battery Lifetime Analysis for Residential PV-Battery System used to Optimize the Self Consumption - A Danish Scenario". In: *2019 IEEE Energy Conversion Congress and Exposition, ECCE 2019*. Institute of Electrical and Electronics Engineers Inc., Sept. 2019, pp. 6693–6698. ISBN: 9781728103952. DOI: 10.1109/ECCE.2019.8912280.

[194] Hector Beltran, Pablo Ayuso, and Emilio Pérez. "Lifetime Expectancy of Li-Ion Batteries used for Residential Solar Storage". In: *Energies* 13.3 (Jan. 2020), p. 568. ISSN: 19961073. DOI: 10.3390/en13030568. URL: https://www.mdpi.com/1996-1073/13/3/568.

[195] Evangelos Panos and Martin Densing. "The future developments of the electricity prices in view of the implementation of the Paris Agreements: Will the current trends prevail, or a reversal is ahead?" In: *Energy Economics* 84 (Oct. 2019), p. 104476. ISSN: 01409883. DOI: 10.1016/j.eneco.2019.104476.

[196] European Commission. *Fit for 55 - EU Commission Legislative Train Schedule*. 2021. URL: https://www.europarl.europa.eu/legislative-train/theme-a-european-green-deal/package-fit-for-55 (visited on 01/26/2022).

[197] IRENA. *World Energy Transitions Outlook: 1.5°C Pathway*. Tech. rep. 2021, p. 58. URL: https://www.irena.org/publications/2021/Jun/World-Energy-Transitions-Outlook.

[198] Bingjie Xu et al. "Have electric vehicles effectively addressed CO2 emissions? Analysis of eight leading countries using quantile-on-quantile regression approach". In: *Sustainable Production and Consumption* 27 (2021), pp. 1205–1214. ISSN: 23525509. DOI: 10.1016/j.spc.2021.03.002. URL: https://doi.org/10.1016/j.spc.2021.03.002.

[199] Md Mamunur Rahman et al. "A comparative assessment of CO2 emission between gasoline, electric, and hybrid vehicles: A Well-To-Wheel perspective using agent-based modeling". In: *Journal of Cleaner Production* 321.October 2020 (2021), p. 128931. ISSN: 09596526. DOI: 10.1016/j.jclepro.2021.128931. URL: https://doi.org/10.1016/j.jclepro.2021.128931.

[200] Mehmet Efe Biresselioglu, Melike Demirbag Kaplan, and Barbara Katharina Yilmaz. "Electric mobility in Europe: A comprehensive review of motivators and barriers in decision making processes". In: *Transportation Research Part A: Policy and Practice* 109 (Mar. 2018), pp. 1–13. ISSN: 0965-8564. DOI: 10.1016/J.TRA.2018.01.017.

[201] Mattia Secchi et al. "Multi-objective battery sizing optimisation for renewable energy communities with distribution-level constraints: A prosumer-driven perspective". In: *Applied Energy* 297 (Sept. 2021), p. 117171. ISSN: 0306-2619. DOI: 10.1016/J.APENERGY.2021.117171.

[202] "A photovoltaics-aided interlaced extended Kalman filter for distribution systems state estimation". In: *Sustainable Energy, Grids and Networks* 26 (June 2021), p. 100438. ISSN: 2352-4677. DOI: 10.1016/J.SEGAN.2021.100438.

[203] Bijan Bibak and Hatice Tekiner-Mogulkoc. "Influences of vehicle to grid (V2G) on power grid: An analysis by considering associated stochastic parameters explicitly". In: *Sustainable Energy, Grids and Networks* 26 (2021), p. 100429. ISSN: 23524677. DOI: 10.1016/j.segan.2020.100429. URL: https://doi.org/10.1016/j.segan.2020.100429.

[204] Sang Keun Moon and Jin O. Kim. "Balanced charging strategies for electric vehicles on power systems". In: *Applied Energy* 189 (2017), pp. 44–54. ISSN: 03062619. DOI: 10.1016/j.apenergy.2016.12.025. URL: http://dx.doi.org/10.1016/j.apenergy.2016.12.025.

[205] Linni Jian et al. "A scenario of vehicle-to-grid implementation and its double-layer optimal charging strategy for minimizing load variance within regional smart grids". In: *Energy Conversion and Management* 78 (2014), pp. 508–517. ISSN: 01968904. DOI: 10.1016/j.enconman.2013.11.007. URL: http://dx.doi.org/10.1016/j.enconman.2013.11.007.

[206] Linni Jian et al. "Optimal scheduling for vehicle-to-grid operation with stochastic connection of plug-in electric vehicles to smart grid". In: *Applied Energy* 146 (2015), pp. 150–161. ISSN: 03062619. DOI: 10.1016/j.apenergy.2015.02.030. URL: http://dx.doi.org/10.1016/j.apenergy.2015.02.030.

[207] Mohd Syahmi Hashim et al. "Priority-based vehicle-to-grid scheduling for minimization of power grid load variance". In: *Journal of Energy Storage* 39 (2021), p. 102607. ISSN: 2352152X. DOI: 10.1016/j.est.2021.102607. URL: https://doi.org/10.1016/j.est.2021.102607.

[208] J García-Villalobos et al. "Multi-objective optimization control of plug-in electric vehicles in low voltage distribution networks". In: *Applied Energy* 180 (2016), pp. 155–168. ISSN: 03062619. DOI: 10.1016/j.apenergy.2016.07.110.

[209] Vincenzo Marano et al. "Lithium-ion batteries life estimation for plug-in hybrid electric vehicles". In: *5th IEEE Vehicle Power and Propulsion Conference, VPPC '09* (2009), pp. 536–543. DOI: 10.1109/VPPC.2009.5289803.

[210] Anderson Hoke et al. "Electric vehicle charge optimization including effects of lithium-ion battery degradation". In: *2011 IEEE Vehicle Power and Propulsion Conference, VPPC 2011* (2011). DOI: 10.1109/VPPC.2011.6043046.

[211] Vasileios Boglou et al. "A Fuzzy Energy Management Strategy for the Coordination of Electric Vehicle Charging in Low Voltage Distribution Grids". In: *Energies 2020, Vol. 13, Page 3709* 13 (14 July 2020), p. 3709. ISSN: 19961073. DOI: 10.3390/EN13143709. URL: https://www.mdpi.com/1996-1073/13/14/3709/htmhttps://www.mdpi.com/1996-1073/13/14/3709.

[212] Enrico Dalla Maria, Mattia Secchi, and David Macii. "A Flexible Top-Down Data-Driven Stochastic Model for Synthetic Load Profiles Generation". In: *Energies 2022, Vol. 15, Page 269* 15 (1 Dec. 2021), p. 269. ISSN: 1996-1073. DOI: 10.3390/EN15010269.

[213] Andrea Mangipinto et al. "Impact of mass-scale deployment of electric vehicles and benefits of smart charging across all European countries". In: *Applied Energy* 312 (Apr. 2022), p. 118676. ISSN: 0306-2619. DOI: 10.1016/J.APENERGY.2022.118676.

[214] Snezana Cundeva, Aleksandra Krkoleva Mateska, and Math H.J. Bollen. "Hosting capacity of LV residential grid for uncoordinated ev charging". In: *Proceedings of International Conference on Harmonics and Quality of Power, ICHQP* 2018-May (June 2018), pp. 1–5. ISSN: 21640610. DOI: 10.1109/ICHQP.2018.8378892.

[215] Justine Sears, David Roberts, and Karen Glitman. "A comparison of electric vehicle Level 1 and Level 2 charging efficiency". In: *2014 IEEE Conference on Technologies for Sustainability, SusTech 2014* (Feb. 2014), pp. 255–258. DOI: 10.1109/SUSTECH.2014.7046253.

[216] "Electric Vehicle Use and Energy Consumption Based on Realworld Electric Vehicle Fleet Trip and Charge Data and Its Impact on Existing EV Research Models". In: *World Electric Vehicle Journal 2015, Vol. 7, Pages 436-446* 7 (3 Sept. 2015), pp. 436–446. ISSN: 2032-6653. DOI: 10.3390/WEVJ7030436. URL: https://www.mdpi.com/2032-6653/7/3/436.

[217] Cristina González-Morán, Pablo Arboleya, and Valeria Pilli. "Photovoltaic self consumption analysis in a European low voltage feeder". In: *Electric Power Systems Research* 194.December 2020 (May 2021), p. 107087. ISSN: 03787796. DOI: 10.1016/j.epsr.2021.107087. URL: https://doi.org/10.1016/j.epsr.2021.107087.

[218] Yassir Dahmane et al. "Optimized time step for electric vehicle charging optimization considering cost and temperature". In: *Sustainable Energy, Grids and Networks* 26 (June 2021), p. 100468. ISSN: 2352-4677. DOI: 10.1016/J.SEGAN.2021.100468.

[219] Mohammad Sameti and Fariborz Haghighat. "Integration of distributed energy storage into net-zero energy district systems: Optimum design and operation". In: *Energy* 153 (June 2018), pp. 575–591. ISSN: 0360-5442. DOI: 10.1016/J.ENERGY.2018.04.064.

[220] Rutooj D. Deshpande and Kotub Uddin. "Physics inspired model for estimating 'cycles to failure' as a function of depth of discharge for lithium ion batteries". In: *Journal of Energy Storage* 33 (Jan. 2021), p. 101932. ISSN: 2352-152X. DOI: 10.1016/J.EST.2020.101932.

[221] ARERA. "Regolazione tariffaria dei servizi di trasmissione, distribuzione e misura dell'energia elettrica, per il periodo di regolazione 2016-2023." In: (2015). URL: https://www.arera.it/it/docs/15/654-15.htm.

[222] Julio A. Sanguesa et al. "A Review on Electric Vehicles: Technologies and Challenges". In: *Smart Cities 2021, Vol. 4, Pages 372-404* 4 (1 Mar. 2021), pp. 372–404. ISSN: 2624-6511. DOI: 10.3390/SMARTCITIES4010022. URL: https://www.mdpi.com/2624-6511/4/1/22.